Title	Phenomenological and cosmological aspects of string axion and supersymmetric standard models
Author(s)	大本, 直哉
Citation	北海道大学. 博士(理学) 甲第13561号
Issue Date	2019-03-25
DOI	10.14943/doctoral.k13561
Doc URL	http://hdl.handle.net/2115/74271
Type	theses (doctoral)
File Information	Naoya_Omoto.pdf

Phenomenological and cosmological aspects of string axion and supersymmetric standard models

（弦理論アクシオンと超対称標準模型の現象論的かつ宇宙論的側面についての研究）

Naoya Omoto

Department of Cosmosciences, Graduate school of Science

Hokkaido University

A thesis submitted for the degree of

Doctor of Science

March, 2019

Abstract

Recent discoveries and insights depended on some experimental results have already deeply impacted our understanding. Although the standard model in particle physics is consistent with almost all the experimental results obtained so far, there also exist unsolvable problems, even in the cosmology. It suggests that our standard model should be extended, beyond from the electroweak scale to higher energy scale. It is the time that we have to solve these serious problems facing now using all the knowledge we have gained until now.

In this thesis, we have studied these relational extended models by considering the following two approaches. First, we concentrate on the inflation models as a high energy physics in the early universe. So far, there are found many kinds of slow-roll inflation models, in this thesis, we pursue mainly inflation related to axion. Typically, the axions are particularly attractive inflation candidates because they have shift symmetry to all orders in perturbation theories. Motivated above a key ingredient, we have studied an axion inflation model recently proposed within the framework of type IIB superstring theory, where we pay particular attention to a sub-Planckian axion decay constant. Further, we study a general class of small-field axion inflations which are the mixture of polynomial and sinusoidal functions suggested by the natural and axion monodromy inflations. In such a case, the axion decay constants, leading to the successful axion inflations are severely constrained in order not to spoil the Big-Bang nucleosynthesis and overproduce the isocurvature perturbation originating from the QCD axion. We, in turn, find that the cosmological favorable axion decay constants are typical of order the grand unification scale or the string scale which is consistent with the prediction of closed string axions. Our axion potential can lead

to the small field inflation with a small tensor-to-scalar ratio, and a typical reheating temperature can be as low as GeV.

Second, we have concentrated on about the cosmology in the viewpoint of supersymmetry phenomenology. After we briefly review a few variations on the basic picture of the minimal supersymmetric standard model (MSSM) and its application to the cosmology, we consider domain walls in the Z_3 symmetric Next-to-MSSM. The spontaneous Z_3 discrete symmetry breaking produces domain walls, and the stable domain walls are problematic. Thus, we assume the Z_3 symmetry is slightly, but explicitly broken and the domain walls decay. Such a decay causes a large late-time entropy production. We study its cosmological implications on unwanted relics such as moduli, gravitino, lightest supersymmetric particle (LSP) and axion. Moreover, we also propose an Affleck-Dine leptogenesis model with right-handed neutrino as a minimal extension of MSSM, which is based on LH_u direction, and we have pointed out that sufficient amounts of baryon asymmetry can be generated in our model.

Through this thesis, we hope that our scenario would clearly contribute to our understanding of the feature of the universe.

List of auther's publications

This is a Ph.D. thesis on cosmological inflation and cosmology in supersymmetric standard models. The thesis [1] is based on the auther's works (d, e) and (c). There are unpublished works in chapter 6, and some new contents beyond Refs. (d, e) in chapter 3 which is based on (f).

[a] D. Kikuchi, N. Omoto, K. Yamada and H. Asada, "Possible altitudinal, latitudinal, and directional dependence of the relativistic Sagnac effect in Chern-Simons modified gravity," Phys. Rev. D **90** (2014) no.6, 064036 doi:10.1103/PhysRevD.90.064036 [arXiv:1405.7472 [gr-qc]].

[b] H. Hattori, T. Kobayashi, N. Omoto and O. Seto, "Dilution of axion dark radiation by thermal inflation," Phys. Rev. D **92** (2015) no.2, 023517 doi:10.1103/PhysRevD.92.023517 [arXiv:1505.01294 [hep-ph]].

[c] H. Hattori, T. Kobayashi, N. Omoto and O. Seto, "Entropy production by domain wall decay in the NMSSM," Phys. Rev. D **92** (2015) no.10, 103518 doi:10.1103/PhysRevD.92.103518 [arXiv:1510.03595 [hep-ph]].

[d] K. Kadota, T. Kobayashi, A. Oikawa, N. Omoto, H. Otsuka and T. H. Tatsuishi, "Small field axion inflation with sub-Planckian decay constant," JCAP **1610** (2016) no.10, 013 doi:10.1088/1475-7516/2016/10/013 [arXiv:1606.03219 [hep-ph]].

[e] T. Kobayashi, A. Oikawa, N. Omoto, H. Otsuka and I. Saga, "Constraints on small-field axion inflation," Phys. Rev. D **95** (2017) no.6, 063514 doi:10.1103/PhysRevD.95.063514 [arXiv:1609.05624 [hep-ph]].

[1] See auther's profile on INSPIRE HEP.

[f] T. Kobayashi, N. Omoto, H. Otsuka and T. H. Tatsuishi, "Supersymmetry preserving and breaking degenerate vacua, and radiative moduli stabilization," Phys. Rev. D **96** (2017) no.4, 046004 doi:10.1103/PhysRevD.96.046004 [arXiv:1704.04875 [hep-th]].

[g] T. Kobayashi, N. Omoto, H. Otsuka and T. H. Tatsuishi, "Radiative Khler moduli stabilization," Phys. Rev. D **97** (2018) no.10, 106006 doi:10.1103/PhysRevD.97.106006 [arXiv:1711.10274 [hep-th]].

[h] T. Abe, N. Omoto, O. Seto and T. Shindou, "Electric dipole moments and dark matter in a CP violating MSSM," Phys. Rev. D **98**, no. 7, 075029 (2018) doi:10.1103/PhysRevD.98.075029 [arXiv:1805.09537 [hep-ph]].

[i] T. Kobayashi, N. Omoto, Y. Shimizu, K. Takagi, M. Tanimoto and T. H. Tatsuishi, "Modular A_4 invariance and neutrino mixing," JHEP **1811**, 196 (2018) doi:10.1007/JHEP11(2018)196 [arXiv:1808.03012 [hep-ph]].

Acknowledgements

First of all, I would like to express my sincere gratitude and appreciation to my supervisor, Tatsuo Kobayashi for valuable scientific discussions, for instructive suggestions, for a good research environment, and for constant encouragements to my study. Without him, this thesis would not exist, on the contrary, I would not advance in the Ph.D. course at Hokkaido University. I also thank him for kindly advice on an academic career and so on. I learned a lot from his critical advice as a scientist. Further, I would like to thank Osamu Seto for helping me throughout my Ph.D. course, and for useful discussions and comments. Motivated by the discussion with him, I decided to study the cosmology and SUSY phenomenology. It is my great pleasure to collaborate and to study with them.

I am also grateful to Hironori Hattori, Hajime Otsuka, Takuya H. Tatsuishi, Akane Oikawa, Ikumi Saga, Kenji Kadota, Yusuke Shimizu, Kenta Takagi, Morimitsu Tanimoto, Shindo Tetsuo, Abe Tomohiro for valuable advice and discussions on the papers which we have published.

I thank all staffs and the past and present student members of theoretical particle physics group at Hokkaido University.

Finally, I want to express my appreciation to my family for their continuing hearty supports.

I have been financially supported since April 2018 by Grant-in-Aid JSPS Fellows, and a Grant-in-Aid of the JSPS under No. 18J109080

Contents

1

Introduction -Our landscape-

The "cosmolog" is one of the most active research topics in modern physics, which many physicists have studied vigorously since especially the ancient time. The law of cosmology is deeper and more fundamental questions, and it is quite important in order to understand; what particles are, what interactions among them are, and what some unknown phenomena detected current experiments are, relating to the high energy physics beyond the standard model in the particle physics, discussed in this thesis. We think that the goal of cosmology is to explain the present state of the universe within the basis of physical law, which we hope that it would clearly elucidate these mysterious features of the universe. In this sense, the inflation and supersymmetry are assumed to be attractive candidates, and we have tried to describe the universe by our original approach depending on these established theories.

Here, let us mention about the particle physics so far briefly. By developing the technology of experiments dramatically, our understanding is summarized in the standard model of particle physics. It is described by the quantum field theory with the gauge group; $SU(3)_c \times SU(2)_L \times U(1)_Y$, and almost all people persist that the standard model is an effective theory constructed by more fundamental theory in high energy physics. The standard model or such effective theory explains almost all experimental results observed until now. It is remarkable that these observables are consistent with the standard model, however, there are also a few phenomena that cannot be explained by our understandings; neutrino mass, dark matter candidate, baryon asymmetry of the universe, mechanisms of inflation and its inflation candidate, and also theoretical problems, like domain wall problems, the gauge hierarchy problem and fine tunings on them, and so on. In order to explain these issues, naively, we assume that the standard model has to be extended beyond the electroweak scale.

From the viewpoint of the potentiality of the particle physics, one naively supposes the gauge couplings are close to or unified each other at a high energy scale, which means that there exist some unified models beyond the standard model. In spite of the success in the standard model, there are also problems as mentioned above. In this sense, the supersymmetry becomes a key ingredient to solve such problems and to propose new perspectives. This is advantageous for supersymmetry.

The supersymmetry is a symmetry to transform between bosonic state and fermionic state each other, and it is symmetry which extends the Poincare symmetry of space-time [1]. Especially motivated us by a dark matter candidate, which dominate the current energy density of the universe, and unwanted relics problems, like kind of gravitino, moduli, and monopole, supersymmetry solves them both phenomenologically and theoretically. As for the cosmology, it has also a possibility to solve the mysteries consequently. As discussed in chapter 4, we will revisit relations between supersymmetry and cosmology, and propose our original approach to solve them.

On the other hand, related to the cosmology, there is a successful scenario to explain our universe; the Big-Bang scenario. The standard Big-Bang cosmology scenario has strong observational shreds of evidence. However, the cosmological problems still remain, the standard model also cannot explain these problems. One of the topics of this thesis is about inflation. Advantages of this approach are that it provides testable predictions for the cosmological observables. The primordial gravitational wave is also one of the main desirable observations especially. Inflation solves the problems of the Big-Bang theory; flatness problem, horizon problem, and unwanted relics to realize successful nucleosynthesis, and so on. Further, it generates a seed of the primordial density perturbation observed today, growing the large-scale structure of our universe.

This mechanism is caused by the potential of the scalar field, so-called inflation. In the standard model, it has only the Higgs field as a scalar field, however, the pure standard model Higgs cannot reproduce suitable prediction for current observables. Although there are many possibilities to describe the inflation so far, at the present we cannot determine which model is true, unfortunately. In chapter 2, we will revisit about the inflation, and we propose some possibilities of inflation models, the small field

[1] The details, what is the supersymmetry, are discussed in chapter 4. We will review there.

axion inflation scenarios in chapter 4, in which models were recently derived within the framework of type IIB superstring theory (1).

Going back to the previous topic, the Big-Bang theory suggests that the universe would shrink and dense at one point by going back our time. This prediction is the key ingredient. The universe at a such very early stage, every matter is decomposed to elementary particles due to high energy interaction particle physics, therefore the cosmology is related to low energy theory, the standard model seriously. In this sense, it is quite useful to discuss for extended models of UV theory (or theory in the Planck scale) beyond our understanding, further, for future study. Moreover, we all want to know nature in a unified framework of particle physics. Then again, motivated the above interests, we have tried to describe the universe by our original approach comprehensively, and we hope that our scenarios would clearly elucidate mysteries feature of the universe.

In this thesis, we aim to investigate and understand the cosmological problems which are suggested by experiments, especially in the viewpoint of the supersymmetry (and string theory), and to propose our insights on my current approach toward these problems. Actually, we will find that our models could explain the above problems naturally.

This thesis consists of two parts, organizing as follows: The first part is composed of the inflation. In chapter 2, we review on the set up of slow-roll inflation depended on a scalar field dynamics, and summarize cosmological perturbation and current observable. Then the next chapter 3, we propose our small field axion inflation scenarios, in which models were recently derived within the framework of type IIB superstring theory (1). This chapter is based on our works (d, e), and there are some new contents beyond Refs.(d, e) which is based on Ref.(f) with considering the moduli stabilization there. The second part is considered on about cosmology in the viewpoints of supersymmetry phenomenology. In chapter 4, we provide a fundamental introduction of supersymmetry including topics are motivated for the supersymmetry, the Higgs scalar potential constructed from a supersymmetric Lagrangian, and some extension of the minimal framework, the minimal supersymmetric standard model (MSSM) for the next-to MSSM (NMSSM) and Affleck-Dine mechanism which is one of the baryogenesis scenarios. These are preparations of our studies on chapter 5 and chapter 6. Then, in chapter 5, we consider domain walls in the Z_3 symmetric NMSSM based on our works (c), where domain walls due to the spontaneous Z_3 discrete symmetry are characterized, and we study its cosmological implications on unwanted relics. In chapter 6, we propose a model of Affleck-Dine mechanism for the leptogenesis with a right-handed Dirac neutrino. In this model, the baryon number can be explained, and we will show that several phenomenological consequences of our scenario give some interesting bounds on supersymmetric parameter space. Finally, chapter 7 is devoted to the summary in this thesis and to remark on our future works. At the rest of this thesis, in Appendix A, we manifest the conventions and notations of supersymmetry in our study, in Appendix B, we show the review of a moduli stabilization depended on (g), and, in Appendix C, we add the preparation of the Affleck-Dine mechanics.

Part I

INFLATION

2

A brief review of inflation

2.1 Overview

Einstein proposed the General Relativity in 1915 (2), which made it possible to discuss the structure of space-time and the evolution of the universe in terms of physical law. The general solution of Einstein's equations is very complicated. Meanwhile, in 1992 Friedmann found the special cosmological solution of Einstein field equation (2), which is isotropic and even homogeneous. After that, in 1946 Hubble suggested that our universe is expanding by his observations in the redshift of galaxies (2), as Einstein theory predicts. Such theoretical predictions are now supported by powerful evidence, CMB. If the expansion of the universe is not isotropic, the expansion anisotropy would mean a temperature anisotropy in the CMB. Likewise, inhomogeneity in the density of the universe would lead to temperature anisotropy. Today there is a simple and remarkably successful picture; Big-Bang.

In standard Big-Bang cosmology, our universe is described that the state of the universe experiences the radiation and matter dominated era. At an early stage of the universe, everything is decomposed into elementary particles due to high energy interactions. These events predict the existence of expansion of the universe. The standard big-bang cosmology scenario has strong observational pieces of evidence and we believe that our universe started out from a hot and dense state. However, the cosmological problems still remain; why is the space flat, and why are the causality regions restricted to be small? These new problems are so-called flatness and horizon problem, respectively.

Even if the universe is an apparent feasible explanation of such problems, there is another puzzle for the standard cosmology, unwanted relics. Within the context of unified theories, e.g. string theory and supersymmetry, there are a variety of stable and heavy particles which should have been produced in the early universe. According to the viewpoint of particle physics, the breaking of symmetry also leads to the production of many unwanted relics such as cosmic string and topological defects. If these particles exist in the early stage of the universe, these massive relics could dominant in the universe, which contradicts with observation. The standard cosmology has no mechanism to avoid the universe of relics which are overproduced in the early universe.

In order to overcome new fundamental problems, it is required to consider an epoch of accelerated expansion in the early universe, i.e., inflation. An original inflation was proposed by Guth (3) and Sato (4) independently in 1981 (2), which is now called old inflation. The basic ideas of inflation are that the universe experienced accelerating expansion when the vacuum energy dominates component of the energy density of the universe. The definition of the inflation is given as

$$\ddot{a} > 0, \tag{2.1}$$

which a, dynamical variable, is the scale factor. In the case for example on Robertson-Walker metric, the dynamics of the expanding universe only appeared implicitly in the time dependence of the scale factor $a(t)$. The old inflation has a serious problem that the universe becomes inhomogeneous by the bubble collision due to the first order phase transition to the true vacuum after inflation ends. In 1982, Linde (5), and Albrecht and Steinhardt (6) proposed the revised version of old inflation (2), which is now termed as new inflation. New inflation corresponds to the slow roll inflation with the second order phase transition to true vacua.

The inflation scenario does not only provide an elegant way to solve the flatness problem, horizon problem and dilute unwanted relics but also generates density perturbation as an origin for large-scale structure in the universe. By freezing inflation which provides quantum fluctuations of the field during the inflation by accelerating expansion, the scales of fluctuations leave the Hubble radius. After inflation, the scales cross Hubble radius again. Therefore the perturbations originated inflation can be the origin of large-scale structure in the universe. Recent observation of the Planck detas (7, 8, 9) show the strong evidnces for inflation.

So far, we do not mention the concrete form of the scalar potentials, $V(\phi)$. Originating from the scenario proposed by Linde (5), and Albrecht and Steinhardt (6) in 1982, many kinds of inflationary models have been constructed in these thirty years. We now have varieties inflation models: Higgs, chaotic, power-law, hybrid, natural, F-term and D-term based on supersymmetry, and so on. In contrast, we are more interested in 'axion inflation' and mechanisms itself of axion potential based on the string theory, and some special classes of the models. Also, we would like to discuss phenomenologies after inflation, reheating temperature and dark matter abundance. For complimentary, information on the axion inflation in string theory framework and beyond our previous works, see our some recent articles (d, e) and the references therein.

In this chapter, we review the cosmic inflation briefly. First, we see a slow-roll inflation model and its dynamics using a scalar field. The perturbation theory and observables are shown in section 2.2 and section 2.3. After we show probing the inflation in section 2.4, then we will introduce the specific inflation models with axion in section 2.5, which relate to our main study in chapter 3.

2.2 Slow-roll inflation as scalar field dynamics

Here, we review aspects of inflation using the most simple potential driven slow-roll inflation model. In the last section, we did not specify the physical origin of the inflationary background. Inflationary expansion requires somewhat unconventional matter contents. The spatially flat Friedmann-Lemaitre-Robertson-Walker (FLRW) metric universe supported by a perfect fluid (which mean the homogeneous isotropic background metric) is given as [1]

$$ds^2 = -dt^2 + a^2(t)d\sigma^2, \qquad d\sigma^2 = \frac{dr^2}{1-Kr^2} + r^2(d\theta^2 + \sin^2\theta d\phi^2). \tag{2.2}$$

The dynamics of $a(t)$ is calculated from the Einstein equation ,which is given by

$$R_{\mu\nu} - \frac{1}{2}g_{\mu\nu} + \Lambda g_{\mu\nu} = 8\pi G T_{\mu\nu}, \tag{2.3}$$

[1]Since it becomes quite small during the inflation, throughout this thesis, we ignore the spatial curvature K of the universe. Actually the achievement of small curvature $|\Omega_k| < 0.005$ Ref.(8) (see also latest Planck data ref.(9)) is one of the motivation if the inflation scenario.

where Λ is the cosmological constant and $T_{\mu\nu} = \text{diag.}(-\rho,\ p,\ p,\ p)$ is the energy-momentum tensor for all components in the universe. From the assumption of homogeneity and isotropicity, $T\mu\nu$ has only diagonal components at zeroth order of perturbation. ρ is the energy density and p is corresponding to a pressure of the fluid. In a spatially flat FLRW universe supported by a perfect fluid, the components of (00), and (11) (components of (22) and (33) also derive the same equation (11)) of the Einstein equation eq.(2.3) lead to the so-called Freedman equations,

$$\left(\frac{\dot{a}}{a}\right)^2 = \frac{8\pi G}{3}\rho + \frac{\Lambda}{3}, \qquad 3H^2 + 2\dot{H} = -8\pi G p - \Lambda, \tag{2.4}$$

which we could obtain with a simple calculation. Further, combining the above equations, we find

$$\frac{\ddot{a}}{a} = -\frac{4\pi G}{3}(\rho + 3p) - \frac{\Lambda}{3}, \tag{2.5}$$

dependently. Here, the Hubble parameter H is defined as

$$H \equiv \frac{1}{a}\frac{da}{dt}. \tag{2.6}$$

If the accelerated expansion universe had been induced by the cosmological constant Λ, the above equations can be easily solved and we can obtain the solution as $a(t) \propto \exp\left(\sqrt{\Lambda/3}t\right)$.

The scalar field is the important ingredients in particle physics theories. Let us consider one of the easiest models of the slow-roll inflation in the Einstein frame; use a canonically normalized single scalar field, inflaton ϕ, minimally coupled to gravity (5, 6),

$$S = \int d^4x\sqrt{-g}\left[\frac{M_{pl}}{2}R - \frac{1}{2}g^{\mu\nu}\partial_\mu\phi\partial_\nu\phi - V(\phi)\right], \tag{2.7}$$

where g is the determinant of the metric, R is the Ricci scalar curvature, and $V(\phi)$ is the inflaton potential that we have allowed for an arbitrary potential form. See also AppendixA. The equation of motion, Klein-Gordon equation for the inflaton ϕ

$$\ddot{\phi} + 3H\dot{\phi} + V' = 0, \tag{2.8}$$

where the prime denotes derivative with respect to the inflaton ϕ, $V' \equiv \partial_\phi V$, and H is the Hubble paramter defined in eq.(2.6) before. If we assume that the inflaton was a constant, or equivalently inflaton potential $V(\phi)$ were constant, naively we could easily reproduce the exponential expansion which is derived as in the case of the cosmological constant. Therefore, we impose the following two conditions in the slow-roll approximation in order to derive the inflation,

$$\frac{1}{2}\dot{\phi}^2 \ll V(\phi), \qquad \ddot{\phi} \ll 3H\dot{\phi}. \tag{2.9}$$

The first condition means that the kinetic term is efficiently smaller than the potential height, and the second one that the acceleration term in the equation of motion can be neglected. We call this slow-roll condition. Inflation, therefore, occurs when these slow-roll conditions are satisfied.

In this model, The energy momentum tensor $T^{\mu\nu}$ is given by

$$T^{\mu\nu} = g^{\mu\alpha}g^{\nu\beta}\partial_\alpha\phi\partial_\beta\phi + g^{\mu\nu}\left(-\frac{1}{2}g^{\alpha\beta}\partial_\alpha\phi\partial_\beta\phi - V(\phi)\right). \tag{2.10}$$

Here, we assume the perfect fluid and homogeneousity and isotropicity on FLRW universe, it gives us $\partial_i\phi = 0$. Thus, neglecting spatial derivatives, the energy density and pressure density of inflaton are defined respectivity as

$$\rho = \frac{1}{2}\dot{\phi}^2 + V(\phi), \qquad p = \frac{1}{2}\dot{\phi}^2 - V(\phi). \tag{2.11}$$

Under the slow-roll conditions, the first terms are neglected: $\rho \simeq V$, $p \simeq -V$. Substituting eq.(2.11) for eq.(2.4), we get

$$3M_pH^2 = \frac{1}{2}\dot{\phi}^2 + V(\phi). \tag{2.12}$$

Here, we take $\Lambda = 0$. An almost flat potential of the inflaton acts as the role of cosmological constant depending on its height (also its tilt). Note that if we put $\dot{\phi} = 0$ in accordance with slow-roll conditions, we can realize the cosmological constant when $V = \Lambda/8\pi G$.

Again, during inflation, we assume that the inflaton ϕ and its potential $V(\phi)$ satisfy following reduced equations,

$$3H\dot{\phi} = -V', \qquad 3M_pH^2 = V(\phi). \tag{2.13}$$

We will see that these equations play an importnat role to discribe not only the classical dynamics of inflaton but also the quantum dynamics of it.

2.3 Cosmological perturbaion and obserbables

Although, the dependence of density perturbation derived from the inflation theory is universal, its absolute amplitude has a dependence on models. Here, we consider two-point function of curvature perturbation, which is given as

$$\langle \mathcal{R}(\mathbf{k})\mathcal{R}(\mathbf{k}')\rangle = \delta(\mathbf{k}+\mathbf{k}')P_{\mathcal{R}}(k) \tag{2.14}$$

where $P_{\mathcal{R}}(k)$ is power specrtrum of $\mathcal{R}(\mathbf{k})$. Naively, the amplitude of the scalar perturbation is directly connected to the temperature perturbation, CMB. When we sum up $P_{\mathcal{R}}(k)$ with the wevenumber k mode, the expectation value of $\langle \mathcal{R}^2\rangle = (1/2\pi^2)\int dk\, k^2 P_{\mathcal{R}}(k)$ is given as $\langle \mathcal{R}^2\rangle = \int d\ln k \mathcal{P}_{\mathcal{R}}(k)$. We often call $\mathcal{P}_{\mathcal{R}}(k)$ power spectrum, which is defined as

$$\mathcal{P}_{\mathcal{R}}(k) = \frac{k^3}{2\pi^2}P_{\mathcal{R}}(k). \tag{2.15}$$

Futher, we define the amplitude at the horizon crossing time A_s as

$$A_s \equiv \left.\mathcal{P}_{\mathcal{R}}(k)\right|_{k=aH}. \tag{2.16}$$

Since generally $\mathcal{P}_{\mathcal{R}}(k)$ has a dependence of the wavenumber k, we define the spectral index of curvature perturbation,

$$n_s - 1 \equiv \left.\frac{d\ln \mathcal{P}_{\mathcal{R}}(k)}{d\ln k}\right|_{k=aH}. \tag{2.17}$$

If the infation is derived from the cosmological constant, it is known that the demensionless power spectrum of CMB becomes Harrison-Zel'dovich spectrum (10, 11), which is scale invariant, $n_s = 1$.

The metric has the tensor modes [1] for perturbations which can be observed as the polarization of the gravitational waves. Simirally, as in the case of scalar perturbation, we define the amplitude of the power spectrum at the horizon crossing time as

$$\left.\mathcal{P}_h(k)\right|_{k=aH} = \left.\frac{2H^2}{\pi^2 M_{pl}^2}\right|_{k=aH}. \tag{2.18}$$

Combining the eqs.(2.15), (2.18), we obtain the tensor-to-scalar ratio r,

$$r \equiv \left.\frac{\mathcal{P}_{\mathcal{R}}(k)}{\mathcal{P}_h(k)}\right|_{k=aH}. \tag{2.19}$$

[1]There are also the vector modes. However, since it decays rapidly, we do not consider seriously.

If the inflation is derived by the cosmological constant, the tensor-to-scalar ratio becomes also zero.

If the inflation was occurred by inflaton depending on the slow-roll condition eq.(2.9), a gap of Harrison-Zel'dovich spectrum is decided by a degree of slow-roll. Here, we define the so-called slow-roll parameters

$$\epsilon \equiv \frac{M_p^2}{2}\left(\frac{V'}{V}\right)^2, \qquad \eta \equiv M_p^2 \frac{V''}{V}, \qquad \xi \equiv M_p^4 \frac{V'V'''}{V^2}, \tag{2.20}$$

which we can easily verify that the above slow-roll approximation is valid when

$$\epsilon \ll 1, \qquad |\eta| \ll 1, \tag{2.21}$$

whereas the inflation will end when ϵ and η grow of order unity.

In order to quantify whether inflationary expansion sufficiently keeps a long time, usually the e-fording number N is used,

$$N \equiv \ln \frac{a_f}{a_i} = \int_t^{t_{\rm end}} dtH \simeq \frac{1}{M_p}\int_{t_{\rm end}}^{\phi} \frac{V}{V'} d\phi \simeq \int_{t_{\rm end}}^{\phi} \frac{1}{\sqrt{2\epsilon}} d\phi, \tag{2.22}$$

where subscripts i and f denote the quantities at the beginning and the end of the inflation, respectively, and we used the slow-roll condition eq.(2.9). This value we observe today should be in the range $40 \leq N \leq 60$ typically, which is depending on the details of the models [1].

As we mentioned, quantum fluctuation of the inflation is approximately (but, not exactly) scale invariant. It is expanded by inflation and becomes the origin of density perturbations. The power spectra of scalar and tensor perturbation are parameterized as

$$\mathcal{P}_s(k) = A_s \left(\frac{k}{k^*}\right)^{n_s - 1 + \frac{1}{2}\frac{dn_s}{d\ln k}\ln\frac{k}{k_*} + \cdots}, \tag{2.23}$$

$$\mathcal{P}_t(k) = A_t \left(\frac{k}{k^*}\right)^{n_t + \frac{1}{2}\frac{dn_t}{d\ln k}\ln\frac{k}{k_*} + \cdots}, \tag{2.24}$$

where $A_{s,\,t}$ are the amplitude at the horizon crossing time, $\alpha_{s,\,t} \equiv dn_{s,\,t}/d\ln k$ are the runnings of the spectral index, and index * denotes the pivot scale implicitly [2]. Using

[1] Also, it depends on which reheating model we take.

[2] In the WMAP analysis the pivot scale was chosen to be $k^* = 0.002$ Mpc^{-1}, while for Planck $k^* = 0.05$ Mpc^{-1}(12).

the slow-roll paremeters, eq.(2.20), they are given by [1]

$$A_s = \frac{V}{24\pi^2 M_p^4 \epsilon} \quad , \qquad A_t = \frac{2V}{3\pi^2 M_p^4}, \tag{2.25}$$

$$n_s - 1 = -6\epsilon + 2\eta \quad , \qquad n_t = -2\epsilon, \tag{2.26}$$

$$\frac{dn_s}{\ln k} = 16\epsilon\eta - 24\epsilon^2 - \xi^2 \quad , \qquad \frac{dn_t}{\ln k} = 4\epsilon\eta - 8\epsilon^2. \tag{2.27}$$

Especially, the tensor-to-scalar ratio of the amplitude of the power spectrum is given as

$$r = 16\epsilon. \tag{2.28}$$

Finally, let us mention about the Lyth bound, which we quite use in our works (d, e). Substituting field equations, eq.(2.13) into $r = 16\epsilon$, we can relate the tensor-to-scalar ratio r to the evolution of the inflaton field,

$$r = 8\left(\frac{1}{M_p}\frac{d\phi}{dN}\right)^2, \qquad \text{where } \frac{dN}{dt} \equiv H. \tag{2.29}$$

Integrating eq.(2.29) from the time N^* when modes that are observable at the horizon crossing time, until the end of the inflation at (approximately) $N_{\rm end} \equiv 0$, we get

$$\frac{\Delta\phi}{M_p} = \int_0^{N^*} dN \sqrt{\frac{r(N)}{8}} \simeq \mathcal{O}(1) \times \left(\frac{r}{0.01}\right)^{1/2}. \tag{2.30}$$

Here, we combined with the observational constraints on $n_s - 1$ and r described next section, and we assume that $N_* \simeq 50$ – 60 in the second approximation. We strongly caution against viewing $\Delta\phi = M_p$ as an absolute dividing line. Like such a case of chaotic inflation, when $\Delta\phi > M_p$, we call them 'large-field inflation', while for 'small-field inflation' when $\Delta\phi < M_p$, or $r \gtrsim 0.01$. In particular, although gravity itself becomes strongly coupled around the scale M_p, parametrically controlled ultraviolet completion of gravity generally involves additional scales $\Lambda < M_p$. For examples, the string scale and the Kaluza-Klein scale are typically well below the Planck scale. Field excursion that is large compared to those scales connected to the super-Planckian scale, but we are not interested and do not treat in the thesis [2].

[1] Of cause, we can second order Taylor expand around the k^*, but the contributions are expected to be tiny. Thus, we will ignore them in the follwing calculations.

[2] If you want details, See Ref.(12).

2.4 Probing the inflations

The Planck collaboration has tested for primordial scalar and tensor fluctuations from standard assumptions for some initial conditions (7, 8, 9). These observations are in agreement with the predictions of inflation both qualitatively and quantitatively. In this section, we summarize their data briefly [1].

We have shown that the slow-roll inflation predicts a deviation from the scale invariance background, which has been detected at high significance by Planck collaborations. At scond order in the slow-roll expansion, the inflations predict a small correction to the spectrum,

$$\mathcal{P}_s(k) = A_s \left(\frac{k}{k^*}\right)^{n_s - 1 + \frac{1}{2}\frac{dn_s}{d\ln k}\left(\ln\frac{k}{k_*}\right)}. \tag{2.31}$$

According to the Plank 2015 data (8), the amplitude of the curvature perturbation and spectral index are proposed as

$$A_s = 2.198^{+0.076}_{-0.085} \times 10^{-9} \qquad (68\%\mathrm{CL},\ \mathrm{Planck},\ \mathrm{TT} + \mathrm{lowP}), \tag{2.32}$$

$$n_s = 0.9655 \pm 0.0062 \qquad (68\%\mathrm{CL},\ \mathrm{Planck},\ \mathrm{TT} + \mathrm{lowP}), \tag{2.33}$$

with the pivot scale $k_0 = 0.05\mathrm{Mpc}^{-1}$. The data is not yet precise enough to detect the expected running of the spectrum $\alpha_s \sim (n_s - 1)^2$.

Measuring α_s would test the consistency of the slow-roll expansion. However, since its running is second order in the slow-roll, we can naively expect it to be small. Actuarry, current bounds on α_s are small,

$$\alpha_s \equiv \frac{dn_s}{d\ln k} = -0.0084 \pm 0.0082 \qquad (68\%\mathrm{CL},\ \mathrm{Planck},\ \mathrm{TT} + \mathrm{lowP}), \tag{2.34}$$

which the central value for the running has decreased in magnitude with respect to the Planck 2013 (7). We hope that future galaxy surveys may allow such a measurement (13) [2]. Any detection of a larger level of running would be a challenge for slow-roll inflations.

[1] Recently, latest data from Planck is proposed, see Ref.(9). However, Since our studies do not consider its latest data, in this section we just summarize only their findings on Planck 2013 (7), and Planck 2015 (8).

[2] See also Ref.(14).

Also, tensor modes are constrained by the Planck analysis. They give an upper limit on the tensor-to-scalar ratio (8),

$$r < 0.103 \qquad (95\%\mathrm{CL},\ \mathrm{Planck},\ \mathrm{TT} + \mathrm{lowP}), \tag{2.35}$$

with the pivot scale $k_0 = 0.05\mathrm{Mpc}^{-1}$.

Most important observables in order to classify the slow-roll inflation models are the spectral index of curvature perturbation, n_s and tensor-to-scalar ratio, r. Planck collabrators have plotted 68 % and 95 % CL regions for n_s and r at $k_0 = 0.002\mathrm{Mpc}^{-1}$ compared to the theoretical predictions of selected inflationary models (8) (See Figure 2.1). We can find generally, slow-roll parameters, ϵ and η, are not zero, and as mentioned above, these parameters depend on the concrete potential form of inflation models. This fact suggests that we are able to select concrete inflationary models by observing the gap of the scale invariance. In the following subsection, we can find that realizing the slow-roll conditions eq.(2.9) in a theory of inflation is a non-trivial task.

2.5 Specific inflation models with axion

The slow-roll models favor a nearly-flat scalar potential as mentioned above. So far, there are found many kinds of slow-roll inflation models, in this thesis, we pursue mainly inflation driven by 'axion'. Following models introduced in this section are useful to embed various kinds of inflationary models, especially for our models introduced in the next chapter.

Note that here we will not provide a comprehensive slow-roll inflation model, but instead, we give a few brief examples of the most important classes of slow-roll models, and give these observational predictions.

2.5.1 Inflation with axions in string thery

In 1977, Pecci and Quinn have proposed the light scalar field, called an axion, as the solution to the strong CP problem (15). In QCD, there is a CP violated phase related with topological strucuture of QCD generically,

$$\mathcal{L} = L_{\mathrm{QCD}} + \frac{\theta}{32\pi^2} G_{\mu\nu}\tilde{G}^{\mu\nu}, \tag{2.36}$$

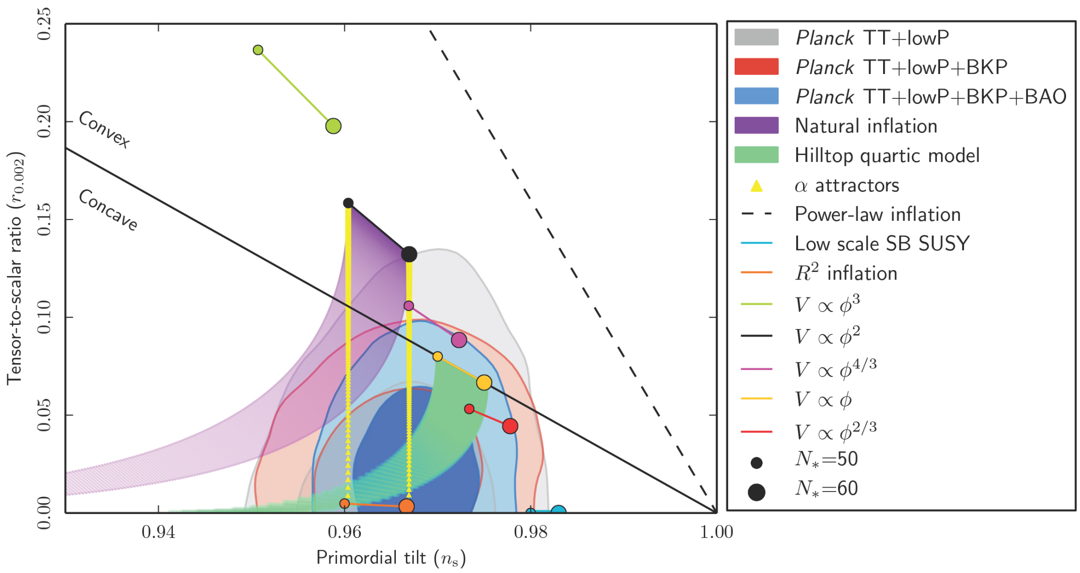

Figure 2.1: - Marginalized joint 68 % and 95 % CL regions for n_s and r at $k_0 = 0.002\text{Mpc}^{-1}$ from Planck compared to the theoretical predictions of selected inflationary models. Note that the marginalized joint 68 % and 95 % CL regions have been obtained by assuming $dn_s/d\ln k = 0$. See Ref.(8) in detail.

where G and $\tilde{G}$ are the field strength of gluons and its dual form, respectively. Depending on the effective action of meson and baryons, the no-observations of the electric dipole moment of neutron and Hg (16, 17) show that the experimental bound of θ should be smaller than 10^{-10}. Although the θ is an arbitrary parameter, this fact suggests that θ in eq.(2.36) has to be zero for some reason. This problem is the strong CP problem. As the solution to this problem, Pecci-Quinn introduced the global symmetry, called as PQ symmetry $U(1)_{\rm PQ}$. Under the PQ symmetry, axion, a as a Pseudo-Numbu-Goldstone boson which has shift symmetry of the form $a \to a + \text{const.}$ (while, other fields do not transform under the PQ symmetry), will appear through the following coupling,

$$\mathcal{L} = \frac{1}{2}\left(\partial_\mu a\right)^2 + \frac{1}{f_a}\left(\partial_\mu a\right) J^\mu + \frac{1}{32\pi^2}\frac{a}{f_a} G_{\mu\nu}\tilde{G}^{\mu\nu} + (U(1)_{\rm PQ} \text{ inv. terms}), \tag{2.37}$$

where f_a is the scale of PQ symmetry breaking, and J^μ is axial currents of quarks. When axion, a develops the vacuum expectation value, then, the θ can be absorbed into a by field redefinition, and CP on the QCD is preserved.

The 'QCD' axion is the original and most famous examples of axion. However, some authors, or especially we mention the word 'axion' for also string axion in this thesis. In contraction to QCD axion, the axions defined in the string theory are different and do not need to couple to QCD, generally, arise in the string compactifications from the integration of p-form gauge potentials over p-cycle of compact space (12). Typically, these axions are particularly attractive inflation candidates because they have shift symmetries to all orders in perturbation theories. As we can see easily, such shift symmetry is a key ingredient, and in the following, we discuss the rich phenomenology of the axion inflations.

2.5.2 Naturarl inflation and its application

In the following sections, we just give a summary of the main ingredients of the natural inflation model with axion and critically discuss their shortcomings.

In order to achieve the flat potential for successful inflation, shift symmetry $\phi \to \phi + \text{const.}$ can forbid the sort of corrections. We refer to a field possessing this symmetry as an 'axion'. The first model of axion inflation was proposed for a long time ago and named natural inflation (18) (see its review Ref.(19)), and so far several other models have been proposed.

At perturbative level, an axion has a flat potential, but this is broken down by nonperturbative effect to a discrete symmetry $\phi \to \phi + 2n\pi f$, leading to the following potential form [1],

$$V(\phi) = \Lambda^4 \left[1 - \cos\left(\frac{\phi}{2n\pi f}\right)\right] \tag{2.38}$$

where f is the axion decay constant, and Λ is some non-perturbatively generated scale, namely proportional to $e^{-1/g}$ for some gauge coupling g. For the successful inflation, or for enough e-folding number, this model is compatible with phenomenology only for $f \gg M_p$. However, Figure 2.1 shows how much natural inflation inconsistent with the Planck results [2]. Naively speaking, the simplest implementation of axion inflation (namely, natural inflation (18)) results that n_s is too small if the theoretical bound $f < M_p$ is respected. One scale that plays an important role in some axion models is the axion decay constant f as defined above which can be thought of as determining the strength of the least irrelevant shift symmetric coupling. The predictions for axion inflation are under theoretical control for naively $f < M_p$. The upper bound comes from the fact that we assume all known controlled string theory constructions are characterized. Since, the axion periodicity is lifted, allowing for superPlanckian displacements, we suppose that the UV corrections to the potential should still be constrained by some underlying symmetry. In general, it is hard to realize such an axion decay constant beyond the Planck scale in the 4D effective theory, since the scale of axion decay constant is connected to the volume of an internal manifold and the cut-off scale of higher-dimensional theories.

In order to avoid these conflicts, many ideas are proposed. One is to break the shift symmetry in a controlled way, either explicitly or spontaneously. Another one is to invoke some additional dynamics that arise from the coupling to other fields (in particular, gauge fields), and one possibility is to use non-local operators that arise in extra-dimensional contexts, and so on.

In addition to the above ideas, there is one simple solution that uses more than one axion, instead of breaking the shift symmetry. In such a case, a super-Planckian excursion of the inflaton can be achieved [3]. The first implementation of this idea

[1] Note that ϕ here and in the rest of this review, we assumed has always a canonical kinetic term.

[2] Also, it is disfavored by the Planck 2018 (9).

[3] We can think several approaches to realize the natural inflation with 'subPlnankian' axion decay constant to overcome such a problem. We consider such the approach in the next section.

was given in (20) where it was assumed that two axions are present and they interact through some non-perturbative potential (19)

$$V(\phi_1,\ \phi_2) = \Lambda_1^4\left[1 - \cos\left(\frac{\phi_1}{f_1} + \frac{\phi_2}{g_1}\right)\right] + \Lambda_2^4\left[1 - \cos\left(\frac{\phi_1}{f_2} + \frac{\phi_2}{g_2}\right)\right] \tag{2.39}$$

where $f_{1,\ 2}$ and $g_{1,\ 2}$ are different axion decay constants. For simplicity, if we assume $\Lambda_2^4 \gg \Lambda_1^4$, there appears a heavy and light linear combination of axions. After integrating out the heavy axion, the effective potential for light axion becomes

$$V(\phi_{\text{light}}) = \Lambda_2^4\left[1 - \cos\left(\frac{\phi_{\text{light}}}{f}\right)\right], \tag{2.40}$$

with

$$f = \sqrt{g_1^2 + g_2^2}\left(\frac{f_1 f_2}{g_1 g_2}\right)\left(\frac{f_2}{g_2} - \frac{f_1}{g_1}\right)^{-1}. \tag{2.41}$$

Allowing some tuning of g_1 and g_2, one can make f arbitrarily large, hence achieving an effective superPlanckian axion decay constant and the phenomenological predictions of natural inflation.

Let us focus on other popular axion inflation, the axion monodromy inflation, which is naively combined chaotic inflation [1] and natural inflation. In the string theory, the axion shift symmetry is broken by the D-brane, and then, the inflation potential has a structure of monodromy. The axion monodromy inflation is characterized by the additional following potential,

$$V(\phi) = \mu^{4-p}\phi^p, \tag{2.42}$$

where μ is some energy scale, and p is the model dependent fractional number (See Ref. (12) and references therein). Instead of the model of multi axion inflation, we do not need the superPlankian axion decay constant. The first realization of this idea involved D-branes moving around a Nilmanifold in type IIA string theory, produced a potential $\phi^{2/3}$ (19). A different construction using model-dependent axions in type IIB was proposed in (21) and further studied in Refs. (22, 23, 24).

[1] One of the simplest large field inflation models which we would not mention here.

3

Small field axion inflations

In this chapter, we consider and summarize the small field axion inflation scenarios, in which models were recently derived within the framework of type IIB superstring theory (1). This chapter is based on our works (d, e), and there are some new contents beyond Refs.(d, e) which is discussed in Ref.(f).

3.1 Introduction

In order to construct the inflationary favorable axion potential, the axion decay constant is required to be large enough to obtain the flat direction in the axion potential, in particular, the super-Plankian decay constant for the natural inflation (18). However, in the string theory, the decay constant of a closed-strung axion is typically around the string scale or grand unified scale 10^{16} GeV (25, 26, 27). When the axion decay constant is of order the Planck scale, the axion inflation generically predicts $\mathcal{O}(1)$ tensor-to-scalar ratio r as can be seen in the Lyth bound (28), which argues that the tensor-to-scalar ratio$r$ us closely related to the inflation field range, $\Delta\phi$, during the inflation. Under the assumption that the valuation of r is negligible over the period $\Delta\phi$, the approximate relation is obtained as (28)

$$\frac{\Delta\phi}{M_P} \simeq \mathcal{O}(1) \times \left(\frac{r}{0.01}\right)^{1/2}. \tag{3.1}$$

This relation indicates that if $\Delta\phi < M_p$, $r \leq 0.01$ are obtained, and we call this class of inflation model the small field inflation throughout this paper. Although the large field axion inflations ($r \geq 0.01$) consistent with the recent Plank data (7, 8) [1], the weak gravity conjecture (29) suggests that the higher-order instanton effects give a sizable effect for the axion potential with a super-Planckian axion decay constant, and these would generally violate the slow-roll axion inflation.

As mentioned above, some axion inflation models in the string theory discussed in the literature typically involve the super-Plankian inflation amplitudes and potentially large tenser-to-scalar ratio r is featured for the Lyth bound. On the contrary, in our work, we study the small-field axion inflation where the field excursion of the axion inflation is small compared with Plank scale M_p (see, e.g. Refs. (30, 31, 31, 32)). The tenser-to-scalar ratio can be consequently small and, in our string axion models with a sub-Plankian axion decay constant, the reheating temperature can be as low as GeV, on the contrary, a notable requirement for the successful natural inflation model is super-Plankian axion decay constant, i.e. $f \sim 5M_p$ [2]. For the illustrative purpose, we study in details the concrete axion inflation model which was recently derived within the framework of type IIB superstring theory (1). It is the extension of the work (33) to the compactification with generic fluxes, and the inflation potential consists of the mixture of polynomial function and sinusoidal function of the axion (see also Refs. (34, 35)).

Related to the work (d), we conjectured that, in a certain class of small-field inflation derived from type IIB superstring theory (1) [3], the tensor-to-scalar ratio r correlates with the axion decay constant f as follows (d),

$$r \sim 10^{-6} f^{2q}, \tag{3.2}$$

where the fractional number q depends on the model. In the example of refs.(1, d), we obtain $q = 2$. This behavior originates from sinusoidal functions in the axion inflation potential. The above relation could also predict the magnitude of the inflation potential and the inflaton mass by f. In general, certain theory leads to the axion potential with one or more sinusoidal terms induced by several nonperturbative terms. Thus, it is important to extend the previous analysis to other axion inflation scenarios. In our work, we further study such dependence of the axion decay constant for not only cosmological observables but also the reheating temperature and dark matter

[1] The Planck 2018 results have been reported. See Ref.(9).

[2] Here and hereafter, M_p denotes the reduced Plank scale $M_p = 2.4 \times 10^{18}$ GeV.

[3] The model in Ref.(1) can lead to both small-field and large-field inflations.

abundance for the general class of small-field axion inflations, which are the mixture of polynomial and sinusoidal functions suggested in the axion monodromy inflation (36, 37, 38) and general form of sinusoidal functions suggested in the natural and multi-natural inflations (18, 30, 39, 40) [1].

3.2 Small field axion inflation with sub-Planckian decay constant

We, in this section 3.2, present the axion inflation model based on type IIB superstring theory (1). In particular, we consider the inflation model with a sub-Planckian axion decay constant which can lead to a small tensor-to-scalar ratio r. We give the quantitative discussions for our axion inflation scenarios in terms of the slow-roll parameters.

The rest of this section is organized as follows. In section 3.2.2, we study the inflation dynamics for our axion inflation scenarios with a sub-Planckian decay constant and demonstrate that the axion inflation energy scale can be quite low compared to the conventional axion inflation scenarios with a super-Plankin axion decay constant. In section 3.2.3, we study the reheating temperature in our model and discuss the thermal history after the inflation ends.

3.2.1 Axion inflation potential in type IIB string theory

Recently, within the framework of type IIB superstring theory, the following form of the axion potential was derived (1),

$$V(\phi) = \Lambda_1 \phi^2 + \Lambda_2 \phi \sin\left(\frac{\phi}{f}\right) + \Lambda_3 \left(1 - \cos\left(\frac{\phi}{f}\right)\right), \tag{3.3}$$

where $\Lambda_{1,2,3}$ are constant, and f is the axion decay constant. We consider the flux compactification of type IIB superstring theory. We can, in general, stabilize all of the complex structure moduli and the dilaton by choosing proper 3-form fluxes (42, 43). We here choose the 3-form fluxes such that only one of the complex structure moduli, Φ, does not appear in the tree-level superpotential, while the other complex structure

[1] The scalar potential including modular functions in superstring theory can effectively lead to such a multi-natural inflation (41)

moduli, as well as the dilaton, are stabilized by the 3-form fluxes [1]. However, the geometrical corrections induce the superpotential,

$$W = w_0 + (c + c'\Phi)e^{-\Phi/f}, \tag{3.4}$$

where ω_0, c, c' are constants determined by fluxes and vacuum expectation values of other moduli. The Kähler potential of Φ also receives the correction,

$$\Delta K = \big(k + k'\mathrm{Re}(\Phi)\big)\cos(\mathrm{Im}(\Phi)/f)e^{-\mathrm{Re}(\Phi)/f}, \tag{3.5}$$

in addition to the tree-level Kähler potential $K = -\ln i\int_{\mathcal{M}}\Omega\wedge\bar{\Omega}$ with the holomorphic three-form Ω of the CY manifold $\mathcal{M}$, where k and k' are constants determined by fluxes and other moduli vacuum expectation values. We assume that the real part of Φ, $\mathrm{Re}(\Phi)$, is heavy, and integrating out $\mathrm{Re}(\Phi)$ leads to the above scalar potential eq.(3.3) for the axion $\phi = \mathrm{Im}(\Phi)$. Such a situation is realized by the scenario where Φ is stabilized at the minimum satisfying $\partial_\Phi K = 0$ where K is the ϕ-independent Kähler potential given at the tree-level [2].

We further assume that the Kähler moduli T^i $(i = 1, 2, \cdots, h^{1,1})$ with the hodge number $h^{1,1}$ are stabilized at the minimum realized by the LARGE Volume Scenario (LVS) (50) where the Kähler potential is described by $K = -2\ln(\mathcal{V} + \Delta\mathcal{V})$ with the volume of "Swiss-Cheese" CY manifold $\mathcal{V}$ and loop-correction $\Delta\mathcal{V}$, whereas the superpotential is the sum of contributions from the flux-induced superpotential $W_{\rm flux}$ and non-perturbatively generated superpotential, $W_{\rm non} \simeq \sum_i A_i e^{-a_i T^i}$ with the constants A_i and a_i. Although the energy density of scalar potential changes during and after the inflation, the superpotential can be regarded as the constant in the inflationary era, i.e., $W \simeq w_0$ where w_0 involves both $W_{\rm flux}$ and $W_{\rm non}$. This is because the first term in the superpotential eq.(3.4) can be taken parametrically larger than the second term in eq.(3.4) which induces the inflaton potential. It is then possible that the stabilization of Kähler moduli is achieved at the scale above the inflation scale through the LVS mechanism, since the mass scale of lightest Kähler modulus (volume modulus) $\frac{w_0}{\mathcal{V}^{3/2}}$ can be larger than the Hubble scale for the mild volume of CY manifold $\mathcal{V} \sim 10^2$ in string

[1] We also assume that all of the Kähler moduli are stabilized by non-perturbative effects (44) and a proper uplifting scenario is available such as Refs.(45, 46, 47, 48).

[2] Recently, the authors of Ref.(49) pointed out that the light complex structure moduli appear in the explicit Calabi-Yau (CY) manifolds.

units. As discussed in Refs.(1, 33), the back reaction from the Kähler moduli are also suppressed, since the energy scale of scalar potential determined by the LVS is larger than that of inflaton potential.

Note that the superpotential, as well as the Kähler potential, includes the linear term, exponential term, and their products. This is the origin of the mixture between polynomial functions and sinusoidal functions in the scalar potential. See, for details, Ref.(1). The natural scale for the decay constant would be of order $f \sim 1/2\pi$, even though one can expect a wide range depending on the vacuum expectation values of the real parts of moduli corresponding to the sizes of cycles. For concreteness, in the following discussions, we mainly consider the range

$$0.01 \leq f \leq 1.0. \tag{3.6}$$

Note that we focus on a small axion decay constant which does not exceed the Planck scale, while a large axion decay constant has usually been explored in the previous literature on the axion inflation scenarios (1). The magnitudes and ratios of $\Lambda_{1,2,3}$ can vary depending on the flux magnitudes and vacuum expectation values of moduli (1), and we here treat $\Lambda_{1,2,3}$ as free parameters to make our discussions as general as possible.

This potential consists of a mixture of polynomial functions and sinusoidal functions. It reduces to the simple ϕ^2 chaotic inflation when $\Lambda_2 = \Lambda_3 = 0$, which is in a tight tension with the observations due to a large r (7, 8). For the non-vanishing Λ_2 and Λ_3, the potential consists of many bumps and plateaus, as shown in Figure 3.1 and Figure 3.2, as well as several local minima. The form of the potential eq.(3.3) heavily depends on the oscillation parameter f which determines the width size of the flat plateau region. A small f leads to a high-frequency potential with a small interval between each plateau, and our main focus is on a smaller value of f making each flat plateau close to each other. The potential is shown in Figure 3.1 and Figure 3.2 for $f = 0.1$ and $f = 0.01$, where, for concreteness, we chose $\Lambda_2/\Lambda_3 = 1, \Lambda_1/\Lambda_3 = 7.3$ for $f = 0.1$ and $\Lambda_2/\Lambda_3 = 1, \Lambda_1/\Lambda_3 = 97$ for $f = 0.01$. The inflation can occur on a flat plateau and we, in the following, study the inflation dynamics for our axion inflation scenarios with a sub-Planckian inflaton field excursion.

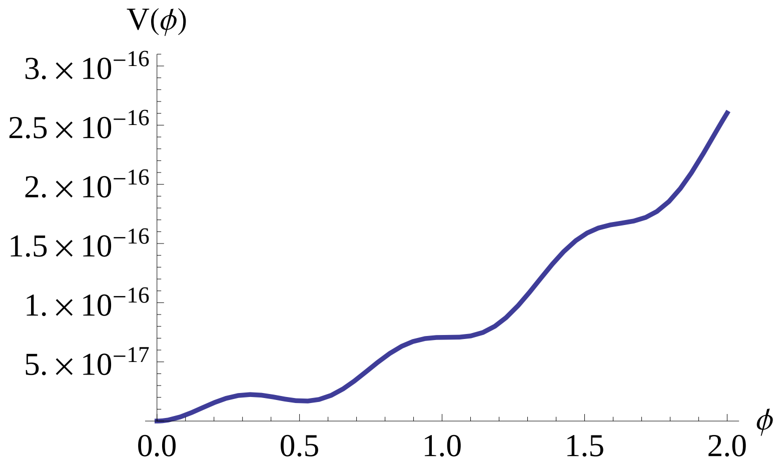

Figure 3.1: - The axion inflation potential with a sub-Planck axion decay constant $f = 0.1$ for the small field axion inflation (the field excursion $\Delta\phi < 1$ during the inflation).

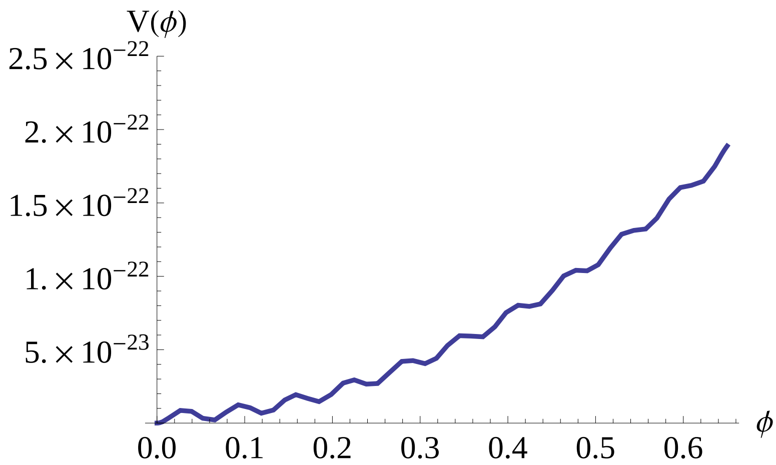

Figure 3.2: - The axion inflation potential with a sub-Planck axion decay constant $f = 0.01$ for the small field axion inflation.

3.2.2 Small field axion inflation

The inflation can occur when an axion inflaton field slowly rolls over a flat plateau region in our axion potential. We shall demonstrate that the small field inflation can be realized for a small axion decay constant f when enough number of e-folds are induced for a sufficiently flat potential [1]. The first derivative of the potential is written by

$$V_\phi = \left(2\Lambda_1 + \frac{\Lambda_2}{f}\cos\left(\frac{\phi}{f}\right)\right)\phi + \left(\Lambda_2 + \frac{\Lambda_3}{f}\right)\sin\left(\frac{\phi}{f}\right). \tag{3.7}$$

For our potential to become flat enough for a sufficient number of e-folds, we require $(V_\phi)^2 \ll V^2$, which is satisfied for $\phi \sim 1$ and $f \ll 1$ (as well as $\cos(\phi/f)$, $\sin(\phi/f) \sim \mathcal{O}(1)$) when

$$\Lambda_1 f \sim \Lambda_2 \sim \Lambda_3, \tag{3.8}$$

with proper signs of $\cos(\phi/f)$ and $\sin(\phi/f)$. Another condition $V_{\phi\phi} \ll V$ can also be satisfied in the same parameter region. The consequent small inflaton field variation results in a small tensor-to-scalar ratio r as estimated in the following.

For the inflaton variation $\Delta\phi$ around $|V_\phi| \approx 0$ and $|V_{\phi\phi}| \approx 0$, the second derivative can be estimated as

$$V_{\phi\phi} \sim V_{\phi\phi\phi}\Delta\phi \sim \left(-\frac{\Lambda_3}{f^3}\sin\left(\frac{\phi}{f}\right) - \frac{\Lambda_2}{f^3}\cos\left(\frac{\phi}{f}\right)\right)\Delta\phi. \tag{3.9}$$

Note, for a small f, the terms with f^{-3} can be dominant in the third derivative $V_{\phi\phi\phi}$. For $V \sim \Lambda_1\phi^2 \sim \Lambda_3/f$, with the relation (3.8) and $\phi = \mathcal{O}(1)$, we estimate

$$\eta \sim \frac{\Delta\phi}{f^2}. \tag{3.10}$$

Demanding $\eta \ll 1$ results in $\Delta\phi \ll f^2$, which leads to $r \ll 0.01 \times f^4$ from Eq. (3.1). Explicitly, we can write

$$r \sim 10^{-6} \times f^4 \times \left(\frac{\eta}{0.01}\right)^2. \tag{3.11}$$

In addition, we can estimate $\eta \sim 10^{-2}$ because $r = 16\epsilon \ll 0.01$ and $2\eta \approx n_s - 1 \approx -0.03$. With this approximation, we estimate $r \sim 10^{-6} \times f^4$ and tensor-to-scalar ratio r can be suppressed greatly as f becomes small.

[1] For small f and ϕ ($f \lesssim 1$ and $\phi \sim 1$ which we assume in the following discussions unless stated otherwise), we require, for our potential to become flat for enough number of e-folds.

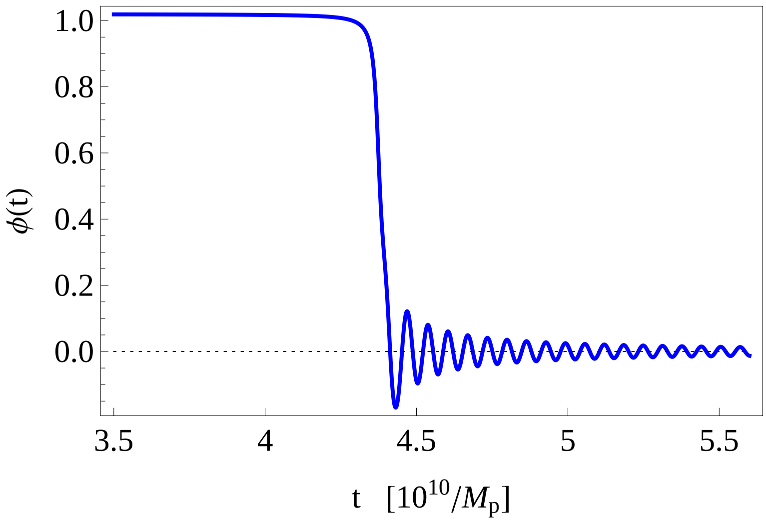

Figure 3.3: - $\phi(0) = 1.0$ for $f = 0.1$, $\Lambda_1/\Lambda_3 = 7.3$, $\Lambda_2/\Lambda_3 = 1$.

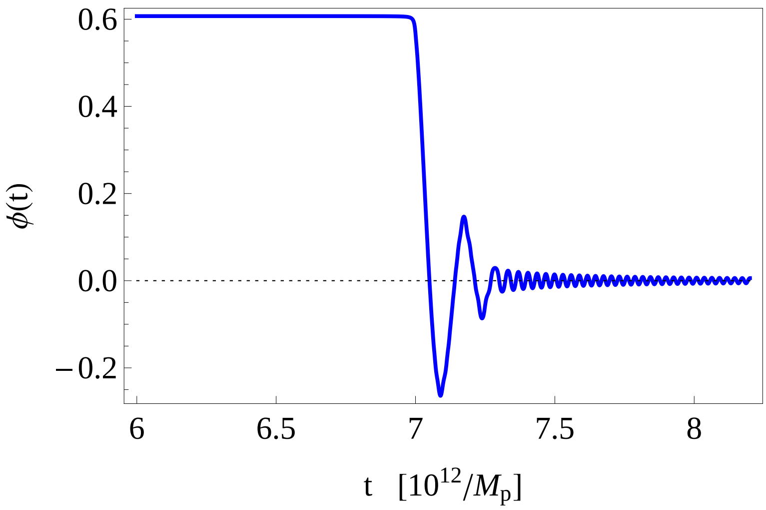

Figure 3.4: - $\phi(0) = 0.6$ for $f = 0.01$, $\Lambda_1/\Lambda_3 = 97$, $\Lambda_2/\Lambda_3 = 1$.

Figure 3.3, 3.4 shows examples of inflaton trajectories. For the illustrative purpose, the initial values of the inflaton field are chosen such that a big enough e-folding number is realized at the second and tenth plateaus, respectively, for $f = 0.1$ and 0.01. The inflaton rolls down through lower plateaus to finally reach the global minimum $\phi = 0$. The e-folding numbers, which are obtained from the other plateaus, are negligible for these examples as we can see in inflaton trajectories, Fig. 3.3, 3.4. We concentrate on such parameter regions for concreteness where the total number of e-folds originates from a single plateau in the following discussions. We then aim to illustrate the characteristic features of our small field axion inflation scenarios which can be applied for a wider range of the parameters.

For $f = 0.1$, Fig. 3.5 shows how the inflaton field evolves as a function of the number of e-folds (counted from the end of inflation), and Fig. 3.6 shows the corresponding tensor-to-scalar ratio r and n_s. In Fig. 3.5,3.6, we consider the scenario where a sufficient number of e-folds are induced while the inflaton axion rolls over the second lowest plateau in the potential shown in Fig. 3.1. As reference values indicate the energy scale of inflation, the Hubble parameter and the potential energy at $N = 55$ in this example are $H_{\rm inf}(N = 55) = 2.2 \times 10^{-9}$ and $V_{\rm inf}^{1/4}(N = 55) = 6.1 \times 10^{-5}$. The inflation on another plateau also can lead to a similar result, so that it can induce enough number of e-folds from a single plateau with a small tensor-to-scalar ratio.

The same story applies for a smaller $f = 0.01$ as shown in Fig. 3.7, 3.8 (the scenario where a sufficient number of e-folds are induced on the tenth lowest plateau in Fig. 3.2) corresponding to $V_{\rm inf}^{1/4}(N = 55) = 4.0 \times 10^{-6}$ and $H_{\rm inf}(N = 55) = 9.0 \times 10^{-12}$.

For completeness, we also show the potential for $f = 1.0$ in Fig.3.9 and the evolution of ϕ along with (n_s, r) in Fig.3.10, 3.11 which corresponds to $V_{\rm inf}^{1/4}(N = 55) = 9.0 \times 10^{-4}$ and $H_{\rm inf}(N = 55) = 4.7 \times 10^{-7}$. The inflaton field excursion during the inflation is sub-Planckian $\Delta\phi < 1$ (we hence call it the small field inflation), even though the amplitude itself can be larger than the Planck scale.

The above numerical analysis demonstrates that our axion potential with a sub-Planckian axion decay constant as well as $f = 1$ can lead to the inflation with a sub-Planckian inflaton field excursion. One notable feature compared with the conventional axion inflation scenarios with the Planckian f and inflaton amplitude is a small tensor to scalar ratio $r \ll 1$. As discussed by Eq. (3.11), r is suppressed as the fourth power of f. A rough estimation Eq. (3.11) fits with our numerical results by taking $\eta \sim 10^{-2}$ as

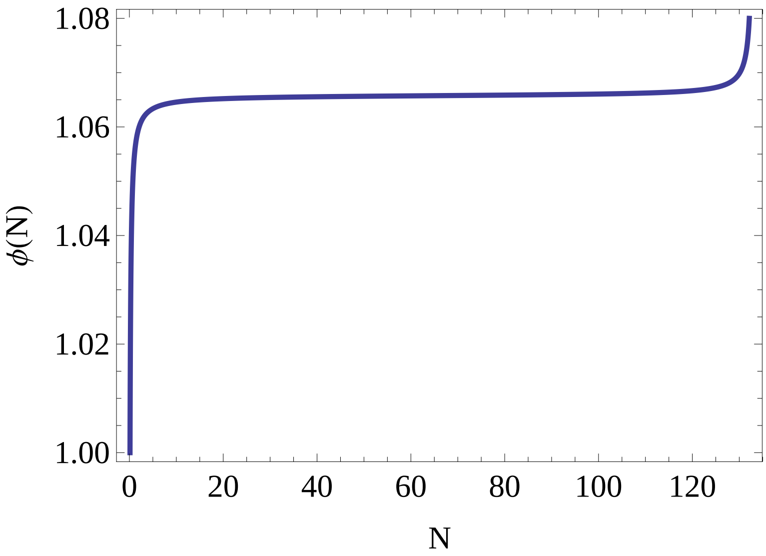

Figure 3.5: - The inflaton amplitude as a function of the number of e-folds $\phi(N)$ for $f = 0.1$, $\Lambda_1/\Lambda_3 = 4.9$ and $\Lambda_2/\Lambda_3 = 0.25$ (corresponding to $V_{\rm inf}^{1/4}(N = 55) = 6.1 \times 10^{-5}$).

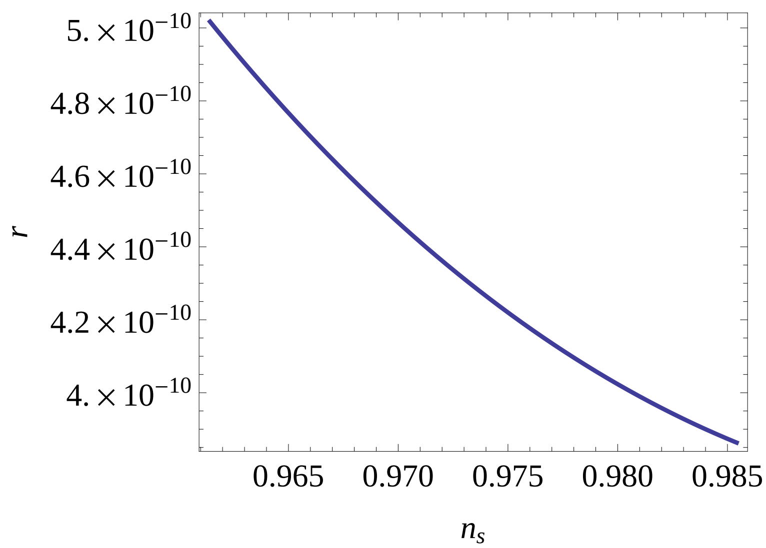

Figure 3.6: - The inflaton amplitude as a function of the number of e-folds (n_s, r) for $N = [50, 60]$ for $f = 0.1$, $\Lambda_1/\Lambda_3 = 4.9$ and $\Lambda_2/\Lambda_3 = 0.25$ (corresponding to $V_{\rm inf}^{1/4}(N = 55) = 6.1 \times 10^{-5}$).

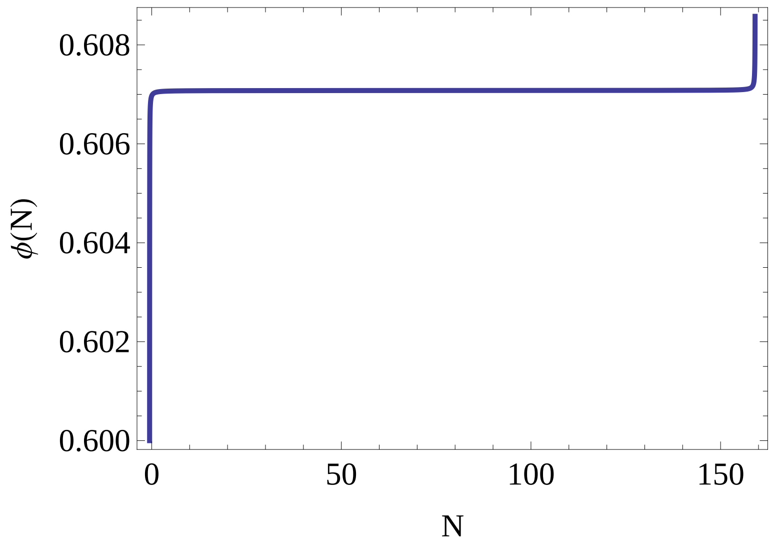

Figure 3.7: - The inflaton amplitude as a function of the number of e-folds $\phi(N)$ for $f = 0.01$, $\Lambda_1/\Lambda_3 = 97$ and $\Lambda_2/\Lambda_3 = 1$ (corresponding to $V_{\rm inf}^{1/4}(N = 55) = 4.0 \times 10^{-6}$).

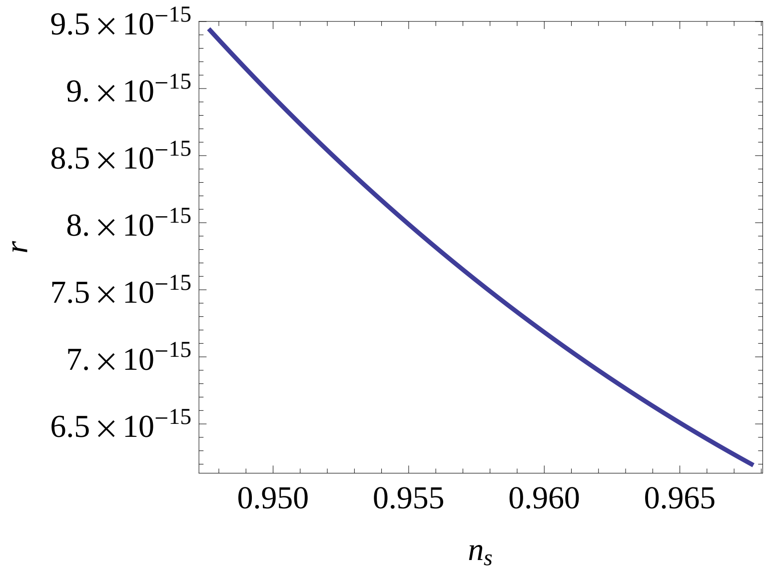

Figure 3.8: - The inflaton amplitude as a function of the number of e-folds (n_s, r) for $N = [50, 60]$ for $f = 0.01$, $\Lambda_1/\Lambda_3 = 97$ and $\Lambda_2/\Lambda_3 = 1$ (corresponding to $V_{\rm inf}^{1/4}(N = 55) = 4.0 \times 10^{-6}$).

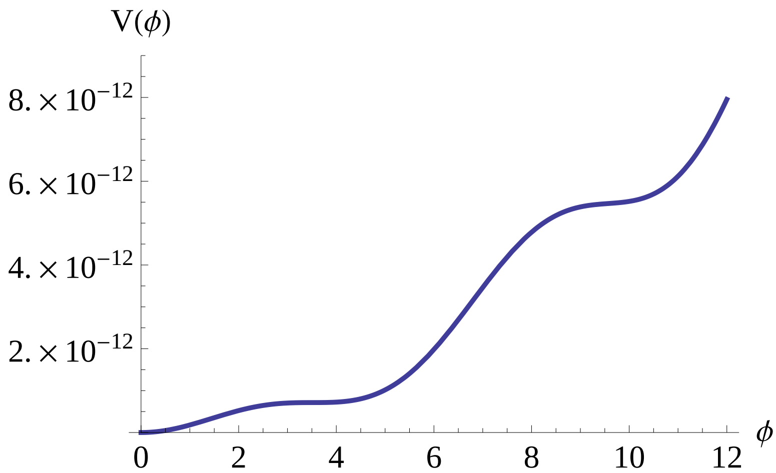

Figure 3.9: - The axion inflation potential with $f = 1.0$ for the small field inflation (the field excursion $\Delta\phi < 1$ during the inflation).

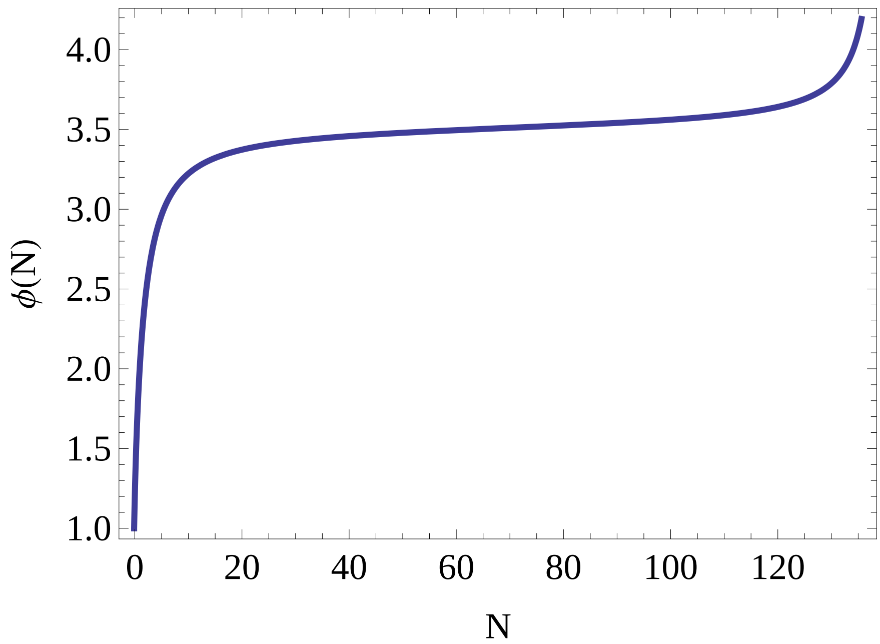

Figure 3.10: - The inflaton amplitude as a function of the number of e-folds $\phi(N)$ for $f = 1.0$, $\Lambda_1/\Lambda_3 = 1.0$ and $\Lambda_2/\Lambda_3 = 1.9$ (corresponding to $V_{\rm inf}^{1/4}(N = 55) = 9.0 \times 10^{-4}$).

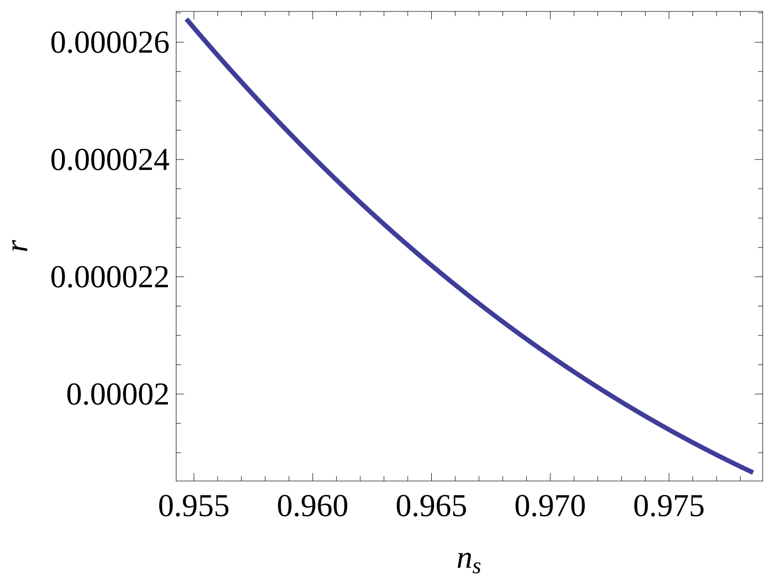

Figure 3.11: - The inflaton amplitude as a function of $(n_s,\, r)$ for $N = [50, 60]$ for $f = 1.0$, $\Lambda_1/\Lambda_3 = 1.0$ and $\Lambda_2/\Lambda_3 = 1.9$ (corresponding to $V_{\rm inf}^{1/4}(N = 55) = 9.0 \times 10^{-4}$).

mentioned above, and we estimate the typical parameter values of our axion inflation scenarios as

$$r \sim 10^{-6} \times f^4, \qquad V_{\rm inf}^{1/4} \sim 5 \times 10^{-4} \times f, \qquad H_{\rm inf} \sim 10^{-7} \times f^2, \qquad \Lambda_3 \sim 6 \times 10^{-14} \times f^5, \tag{3.12}$$

because of $V_{\rm inf} \sim \Lambda_3/f$. The energy scale of our axion inflation scenarios can be quite low compared with the conventional axion inflation with the Planckian decay constant, and we expect the consequent low reheating temperature as discussed in the next section.

Before concluding this section focusing a small f, let us briefly discuss the scenarios for a larger $f \gtrsim 1$ commonly discussed in the literature for comparison. For a Planckian value of the axion decay constant, the large field inflation can be induced. The typical potentials are shown in Fig.3.12, 3.13 for $f = 1$ and $f = 3$ respectively. Compared with our axion potential with a sub-Planckian f, the tensor-to-scalar ratio r, along with the other parameters, can become large. For instance, with $f = 3.0$ for concreteness, the first term $\Lambda_1 \phi^2$ can become dominant in both the potential (3.3) and the first derivative V_ϕ when $\phi \gg 1$ and $\Lambda_1 \sim \Lambda_2 \sim \Lambda_3$. The tensor-to-scalar-ratio ratio r can be estimated

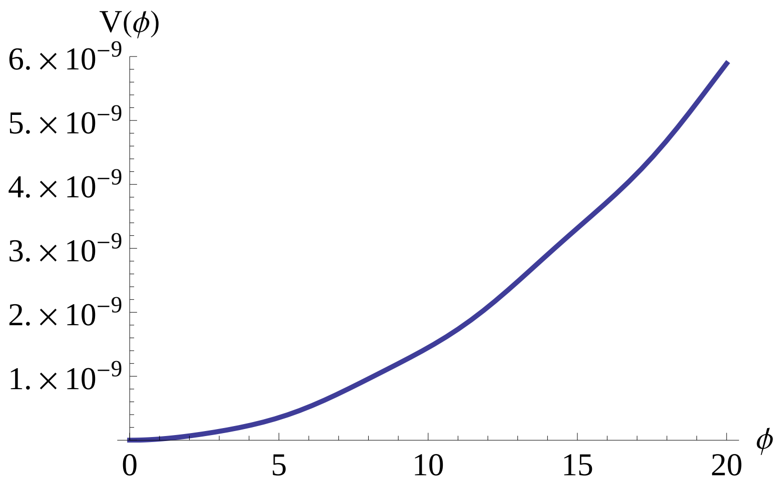

Figure 3.12: - The axion inflation potential with a large axion decay constant for the large field inflation for $f = 1.0$

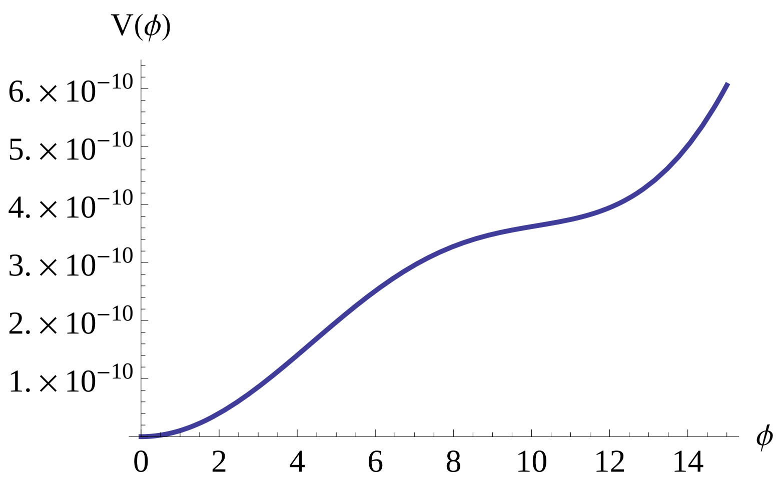

Figure 3.13: - The axion inflation potential with a large axion decay constant for the large field inflation for $f = 3.0$

as $r \sim 10/\phi^2$, e.g. $r \sim 0.1$ for $\phi \sim 10$. The representative examples for a Planckian f are given, for illustration, in Fig.3.12, 3.13 and Table 3.1 showing the observables including the inflaton potential energy scale $V_{\rm inf}$ at the horizon exit $N = 55$.

	N	n_s	r	$V_{\rm inf}^{1/4}$	Λ_1/Λ_3	Λ_2/Λ_3
$f = 1$	55	0.95	0.13	8.0×10^{-3}	5.0	1.0
$f = 3$	55	0.97	0.011	4.3×10^{-3}	1.0	4.9

Table 3.1: The typical parameters for $f = 1, 3$ for the large field inflation.

3.2.3 Phenomenology after inflation

We now discuss the phenomenology after the inflation including the reheating temperature and the dark matter abundance in our small field axion scenarios. The inflaton field is the axionic part of the complex structure modulus, and, in type IIB superstring theory, the complex structure moduli appear in one-loop corrections on gauge kinetic functions (51, 52). The modulus thus couples with the gauge bosons through one-loop effects,

$$-\frac{1}{4g_a^2}F^a_{\mu\nu}F^{a\mu\nu} - \frac{1}{4}\frac{\Delta(\Phi)}{16\pi^2}F^a_{\mu\nu}F^{a\mu\nu}, \tag{3.13}$$

where $a = 1, 2, 3$ correspond to the gauge groups of the standard model, $U(1)_Y$, $SU(2)$ and $SU(3)$, respectively, and $\Delta(\Phi)$ is a function of Φ. Through these couplings, the inflation decays into the gauge bosons $g^{(a)}$, and its decay width is estimated as (1)

$$\begin{aligned}
\Gamma_\phi &= \sum_{a=1}^{3}\Gamma(\phi \to g^{(a)} + g^{(a)}) \\
&= \sum_{a=1}^{3}\frac{N_G^a}{128\pi}\left(\frac{\partial_\phi(\Delta(\Phi))g_a^2}{16\pi^2 d}\right)^2\frac{m_\phi^3}{M_p^2} \\
&\simeq 5.8 \times 10^{-5}c^2\left(\frac{m_\phi}{10^{13}\mathrm{GeV}}\right)^3 \mathrm{GeV},
\end{aligned} \tag{3.14}$$

where $\sum_{a=1}^{3} N_G^a = 12$, $d = \mathcal{O}(\sqrt{K_{\Phi\bar{\Phi}}}) = \mathcal{O}(1)$, $g_a^2 \simeq 0.53$, and for concreteness, we assumed the form $\Delta(\Phi) = c\,\Phi$. When such a decay into the gauge bosons is the dominant decay channel, the reheating temperature can be estimated as

$$T_{\rm reh} = \left(\frac{\pi^2 g_*}{90}\right)^{-1/4}\sqrt{\Gamma_\phi M_{\rm p}} \simeq 6.4 \times 10^6 c\left(\frac{m_\phi}{10^{13}\ \mathrm{GeV}}\right)^{3/2} \mathrm{GeV}, \tag{3.15}$$

where the effective degrees of freedom $g_* = 106.75$. Table 3.2 lists the reheating temperature along with the inflaton mass for the concrete examples of $f = 3.0,\ 1.0,\ 0.1,\ 0.01$ illustrated in the last section. A smaller f corresponds to a smaller inflation energy scale, which hence leads to a smaller $T_{\rm reh}$. The order of magnitude for the inflaton mass can be estimated as follows. For $f \ll 1$ with the relation (3.8), the dominant term of second derivatives, $V_{\phi\phi}$, at $\phi = 0$ is evaluated by $V_{\phi\phi} \sim \Lambda_3/f^2$, i.e. $m_\phi^2 \sim \Lambda_3/f^2$. Then, using Eq. (3.12), we can estimate the inflaton mass by

$$m_\phi^2 \sim 5 \times 10^{-14} \times f^3. \tag{3.16}$$

f	m_ϕ^2	$T_{\rm reh}$
3.0	1.0×10^{-11}	4.3 PeV
1.0	1.9×10^{-13}	220 TeV
0.1	1.2×10^{-16}	860 GeV
0.01	3.4×10^{-20}	1.9 GeV

Table 3.2: Typical reheating temperature for the cases $f = 3.0,\ 1.0,\ 0.1,\ 0.01$ with $c = 1$.

The complex structure moduli may appear in Yukawa couplings and higher dimensional couplings of matter fields within the framework of type IIB superstring theory (see for concrete computations, e.g. Ref.(53, 54)). The inflaton hence can also decay into the matter fields, and, when such a decay channel dominates, the reheating temperature can be estimated as (1)

$$T_{\rm reh} \ \simeq\ 8.8 \times 10^7 (\partial_\Phi Y_{ijk}) \left(\frac{m_\phi}{10^{13}{\rm GeV}}\right)^{3/2} {\rm GeV}, \tag{3.17}$$

where $\partial_\Phi Y_{ijk}$ denotes the first derivative of moduli-dependent Yukawa couplings Y_{ijk}. $T_{\rm reh}$ estimated assuming the dominant decay via the Yukawa couplings is hence comparable or smaller than that estimated assuming the dominant decay into the gauge bosons.

Our models hence lead to the low reheating temperature (as low as GeV). Such a low reheating temperature has important effects on the thermal history following the inflation. Dark matter relic abundance, for instance, could be affected significantly. For example, if the reheating temperature is smaller than the freeze-out temperature of dark matter, $T_{\rm reh} < T_{\rm f}$, the dark matter yield can be estimated by considering the non-thermal abundance from the inflaton decay

$$\frac{n_{\rm dm}}{s} \simeq \frac{n_{\rm inf}}{s}{\rm Br}_{\rm dm} \simeq \frac{\rho}{m_\phi s} \simeq \frac{3T_{\rm reh}}{4m_\phi}{\rm Br}_{\rm dm} \simeq 1.5\times10^{-12}\left(\frac{c}{10}\right)\left(\frac{m_\phi}{10^8\ {\rm GeV}}\right)^{1/2}\left(\frac{{\rm Br}_{\rm dm}}{10^{-4}}\right), \tag{3.18}$$

where $n_{\rm dm}(n_{\rm inf})$ is the number density of dark matter (inflaton), s is the entropy density of the Universe, and ${\rm Br}_{\rm dm}$ is the inflaton decay branching ratio to dark matter. The current dark matter abundance reads

$$\Omega_{\rm dm}h^2 \simeq m_{\rm dm}\frac{n_{\rm dm}}{s}\frac{s_0}{\rho_{\rm cr}} \simeq 0.04\left(\frac{c}{10}\right)\left(\frac{m_{\rm dm}}{100\,{\rm GeV}}\right)\left(\frac{m_\phi}{10^8\ {\rm GeV}}\right)^{1/2}\left(\frac{{\rm Br}_{\rm dm}}{10^{-4}}\right), \tag{3.19}$$

where h denotes the dimensionless Hubble parameter and the ratio of critical density to the current entropy densities of the Universe is given by $\rho_{\rm cr}/s_0 \simeq 3.6h^2\times10^{-9}$.

Our low energy scale axion inflation scenarios hence can be distinguished from the conventional large field axion inflation scenarios with a high reheating temperature $T_{\rm reh} > T_{\rm f}$ where the dark matter abundance can be estimated as the thermal relic abundance [1]. Another notable feature in our axion inflation scenarios with a small decay constant is the suppressed thermal production of the unwanted relics such as the gravitinos due to the low reheating temperature (55, 56). In general, supersymmetric models have the gravitino problem, and the low-energy effective field theory derived from superstring theory has the moduli problem. The non-thermally produced gravitinos from the moduli decay could be still a problem, and a light moduli, which does not contribute to supersymmetry breaking, can help in diluting the relic abundance of unwanted particles (57). The baryogenesis at a low temperature can also be a concern, and the low-energy scale Affleck-Dine mechanism can be a possibility in our scenarios to realize the desired baryon asymmetry of the Universe (58, 59).

In addition to the inflaton axion we have been discussing so far, there can be other axion fields sourcing the isocurvature perturbations which give the tight bounds on the inflation parameters. For example, the isocurvature perturbations due to the QCD axion requires

$$H_{\rm inf} < 0.87\times10^7{\rm GeV}\left(\frac{f_a}{10^{11}{\rm GeV}}\right)^{0.408}, \tag{3.20}$$

[1]We assume that standard model sector is sequestered from supersymmetry breaking sector and then the lightest supersymmetric particle becomes a good candidate of dark matter under the assumption of R-parity.

where f_a is the QCD axion decay constant (different from f), to be consistent with the present observations (7). Such low scale inflation can be realized in our model with a sub-Planckian decay constant f. For instance, the models with $f = 0.1$ and 0.01 can lead to $H_{\rm inf} \sim 10^9$ GeV and 10^7 GeV, respectively, while the model with $f = 1.0$ leads to $H_{\rm inf} \sim 10^{12}$ GeV. It would be interesting to increase f_a, although there is an upper bound $f_a \lesssim 10^{12}$ to avoid the over-abundant axion while its precise upper bounds depend on the model details such as the initial displacement angles and the possible entropy dilution (57, 60, c).

We so far limited our discussions to the case $f \gtrsim 0.01$ as expected in the framework of type IIB superstring theory (1). We could in principle study an even lower f, and compute the reheating temperature with Eqs.(3.16) and (3.15). However, lower f depending on c can lead to the reheating temperature of order MeV or below, and $f \sim \mathcal{O}(0.01)$ would be the lower parameter range of our interest for the successful Big-Bang nucleosynthesis (BBN).

3.2.4 Short summary: discussion

In this section, we have studied the axion inflation model proposed recently within the framework of type IIB superstring theory with a particular emphasis on the sub-Planckian axion decay constant, $0.01 \lesssim f \lesssim 1.0$. The axion potential with such a sub-Planckian decay constant possesses many flat plateaus and the small field inflation can be realized with a sufficient number of e-folds.

A notable feature of our scenario with a small decay constant f is the low inflation energy scale $V_{inf} \propto f^4$ (Eq. (3.12)). The implications of the consequent low reheating temperature in our string axion inflation scenarios were discussed including the dark matter abundance, gravitino/moduli problem and the isocurvature fluctuations of the QCD axion. More detailed studies would be of great interest where we combine concrete mechanism for the moduli stabilization/uplifting, fix the mass scale of light moduli, choose a candidate for dark matter, and embed the QCD axion in superstring theory. We leave such detailed studies through the concrete models and their generalization for our future work.

We have studied one concrete potential which is derived from superstring theory. The shift symmetry of axion is violated by quantum effects inducing the axion potential. Such an axion potential consists of the mixture of polynomial functions and sinusoidal functions with the periodicity $\phi \sim \phi + 2\pi/f$, represented as $V(\phi^m, \cos(\phi/f), \sin(\phi/f))$ [1]. For a small decay constant $f \ll 1$, such a potential can have many bumps and plateaus with the size of the flat regime $f/(2\pi)$, and the small field inflation can be realized on one of the plateaus.

We expect our concrete examples discussed in our paper can capture the generic features for a wider class of axion inflation consisting of the sinusoidal and polynomial terms with a sub-Planckian axion decay constant. For instance, let us assume that the sinusoidal parts are dominant in some derivatives of the potential. We then would find $V^{(n+1)} \sim V^{(n)}/f$ with $n \geq n_0$ for a certain value n_0, where $V^{(n)}$ denotes the n-th derivative ($V^{(n+1)} \sim V^{(n)}/f$ can well happen for a higher derivative of the potential including the sinusoidal terms because a polynomial term vanishes at a sufficiently large n). Analogous to Eq. (3.10), we can then make a similar Ansatz, $\eta \sim \Delta\phi f^{-p}$. Here, p would depend on the form of the potential, e.g. n_0, while $p = 2$ in our model presented in this paper. This would lead to $r \sim 10^{-6} \times f^{2p}$ when the tensor-to-scalar ratio is small $r < \mathcal{O}(10^{-2})$ and we can estimate $2\eta \approx n_s - 1 \approx 0.03$. In such a model analogous to ours discussed in this paper, the inflation energy scale and Hubble parameter could have the power law dependence on f and hence become rapidly small as f becomes small. As a consequence, the reheating temperature would become smaller too, although its precise value depends on the detailed reheating processes such as couplings between the inflaton and light modes. We would also be able to put the tight lower bound on f from the BBN so that $T_{\rm reh} > \mathcal{O}(1)$ MeV. Confirming such a generalization of our study is shown in the next section, and we plan to present the analysis extending our studies here for a wider class of axion inflation models which can be explicitly derived from superstring theory.

3.3 Constraints on small field axion inflation

Based on the discussion in the last section 3.2.4, here we study the general class of small-field axion inflations which are the mixture of polynomial and sinusoidal functions suggested by the natural and axion monodromy inflations.

[1] The similar but different forms including sinusoidal functions could be derived from another setup different from our choice in superstring theory.

Again, we consider we consider the axion inflations with the decay constant below the Planck scale or string scale, which are favorable from the aspects of weak gravity conjecture. The flat direction required in the inflation can be realized by choosing the proper parameters in the axion potential. Since the obtained inflaton potential is categorized into the class of small-field axion inflation, it predicts the small amount of gravitational wave and low inflation scale in comparison with the prediction of large-field axion inflation. Such low-scale inflation is also influential to the isocurvature perturbation originating from the QCD axion. When all the dark matter is dominated by the QCD axion, the current Planck result constrains the Hubble scale during the inflation $H_{\rm inf}$ (7),

$$H_{\rm inf} < 0.87 \times 10^7 \mathrm{GeV} \left(\frac{f_{\rm QCD}}{10^{11}\,\mathrm{GeV}}\right)^{0.408}, \tag{3.21}$$

where $f_{\rm QCD}$ is the decay constant of QCD axion [1]. It is then possible to avoid the isocurvature constraint by the low-scale inflation, although the upper bound of $f_{\rm QCD}$ depends on the initial misalignment angle of axion and dilution mechanism after the inflation (57, 60, c).

In the last section, we conjectured that, in a certain class of small-field axion inflation derived from type IIB superstring theory (1) [2], the tensor-to-scalar ratio r correlates with the axion decay constant f as follows (d):

$$r \sim 10^{-6} f^{2q},$$

where the fractional number q depends on the model. In the example of Refs. (1, d), we obtain $q = 2$. This behavior originates from sinusoidal functions in the axion inflation potential. The above relation could also predict the magnitude of the inflation potential and the inflaton mass by the axion decay constant, f. In general, superstring theory leads to the axion potential with one or more sinusoidal terms induced by several non-perturbative terms. Thus, it is important to extend the previous analysis to other axion inflation scenarios. In this section, we further study such dependence of axion decay

[1] Such a low-scale inflation is also favorable from the view point of fine-tuning problem in the electroweak sector, realized by the relaxion scenario. To dynamically obtain the electroweak vacuum expectation value of the Higgs boson, the relaxion mechanism requires that the Hubble scale during the inflation should be smaller than the QCD scale for the original relaxion model or dynamical scale for the extend relaxion model. However, such mechanisms are beyond the scope of current work, and we do not discuss hereafter.

[2] The model in Ref. (1) can lead to both small-field and larg-field inflations.

constant for not only cosmological observables but also the reheating temperature and dark matter abundance for the general class of small-field axion inflations, which are the mixture of polynomial and sinusoidal functions suggested in the axion monodromy inflation (36, 37, 38) and general form of sinusoidal functions suggested in the natural and multi-natural inflations (18, 30, 39, 40) [1]. We constrain the axion decay constant realizing the small-field axion inflations by the isocurvature perturbation originating from the QCD axion, successful Big-Bang nucleosynthesis (BBN) and dark matter abundance, As will be shown, it is quite interesting that the allowed range of axion decay constant corresponds to the typical decay constant region realized in superstring theory, when our axion is the closed string axion (25, 26, 27).

In the remaining of following subsections, we first discuss the conditions leading to the general class of small-field axion inflations and analytical form of cosmological observables as a function of the decay constant in section 3.3.1, 3.3.2, in which we consider the small-field axion inflations with an emphasis on the multi-natural inflation in section 3.3.1 and axion monodromy inflation with sinusoidal function in section 3.3.2. In section 3.3.3, we derive the constraints for the axion decay constants from the reheating process and dark matter abundance.

3.3.1 Multi-natural inflation

We derive the constraints for the parameters in the axion potentials leading to the successful small-field axion inflation. First of all, we proceed to study the extended natural inflation so-called multi-natural inflation (30, 40), in which the general form of inflaton potential is given by

$$V(\phi) = \sum_{m=1}^{M} A_m \cos\left(\frac{\phi}{f_m} + \theta_m\right) + V_0. \tag{3.22}$$

Here, ϕ is canonically normalized axion with the decay constants f_m with $m = 1, 2, \cdots, M$, θ_m denotes the phase of sinusoidal functions, A_m are the real positive constants, and V_0 is the real constant to achieve the tiny cosmological constant. M depends on the number of hidden gauge sectors which non-perturbatively generate the potential of axion inflaton.

[1] The scalar potential including modular functions in superstring theory can effectively lead to such a multi-natural inflation (41).

Let us demonstrate the small-field axion inflation by the small axion decay constants f_m with $m = 1, 2, \cdots, M$, where sufficiently a large number of e-foldings is achieved under the flat direction in the axion potential. To achieve such a situation, the first derivative of potential in Eq. (3.22)

$$V_\phi = -\sum_{m=1}^{M} \frac{A_m}{f_m} \sin\left(\frac{\phi}{f_m} + \theta_m\right), \tag{3.23}$$

is required to be smaller than its potential during the inflation, i.e., $|V_\phi| \ll |V|$. It can be realized with the region satisfying

$$\sin(\phi/f_m + \theta_m) \sim \cos(\phi/f_m + \theta_m) \sim \mathcal{O}(1), \tag{3.24}$$

with these proper signs and the correlated parameters in the scalar potential,

$$\frac{A_m}{f_m} \sim \frac{A_n}{f_n}, \tag{3.25}$$

for any $m, n = 1, 2, \cdots, M$.

Since the slow-roll inflation is realized under $|V_\phi| \simeq 0$ and $|V_{\phi\phi}| \simeq 0$ during the inflation, the second derivative of the potential can be estimated by employing the inflaton variation $\Delta\phi$,

$$V_{\phi\phi} \sim V_{\phi\phi\phi}\,\Delta\phi \sim \left(-\sum_{m=1}^{M} \frac{A_m}{f_m^3} \sin\left(\frac{\phi}{f_m} + \theta_m\right)\right)\Delta\phi. \tag{3.26}$$

Here, we assume that all f_m^{-3} can be dominated in the third derivative $V_{\phi\phi\phi}$. With the help of Eqs. (3.24) and (3.25), the slow-roll parameter is obtained as

$$\eta \sim \frac{\sum_{m=1}^{M} \frac{A_m}{f_m^3}}{\sum_{n=1}^{M} A_n}\Delta\phi \sim \left(\frac{\sum_m \frac{1}{f_m^2}}{\sum_n f_n}\right)\Delta\phi, \tag{3.27}$$

where $V \sim \sum_m A_m$ is employed. Since we concentrate on the parameter space leading to the small-field inflation, the slow-roll parameter ϵ is expected to be much smaller than unity. It is confirmed later by checking the value of the tensor-to-scalar ratio $r = 16\epsilon$. Thus, slow-roll parameter $|\eta|$ is chosen as 10^{-2} to reproduce the observed spectral index $n_s \simeq 0.96$ reported by Planck.

By fixing $|\eta| \simeq 10^{-2}$, the tensor-to-scalar ratio is estimated by using the Lyth bound Eq. (3.1),

$$r \sim 10^{-2} \times (\Delta\phi)^2 \sim 10^{-6} \times \left(\frac{\sum_m \frac{1}{f_m^2}}{\sum_n f_n}\right)^{-2} \times \left(\frac{\eta}{0.01}\right)^2. \tag{3.28}$$

Furthermore, we can estimate the energy scale of scalar potential during the inflation $V_{\rm inf}$ as functions of axion decay constants from Eqs. (3.28),

$$V_{\rm inf}^{1/4} \quad \sim 4\times 10^{-4}\times\left(\frac{\sum_m f_m}{\sum_n \frac{1}{f_n^2}}\right)^{1/2}, \tag{3.29}$$

and consequently the Hubble parameter $H_{\rm inf}=(V_{\rm inf}/3)^{1/2}$ becomes

$$H_{\rm inf}\sim 10^{-7}\times\left(\frac{\sum_m f_m}{\sum_n \frac{1}{f_n^2}}\right). \tag{3.30}$$

Finally, we estimate the inflaton mass m_ϕ^2 as a function of the decay constant. For small f_m, the dominant term of second derivatives, $V_{\phi\phi}$, at $\phi=0$ is evaluated by using Eq. (3.24), $V_{\phi\phi}\sim\sum_m\frac{A_m}{f_m^2}$ and hereafter the inflaton mass is estimated as

$$\begin{aligned} m_\phi^2 \quad &= \quad V_{\phi\phi}\sim\sum_m\frac{A_m}{f_m^2}\sim\frac{\sum_m\frac{A_m}{f_m^2}}{\sum_n A_n}V_{\rm inf}\sim\left(\frac{\sum_m\frac{1}{f_m}}{\sum_n f_n}\right)V_{\rm inf} \\ &\sim \quad 3\times 10^{-14}\left(\frac{\sum_m\frac{1}{f_m}}{\sum_n f_n}\right)\left(\frac{\sum_n f_n}{\sum_m\frac{1}{f_m^2}}\right)^2. \end{aligned} \tag{3.31}$$

Let us summarize the result for two non-vanishing sinusoidal functions in Eq. (3.22). For $f_1\sim f_2\sim f\ll 1$, the obtained physical quantities have the following decay constant dependence

$$\begin{aligned} r \quad &\sim \quad 10^{-6}\times f^6\,, \qquad V_{\rm inf}^{1/4}\sim 4\times 10^{-4}\times f^{3/2}, \\ H_{\rm inf} \quad &\sim \quad 10^{-7}\times f^3\,, \qquad m_\phi^2\sim 3\times 10^{-14}\times f^4. \end{aligned} \tag{3.32}$$

For another case $f_1\gg f_2$, they are written as

$$\begin{aligned} r \quad &\sim \quad 10^{-6}\times (f_1 f_2^2)^2\,, \qquad V_{\rm inf}^{1/4}\sim 4\times 10^{-4}\times (f_1 f_2^2)^{1/2}, \\ H_{\rm inf} \quad &\sim \quad 10^{-7}\times (f_1 f_2^2)\,, \qquad m_\phi^2\sim 3\times 10^{-14}\times (f_1 f_2^3). \end{aligned} \tag{3.33}$$

Following this line of thoughts, we show the numerical analysis for specific axion potentials. For the illustrative purpose, we consider the axion potential with two sinusoidal functions [1],

$$V(\phi)=A_1\left(1-\cos\left(\frac{\phi}{f_1}\right)\right)+A_2\left(1-\cos\left(\frac{\phi}{f_2}\right)\right), \tag{3.34}$$

[1] For details of bumpy natural inflation with the same scalar potential, see, Ref. (34).

which is achieved under $\theta_1 = \theta_2 = -\pi$ and $V_0 \simeq A_1 + A_2$ in Eq. (3.22). For an illustrating example, we set the decay constants, $f_1 = 0.1$ and $f_2 = 0.01$ [1]. Figures 3.14, 3.15 show the inflaton potential and the trajectory of inflaton as a function of cosmic time t, where the parameters are set as $A_1/A_2 = 22.474579785926$ and $A_2 = 6.47 \times 10^{-25}$. By solving the equation of motion for the inflaton field, we numerically obtain the cosmological observables as shown in Tab. 3.3. It is found that the analytical forms of physical quantities derived in Eqs. (3.28)-(3.31)

$$\begin{aligned}
r &\sim 10^{-6} \times \left(\frac{f_1 + f_2}{\frac{1}{f_1^2} + \frac{1}{f_2^2}} \right)^2 \sim 10^{-6} \times (f_1 f_2^2)^2 \sim 10^{-16}, \\
V_{\rm inf}^{1/4} &\sim 4 \times 10^{-4} \times \left(\frac{f_1 + f_2}{\frac{1}{f_1^2} + \frac{1}{f_2^2}} \right)^{1/2} \sim 4 \times 10^{-4} \times (f_1 f_2^2)^{1/2} \sim 10^{-6}, \\
H_{\rm inf} &\sim 10^{-7} \times \left(\frac{f_1 + f_2}{\frac{1}{f_1^2} + \frac{1}{f_2^2}} \right) \sim 10^{-7} \times (f_1 f_2^2) \sim 10^{-12}, \\
m_\phi^2 &\sim 3 \times 10^{-14} \times \left(\frac{1}{f_1} + \frac{1}{f_2} \right) \left(\frac{f_1 + f_2}{\frac{1}{f_1^2} + \frac{1}{f_2^2}} \right)^2 \sim 3 \times 10^{-14} \times \frac{1}{f_2} (f_1 f_2^2)^2 \sim 3 \times 10^{-22},
\end{aligned} \tag{3.35}$$

are consistent with our obtained numerical results in Tab. 3.3.

Tab. 3.3 also shows the numerical results of the running, $dn_s/d\ln k$, which are large and negative (34). These values can be estimated roughly as follows. The slow-roll parameter, ξ, can be written

$$\xi = \frac{V_\phi V_{\phi\phi\phi}}{V^2} = \left(\frac{r}{8} \right)^{1/2} \frac{V_{\phi\phi\phi}}{V}. \tag{3.36}$$

Then, using Eq. (3.28) and

$$\frac{V_{\phi\phi\phi}}{V} \sim \left(\frac{\sum_m \frac{1}{f_m^2}}{\sum_n f_n} \right), \tag{3.37}$$

we can estimate $\xi = \mathcal{O}(10^{-3})$ for $\eta \sim 0.01$, and this value of ξ is independent of decay constants. In this model, the running is obtained as $dn_s/d\ln k \approx -2\xi$ and other terms

[1] In particular, in the case where the axion decay constants are degenerate $f_1 = f_2 = f$, the flat potential which induces sufficiently large number of e-folding cannot be realized even if we tune the parameters $A_{1,2}$. This is because the shape of potential is not affected by the parameters $A_{1,2}$ for the case of degenerate decay constants. In this regard, we focus on the distinct axion decay constant

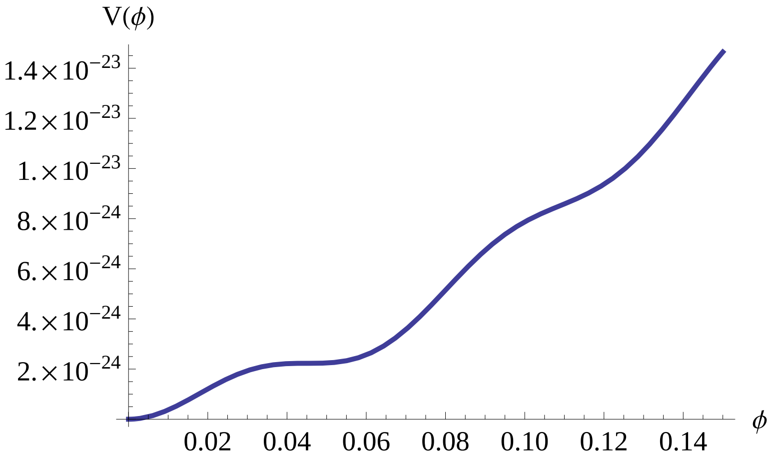

Figure 3.14: - The inflaton potential is drawn by setting the parameters as $A_1/A_2 = 22.474579785926$ and $A_2 = 6.47 \times 10^{-25}$.

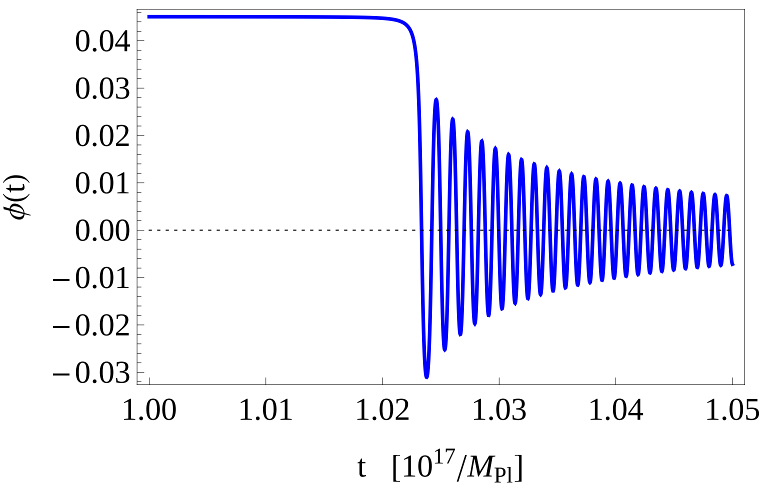

Figure 3.15: - The trajectory of inflaton as a function of cosmic time t for the initial value of inflaton, $\phi_{\rm ini} = 0.04508690783$.

N	n_s	r	m_ϕ^2	$H_{\rm inf}$	$V_{\rm inf}^{1/4}$	$\frac{dn_s}{d\ln k}$
60.0	0.9665	6.85×10^{-17}	7.92×10^{-21}	8.62×10^{-13}	1.22×10^{-6}	2.52×10^{-3}
50.0	0.9665	1.61×10^{-16}	1.86×10^{-20}	1.32×10^{-12}	1.51×10^{-6}	1.65×10^{-3}

Table 3.3: The cosmological observables such as spectral index n_s, tensor-to-scalar ratio r, Hubble scale $H_{\rm inf}$, scalar potential $V_{\rm inf}^{1/4}$ at the pivot scale and the inflaton mass m_ϕ^2 at the vacuum. The parameters are set as $A_1/A_2 = 22.474579785926$ and $A_2 = 6.47\times 10^{-25}$ for the e-folding number $N = 60$, whereas those are set as $A_1/A_2 = 22.474579787160$ and $A_2 = 6.47\times 10^{-25}$ for the e-folding number $N = 50$, respectively. The initial value of inflaton field is also set as $\phi_{\rm ini} = 0.04508690783$ in both cases.

are sub-dominant. Thus, it is found that $dn_s/d\ln k = \mathcal{O}(10^{-3})$. Similarly, the running of running is obtained as $d^2n_s/d\ln k^2 \approx 2\eta\xi$ in this model and other terms are sub-dominant. Then, it is found that $d^2n_s/d\ln k^2 = \mathcal{O}(10^{-5})$, which is independent of decay constants.

Similarly, the potential (3.34) with other values of f_1 and f_2 leads to results consistent with Eq. (3.33).

3.3.2 Axion monodromy inflation with sinusoidal functions

We next discuss the axion monodromy inflation with sinusoidal functions in which the general form of the axion potential is yielded by

$$V(\phi) \quad = A_1\phi^p + \sum_{i=2}^{M} A_i \cos\left(\frac{\phi}{f_i} + \theta_i\right) + V_0. \tag{3.38}$$

Here, ϕ is canonically normalized axion with the decay constants f_i, θ_i denotes the phase of sinusoidal functions, A_i are the real positive constants, and V_0 is the real constant to achieve the tiny cosmological constant. p can be taken as fractional numbers or positive integers such as $p = 1$ (21), $p = 2/3$ (36), $p = 2$ (61, 62) and $p = 4/3,\ 3$ (63) and M depends on the number of hidden gauge sectors which non-perturbatively generate the potential of axion inflaton.

We proceed to demonstrate the small-field axion inflation by the small axion decay constants f_i in the same way as in the previous section. To obtain the sufficiently large number of e-folding, the first derivative of potential in Eq.(3.38)

$$V_\phi = A_1 p \phi^{p-1} - \sum_i \frac{A_i}{f_i} \sin\left(\frac{\phi}{f_i} + \theta_i\right), \tag{3.39}$$

is required to be smaller than the potential energy, that is, $|V_\phi| \ll |V|$. It can be realized with the region satisfying

$$\begin{aligned} \phi &\sim \mathcal{O}(1), \\ \sin(\phi/f_i + \theta_i) &\sim \cos(\phi/f_i + \theta_i) \sim \mathcal{O}(1), \end{aligned} \tag{3.40}$$

with proper signs of $\sin(\phi/f_i + \theta_i)$ and $\cos(\phi/f_i + \theta_i)$, and the correlated parameters in the scalar potential,

$$A_1 p \sim \frac{A_i}{f_i} \sim \frac{A_j}{f_j}, \tag{3.41}$$

for any $i, j = 2, 3, \cdots, M$.

Since the slow-roll inflation is realized under $|V_\phi| \simeq 0$ and $|V_{\phi\phi}| \simeq 0$ during the inflation, the second derivative of the potential can be estimated by employing the inflaton variation $\Delta\phi$,

$$V_{\phi\phi} \sim V_{\phi\phi\phi} \Delta\phi \sim \left(-\sum_i \frac{A_i}{f_i^3} \sin\left(\frac{\phi}{f_i} + \theta_i\right)\right) \Delta\phi, \tag{3.42}$$

for small f_i. Here, we assume that all f_i^{-3} in the third derivative $V_{\phi\phi\phi}$ dominate the second derivative $V_{\phi\phi}$. With the helps of Eqs. (3.40) and (3.41), the slow-roll parameter η is obtained as

$$\eta \sim \frac{\sum_i \frac{A_i}{f_i^3}}{A_1} \Delta\phi \sim p \left(\sum_i \frac{1}{f_i^2} \right) \Delta\phi, \tag{3.43}$$

where the scalar potential during the inflation is approximately given by $V_{\rm inf} \sim A_1$ due to the conditions (3.40) and (3.41). Since we concentrate on the parameter space leading to the small-field inflation, the slow-roll parameter ϵ is expected to be much smaller than unity. It is confirmed later by checking the value of the tensor-to-scalar ratio $r = 16\epsilon$. Thus, the slow-roll parameter $|\eta|$ is chosen as 10^{-2} to reproduce the observed spectral index $n_s \simeq 0.96$ reported by Planck.

By fixing $|\eta| \simeq 10^{-2}$, tensor-to-scalar ratio is estimated by using the Lyth bound Eq.(3.1),

$$r \sim 10^{-2} \times (\Delta\phi)^2 \sim 10^{-6} \times \frac{1}{p^2} \left(\sum_i \frac{1}{f_i^2} \right)^{-2} \times \left(\frac{\eta}{0.01}\right)^2, \tag{3.44}$$

from which the power of decay constants f in r becomes small in comparison with that in the multi-natural inflation.

Furthermore, we can estimate the energy scale of scalar potential during the inflation $V_{\rm inf}$ as functions of axion decay constants from Eq (3.44),

$$V_{\rm inf}^{1/4} \sim 4 \times 10^{-4} \times p^{-1/2} \left(\sum_i \frac{1}{f_i^2} \right)^{-1/2}, \tag{3.45}$$

and consequently the Hubble parameter $H_{\rm inf} = (V_{\rm inf}/3)^{1/2}$ becomes

$$H_{\rm inf} \sim 10^{-7} \times p^{-1} \left(\sum_i \frac{1}{f_i^2} \right)^{-1}. \tag{3.46}$$

Finally, we estimate the inflaton mass m_ϕ^2 as a function of the decay constant. For small f_i, the dominant term of second derivative, $V_{\phi\phi}$, at $\phi = 0$ is evaluated by using Eq. (3.24), $V_{\phi\phi} \sim \sum_i \frac{A_i}{f_i^2}$ and hereafter the inflaton mass is estimated as

$$\begin{aligned} m_\phi^2 &= V_{\phi\phi} \sim \sum_i \frac{A_i}{f_i^2} \sim \frac{\sum_i \frac{A_i}{f_i^2}}{A_1} V_{\rm inf} \sim p \left(\sum_i \frac{1}{f_i} \right) V_{\rm inf} \\ &\sim 3 \times 10^{-14} \times p^{-1} \left(\sum_i \frac{1}{f_i} \right) \left(\sum_i \frac{1}{f_i^2} \right)^{-2}. \end{aligned} \tag{3.47}$$

3.3.3 Reheating temperature and dark matter abundance

In this section, we discuss the reheating process after the inflation dynamics. From now on, we assume that the inflaton axion discussed in the previous section couples to the gauge bosons in the standard model through tree or one-loop corrected gauge kinetic functions. In type IIB superstring theory on toroidal background, it is known that the Kähler axion corresponding to the Kalb-Ramond field couples to the gauge boson at the tree-level, whereas the axion associated with the complex structure modulus appears in the gauge kinetic function at the one-loop level (51, 52). In both cases, the inflaton decays into the gauge bosons $g^{(a)}$ with $a = 1, 2, 3$ corresponding to the gauge groups of the standard model, $U(1)_Y, SU(2)_L, SU(3)_C$ and its decay width is estimated in the instantaneous decay approximation,

$$\begin{aligned} \Gamma_\phi &= \sum_{a=1}^{3} \Gamma(\phi \to 2g^{(a)}) \\ &\simeq 5.8 \times 10^{-5} c^2 \left(\frac{m_\phi}{10^{13}\ {\rm GeV}} \right)^3\ {\rm GeV}, \end{aligned} \tag{3.48}$$

where c becomes $16\pi^2$ and unity for the Kähler moduli and complex structure moduli. When such a decay into the gauge bosons is the dominant process, the reheating temperature is yielded as

$$
\begin{aligned}
T_{\rm ref} &= \left(\frac{\pi^2 g_*}{90}\right)^{-1/4} \sqrt{\Gamma_\phi M_{\rm Pl}} \\
&\simeq 6.4 \times 10^6 c \left(\frac{m_\phi}{10^{13}\ {\rm GeV}}\right)^{3/2}\ {\rm GeV}, \qquad (3.49)
\end{aligned}
$$

with the effective degrees of freedom $g_* = 106.75$ [1].

From the results in section 3.3.2, the reheating temperate is yielded by the axion decay constants,

$$
T_{\rm ref} \simeq 5.4 \times 10^4 c \left(\frac{\sum_{m=1}^{M} \frac{1}{f_m}}{\sum_{n=1}^{M} f_n}\right)^{3/4} \left(\frac{\sum_{n=1}^{M} f_n}{\sum_{m=1}^{M} \frac{1}{f_m^2}}\right)^{3/2}\ {\rm GeV}, \qquad (3.50)
$$

which is illustrated in Fig. 3.16, 3.17 as functions of two axion decay constants for the simplified multi-natural inflation in Eq. (3.34). We now take into account the constraint from the isocurvature perturbation originating from the QCD axion by Eq. (3.21) with $f_{\rm QCD} = 10^{12}\,{\rm GeV}$ and Eq. (3.30) with $m = 1, 2$, which corresponds to the blue shaded region in Fig. 3.16, 3.17. Here and in the following analysis, we employ the maximal value of the QCD axion decay constant constrained by the upper bound of dark matter abundance, although it depends on the initial misalignment angle of axion and dilution mechanism after the inflation (57, 60, c). As can be seen in Fig. 3.16, 3.17, the smallest axion decay constant is bounded as $2 \times 10^{15}\,{\rm GeV} \lesssim f \lesssim 10^{17}\,{\rm GeV}$ for Kähler axion and $10^{16}\,{\rm GeV} \lesssim f \lesssim 10^{17}\,{\rm GeV}$ for axion of complex structure modulus, where the lower bounds are put by $T_{\rm reh} \gtrsim \mathcal{O}(5)$ MeV in order not to spoil the successful BBN, whereas the upper bounds are set by the constraint from the isocurvature perturbation of QCD axion with $f_{\rm QCD} = 10^{12}\,{\rm GeV}$.

Similarly, the reheating temperate for the axion monodromy inflation with sinusoidal functions in section 3.3.2 is also dominated by the axion decay constants,

$$
T_{\rm ref} \simeq 5.4 \times 10^4 c\, p^{-3/4} \left(\sum_{i=2}^{M} \frac{1}{f_i}\right)^{3/4} \left(\sum_{i=2}^{M} \frac{1}{f_i^2}\right)^{-3/2}\ {\rm GeV}, \qquad (3.51)
$$

[1] In addition to the above case, we also consider the case where the decays of inflaton occur instantaneously and the conversion of vacuum energy is perfectly efficient, $\rho_\phi \simeq 3H_{\rm ini}^2 M_{\rm p}^2 = \frac{\pi^2}{30} g_* T_{\rm reh}^4$. This situation gives rise to the maximum reheating temperature (or equivalently, $T_{\rm reh} \simeq 0.41 \times V_{\rm ini}^{1/4}$ GeV) $T_{\rm max} \simeq 2.6 \times 10^{13} \left(\frac{H_{\rm ini}}{10^9\ {\rm GeV}}\right)^{1/2}$ GeV.

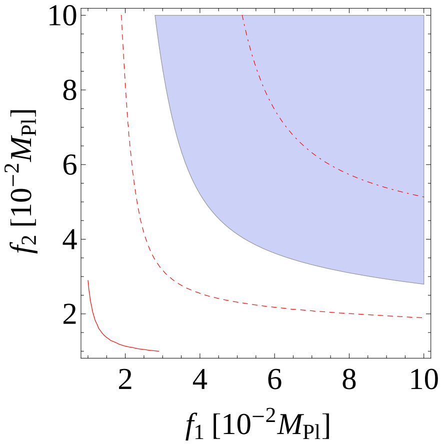

Figure 3.16: - The reheating temperature $T_{\rm reh}$ as functions of two decay constants $f_{1,2}$ for the case of axion of Kähler moduli. The solid, dashed, dot-dashed and dotted curves represent the reheating temperature, $T_{\rm reh} = 1, 10, 10^2, 10^3\,\mathrm{MeV}$, respectively.

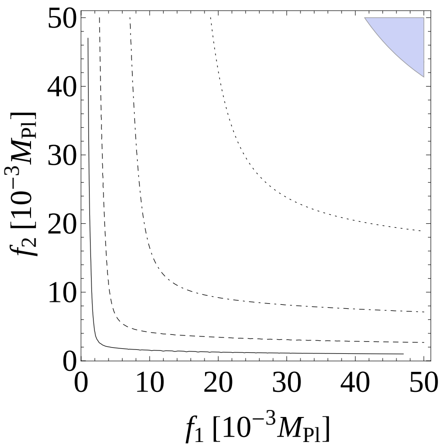

Figure 3.17: - The reheating temperature $T_{\rm reh}$ as functions of two decay constants $f_{1,2}$ for the case of axion of complex structure modulus. The solid, dashed, dot-dashed and dotted curves represent the reheating temperature, $T_{\rm reh} = 1, 10, 10^2, 10^3\,\mathrm{MeV}$, respectively. In above two panels, the blue shaded region is excluded by the isocurvature perturbation originating from the QCD axion.

which is illustrated in Fig. 3.18 as functions of axion decay constant $f = f_2\,(M = 2)$ and the power of polynomial p for the simplified axion monodromy inflation with sinusoidal functions in Eq. (3.38). In Fig. 3.18, 3.19 and in what follows, p is considered as the continuous parameter for simplicity, although it is a fractional number derived in a detailed string setup. In a similar fashion as in the multi-natural inflation, the blue shaded region in Fig. 3.18, 3.19 is excluded by the isocurvature perturbation originating from the QCD axion which is estimated by employing Eq. (3.21) with $f_{\rm QCD} = 10^{12}$ GeV and Eq. (3.46) with $f = f_2$. In order not to spoil the successful BBN and overproduce the isocurvature perturbation due to the QCD axion, Fig. 3.18, 3.19 gives the bounds $2\times10^{14}\,\text{GeV} \lesssim f \lesssim 5\times10^{16}\,\text{GeV}$ for Kähler axion and $2\times10^{15}\,\text{GeV} \lesssim f \lesssim 5\times10^{16}\,\text{GeV}$ for axion of complex structure modulus, respectively. Note that, the smaller $f_{\rm QCD}$ gives the tight upper bound on f from the isocurvature perturbation of QCD axion. As a result, these regions correspond to the typical decay constant for the closed string axions (25, 26, 27). That is surprisingly interesting. Although we focus on the simplified axion potentials in Eqs. (3.34) and 3.38), such severe constraints for the axion decay constant are also applied to the general form of axion potential. Indeed, the larger axion decay constants lead to the large Hubble scale given in Eqs. (3.30) and (3.46).

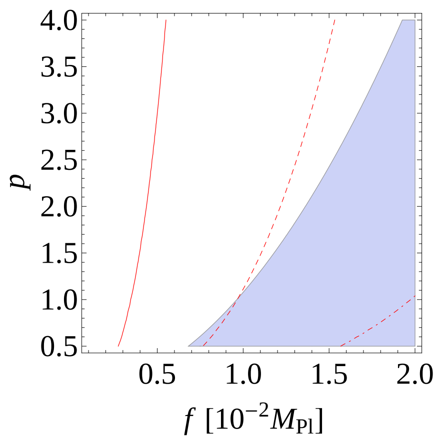

Figure 3.18: - The reheating temperature $T_{\rm reh}$ as functions of the decay constant f and the power of polynomial term p for the case of axion of Kähler moduli. The solid, dashed and dot-dashed curves represent the reheating temperature, $T_{\rm reh} = 1, 10, 10^2, 10^3$ MeV, respectively. The blue shaded region is excluded by the isocurvature perturbation originating from the QCD axion.

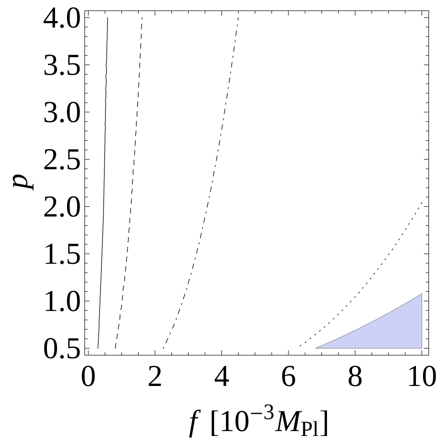

Figure 3.19: - The reheating temperature $T_{\rm reh}$ as functions of the decay constant f and the power of polynomial term p for the case of axion of complex structure modulus.

From these considerations, the low-scale axion decay constants realizing the successful small-field axion inflations generically predict the low reheating temperature. It implies that the freeze-out temperature of dark matter would be smaller than the reheating temperature, and consequently the dark matter yield is determined by the non-thermal process from the inflaton decay

$$\frac{n_{\rm dm}}{s} \simeq \frac{3T_{\rm reh}}{4m_\phi}{\rm Br}_{\rm dm} \simeq 4.8\times 10^{-7}c\,{\rm Br}_{\rm dm}\left(\frac{m_\phi}{10^{13}\ {\rm GeV}}\right)^{1/2}, \tag{3.52}$$

where $n_{\rm dm}$ is the number density of dark matter, s is the entropy density of the Universe and ${\rm Br}_{\rm dm}$ is the branching ratio from the inflaton to dark matter. The relic abundance of dark matter is then given in terms of the ratio of critical density to the current entropy density of the Universe $\rho_{\rm cr}/s_0 \simeq 3.6h^2\times 10^{-9}$,

$$\begin{aligned}\Omega_{\rm dm}h^2 &\simeq m_{\rm dm}\frac{n_{\rm dm}}{s}\frac{s_0}{\rho_{\rm cr}} \\ &\simeq 1.3c\left(\frac{m_{\rm dm}}{100\,{\rm GeV}}\right)\left(\frac{{\rm Br}_{\rm dm}}{10^{-4}}\right)\left(\frac{m_\phi}{10^{13}\ {\rm GeV}}\right)^{1/2},\end{aligned} \tag{3.53}$$

with h being the dimensionless Hubble parameter.

From now on, we for simplicity assume that the current dark matter abundance is mainly consisted of QCD axion compared with another cold dark matter. In Figs. 3.20 and 3.21, we plot the dark matter abundance for the simplified multi-natural inflation in Eq. (3.34),

$$\Omega_{\rm dm}h^2 \simeq 0.27c\left(\frac{m_{\rm dm}}{100\,{\rm GeV}}\right)\left(\frac{{\rm Br}_{\rm dm}}{10^{-4}}\right)\left(\frac{\sum_{m=1}^{2}\frac{1}{f_m}}{\sum_{n=1}^{2} f_n}\right)^{1/4}\left(\frac{\sum_{n=1}^{2} f_n}{\sum_{m=1}^{2}\frac{1}{f_m^2}}\right)^{1/2}, \qquad (3.54)$$

and for the simplified axion monodromy inflation with sinusoidal functions in Eq. (3.38),

$$\Omega_{\rm dm}h^2 \simeq 0.27c\left(\frac{m_{\rm dm}}{100\,{\rm GeV}}\right)\left(\frac{{\rm Br}_{\rm dm}}{10^{-4}}\right)2^{-1/4}f^{3/4} \qquad (3.55)$$

respectively. The relic dark matter abundance should be less than $\Omega_{\rm dm}h^2 \simeq 0.12$ reported by Planck in order not to overclose our Universe (8). Although these predictions depend on the branching ratio ${\rm Br}_{\rm dm}$ and dark matter mass, $\Omega_{\rm dm}h^2 < 0.12$ in Figs. 3.20 and 3.21 is achieved in both inflation models. For example, in simplified multi-natural inflation in Eq. (3.34), $\Omega_{\rm dm}h^2 < 0.12$ can be realized under e.g., ${\rm Br}_{\rm dm} < \mathcal{O}(10^{-3})$ and $m_{\rm dm} \simeq 100\,{\rm GeV}$ with $f_{1,2} \simeq 2\times 10^{-2}\,{\rm M_{Pl}}$ for the Kähler axion and ${\rm Br}_{\rm dm} < \mathcal{O}(10^{-1})$ and $m_{\rm dm} \simeq 100\,{\rm GeV}$ with $f_{1,2} \simeq 4\times 10^{-2}\,{\rm M_{Pl}}$ for the axion of complex structure modulus, whereas in axion monodromy inflation with sinusoidal functions in Eq. (3.38), $\Omega_{\rm dm}h^2 < 0.12$ can be realized under e.g., ${\rm Br}_{\rm dm} < \mathcal{O}(10^{-3})$ and $m_{\rm dm} \simeq 100\,{\rm GeV}$ with $f \simeq 10^{-2}\,{\rm M_{Pl}}$ for the Kähler axion and ${\rm Br}_{\rm dm} < \mathcal{O}(10^{-1})$ and $m_{\rm dm} \simeq 100\,{\rm GeV}$ with $f \simeq 10^{-2}\,{\rm M_{Pl}}$ for the axion of complex structure modulus. However, the low-scale inflation requires enough amount of baryon asymmetry to reproduce the current baryon asymmetry of our Universe. To explain the relic baryon asymmetry, we could combine our inflation models with the baryogenesis scenario, e.g., the Affleck-Dine mechanism (64, 65). It would be studied in future work.

3.4 Kähler moduli inflation

In the paper (f), We propose a new type of moduli stabilization scenario where the supersymmetric and supersymmetry-breaking minima are degenerate at the leading level, and the inclusion of the loop-corrections originating from the matter fields resolves this degeneracy of vacua. Before showing the calculations, let us introduce the motivation of moduli inflation, which we consider in this chapter briefly.

Superstring theory predicts six-dimensional (6D) compact space in addition to four-dimensional (4D) space-time. The size and shape of the 6D compact space are determined by moduli. Thus, moduli are a characteristic feature in superstring theory on

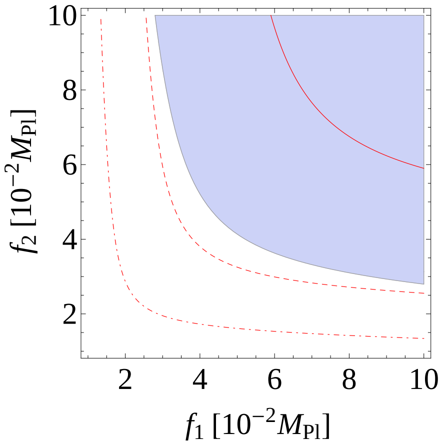

Figure 3.20: - The dark matter abundance $\Omega_{\rm dm}h^2 = 0.1$ as functions of two decay constants $f_{1,2}$ for the case of axion of Kähler moduli. The black solid, dashed and dotdashed curves are drawn by setting $m_{\rm dm}{\rm Br}_{\rm dm} = 10^{-1}, 0.2, 1\,{\rm GeV}$, respectively, whereas the red solid, dashed and dotdashed curves are drawn by setting $m_{\rm dm}{\rm Br}_{\rm dm} = 8, 15, 25\,{\rm GeV}$, respectively.

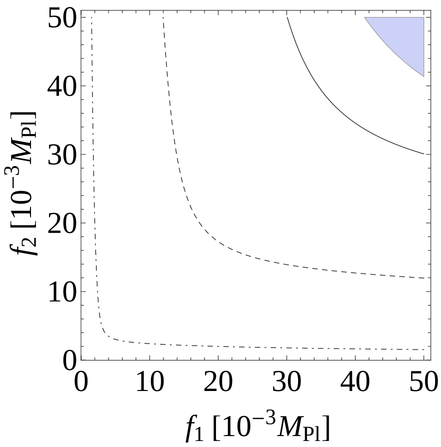

Figure 3.21: - The dark matter abundance $\Omega_{\rm dm}h^2 = 0.1$ as functions of two decay constants $f_{1,2}$ for the case of axion of complex structure modulus. The blue shaded region is excluded by the isocurvature perturbation originating from the QCD axion with $f_{\rm QCD} = 10^{12}\,{\rm GeV}$.

compact space. Indeed, moduli fields play important roles in superstring theory and its 4D low-energy effective field theory, in particular in particle phenomenology and cosmology (See for reviews, e.g. Refs. (52, 66)). Studies on physics relevant to moduli would provide a remnant of superstring theory on compact space.

In the phenomenological point of views, the thermal history of the Universe highly depends on the dynamics of moduli fields as well as axion fields, which are the imaginary parts of moduli fields. Futher, from the theoretical point of view, these moduli fields are originating from the vector and tensor fields in low-energy effective action of superstring theory as well as the higher-dimensional supergravity. The stabilization of moduli field is one of the most important issues to realize a consistent low-energy effective action of superstring theory.

So far, there are several mechanisms to stabilize the moduli, in particular closed string moduli fields, e.g. the Kachru-Kallosh-Linde-Trivedi (KKLT) scenario (44) and the LARGE volume scenario (50) (See e.g. Ref. (66) and references therein). In the paper (f), we propose a new type of moduli stabilization scenario by using the string-derived $\mathcal{N} = 1$ four-dimensional supergravity action. We find that the supersymmetric and SUSY-breaking vacua are degenerate at the tree-level and they are independent of the F-term of certain moduli field. The loop effects originating from the matter fields generate the moduli potential and resolve this degeneracy of vacua.

The moduli potential is prohibited by the higher-dimensional gauge and Lorentz symmetries at the perturbative level. On the other hand, the non-trivial background fields and non-perturbative effects generate the moduli potential. Then, one can stabilize the moduli fields. The vacuum structure of moduli potential is of particular importance. For example, the flat direction of the moduli potential can drive the cosmological inflation [1] and the lifetime of our Universe depends on the (meta)stability of the vacuum.

In this respect, we sutdy the Kähler moduli inflation within the framework of the type IIB superstring theory with stabilizing the modulis, which are the mixture of polynomial and logarithmic functions. Here, we consider some cases that the minimum of the moduli potentials becomes zero, which of course derives successful cosmological inflation. An interesting point is that without up-lifting terms, we can stabilize the vacuum and control the minimum of the potentials with appropriate tunings.

[1]See for the detail of moduli inflations as well as axion inflations, e.g., Ref. (12).

3.4.1 Kähler moduli as an inflaton potential

Now in this section, we derive inflaton potential of Kähler moduli taking into account for supersymmetric and SUSY-breaking minima.

By use of the flux-induced superpotential, the F-term scalar potential is calculated as [1]

$$
\begin{aligned}
V_F &= e^K\Big[\sum_{I,J=S,U_m} K^{I\bar{J}} D_I W D_{\bar{J}}\bar{W} + \Big(K^{T_i\bar{T}_j} K_{T_i} K_{\bar{T}_j} - 3\Big)|W|^2\Big] \\
&= e^K\Big[\sum_{I,J=S,U_m} K^{I\bar{J}} D_I W D_{\bar{J}}\bar{W}\Big],
\end{aligned} \tag{3.56}
$$

where $-3|W|^2$ is canceled by the no-scale structure of Kähler moduli,

$$
\sum_{i,j} K^{T_i\bar{T}_j} K_{T_i} K_{\bar{T}_j} - 3 = 0. \tag{3.57}
$$

Note that the above no-scale structure is valid only at the tree-level.

Then, the dilaton and complex structure moduli are stabilized at the minimum,

$$
D_S W = 0, \qquad D_{U_m} W = 0, \tag{3.58}
$$

which lead to the Minkowski minimum $V_F = 0$. When $W \neq 0$, the supersymmetry is broken by the F-term of Kähler moduli. In contrast to the complex structure modulus case [2], we now assume that all the complex structure moduli and dilaton are stabilized by the flux-induced superpotential. Although the F-terms of S and U vanish at this Minkowski minimum, the F-terms of Kähler moduli are non-vanishing in general

$$
F^{T_i} = -e^{K/2}\sum_j K^{T_i\bar{T}_j} D_{\bar{T}_j}\bar{W} = -e^{K/2}\sum_j K^{T_i\bar{T}_j} K_{\bar{T}_j}\bar{W}, \tag{3.59}
$$

when $W \neq 0$.

For simplicity, we study the model with the overall Kähler modulus with the CY volume $\mathcal{V} = (T+\bar{T})^{3/2}$. Then, the F-term of the Kähler modulus is simplified as

$$
F^T \simeq e^{K(S,U)/2}\frac{T+\bar{T}}{(T+\bar{T})^{3/2}}\bar{W} = e^{K(S,U)/2}\frac{\bar{W}}{(T+\bar{T})^{1/2}}. \tag{3.60}
$$

[1] In the paper (f), we consider two illustrative supergravity models where the moduli fields correspond to the complex strucuture modulus and Kähler moduli within the framework of the type IIB superstring theory. In both scenario, these details are summarized in Appendix B.

[2] Again, see Ref. (f)

Thus, supersymmetric and SUSY-breaking minima are also degenerate in a way similar to the complex structure modulus case, since the scalar potential is independent of T and F^T. However, the supersymmetric vacuum corresponds to $\mathrm{Re}(T) \to \infty$, that is, the decompactification limit.

When the leading α'-corrections are involved, the Kähler potential of the Kähler modulus is corrected as (67)

$$K = -2\ln\left(\mathcal{V} + \frac{\xi}{2}\right), \tag{3.61}$$

where $\xi = -\frac{\chi(CY)\zeta(3)}{2(2\pi)^3 g_s^{3/2}}$ with χ and g_s being the Euler characteristic of CY and string coupling. These α'-corrections break the no-scale structure, and the scalar potential is generated as

$$V_F \simeq e^{K(S,U)}\frac{3\xi}{4\mathcal{V}^3}|W|^2. \tag{3.62}$$

The sign of ξ depends on the number of complex structure moduli and Kähler moduli. When the number of Kähler moduli is smaller than that of complex structure moduli, ξ is positive. In the case of single Kähler modulus, the F-term potential reduces to

$$V_F \simeq e^{K(S,U)}\frac{3\xi}{4(T+\bar{T})^{9/2}}|W|^2 = \frac{3\xi}{4(T+\bar{T})^{7/2}}|F^T|^2. \tag{3.63}$$

Along the same step outlined in section 3.3 of Ref. (f) [1], we take into account the loop-corrections originating from the supersymmetric particles whose soft terms are dominated by the F-term of the Kähler modulus. It is remarkable that the loop corrections give rise to the stabilization of $\mathrm{Re}(T)$ (unlike the case of the complex structure modulus). Then, by assuming that the typical gaugino and supersymmetric scalar fields mainly contribute to the loop-effects, the total scalar potential becomes [1], the

[1] See Appendix B.

total scalar potential becomes

$$
\begin{aligned}
V &\simeq \frac{3\xi}{4(T+\bar{T})^{7/2}}|F^T|^2 + \frac{1}{64\pi^2}\Bigg[a_1\left(c^2 - \left(\frac{|F^T|}{T+\bar{T}}\right)^2\right)^2 \ln\left(c^2 - \left(\frac{|F^T|}{T+\bar{T}}\right)^2\right) \\
&\qquad - a_2\left(\frac{|F^T|}{T+\bar{T}}\right)^4 \ln\left(a_3\left(\frac{|F^T|}{T+\bar{T}}\right)^2\right)\Bigg] \\
&= \frac{3\xi}{4(T+\bar{T})^{3/2}}(\hat{F}^T)^2 + \frac{1}{64\pi^2}\Bigg[a_1\left(c^2 - \left(\hat{F}^T\right)^2\right)^2 \ln\left(c^2 - \left(\hat{F}^T\right)^2\right) \\
&\qquad - a_2\left(\hat{F}^T\right)^4 \ln\left(a_3\left(\hat{F}^T\right)^2\right)\Bigg] \\
&= \frac{3\xi}{4e^{K(S,U)/2}W}(\hat{F}^T)^3 + \frac{1}{64\pi^2}\Bigg[a_1\left(c^2 - \left(\hat{F}^T\right)^2\right)^2 \ln\left(c^2 - \left(\hat{F}^T\right)^2\right) \\
&\qquad - a_2\left(\hat{F}^T\right)^4 \ln\left(a_3\left(\hat{F}^T\right)^2\right)\Bigg], \qquad (3.64)
\end{aligned}
$$

where $\hat{F}^T \equiv |F^T|/(T+\bar{T})$. Here, we employ the same notation of section 3.3 and W is chosen as a real constant, for simplicity.

By setting the illustrative parameters:

$$
a_1 = 10, \quad a_2 = 3, \quad a_3 = 8, \quad c = 1.1, \quad \xi = 1, \quad e^{K(S,U)/2}W \simeq 60.42, \qquad (3.65)
$$

the scalar potential is drawn as in Figure 3.22 [1].

Since those complex structure moduli and dilaton fields have been stabilized at the SUSY-breaking minimum, their masses are typically greater than or equal to the gravitino mass $e^{K(S,U)/2}W/\mathcal{V} \simeq 6.9 \times 10^{-1}$ in our numerical example. Interestingly, the tuning of $e^{K(S,U)/2}W$ allows us to consider the tiny cosmological constant. In the above scenario, $\mathrm{Re}(T)$ can be stabilized at a fine value, but its imaginary part, i.e. the axion, remains massless.

So far, we have studied the model with the overall Kähler modulus. However, we can discuss the model with many Kähler moduli fields T_i. Even in such a model, the tree-level scalar potential is flat along all of the Kähler moduli directions because of the no-scale structure (3.57). Also, the tree-level potential is independent of F-terms of T_i,

[1] As a result, the degeneracy of vacua is resolved by the loop-corrections. The vanishing $|F^T| \propto (T+\bar{T})^{-1/2}$ corresponds to the unphysical domain $\mathrm{Re}(T) \to \infty$. Thus, the SUSY-breaking vacuum is selected. Indeed, the above illustrative parameters give rise to the high-scale SUSY-breaking minimum, where the vacuum expectation value of $\mathrm{Re}(T)$, $\mathrm{Re}(T) \simeq 9.9$, resides in a reliable range of the supergravity approximation.

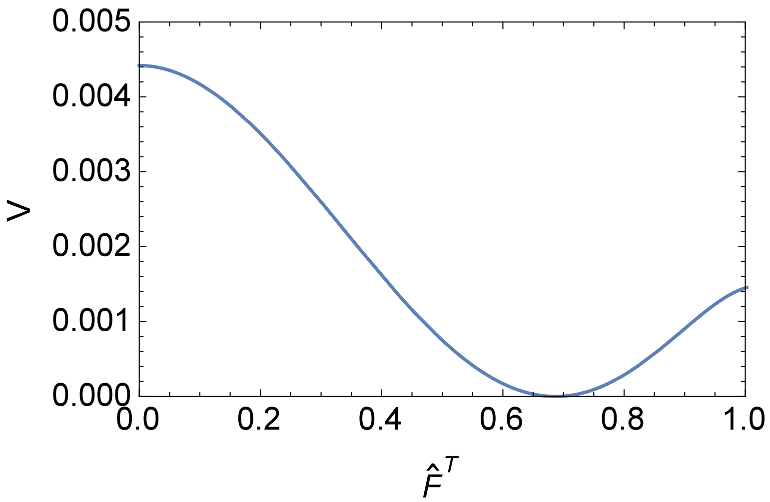

Figure 3.22: - The scalar potential as a function of $\hat{F}^T$ by setting the parameters as in Eq. (3.65).

and these F^{T_i} themselves depend only on $\mathrm{Re}(T_i)$, but not $\mathrm{Im}(T_i)$. In such multi-moduli models, gaugino masses and soft scalar masses would be written by

$$M_a = M_0 + \sum_i k_f^i F^{T_i}, \qquad m_i^2 = m_0^2 - \sum_i k_m^i |F^{T_i}|^2. \tag{3.66}$$

Using these, we obtain the one-loop potential $\Delta V(T_i + \bar{T}_i)$. Then, one can stabilize F^{T_i} and $\mathrm{Re}(T_i)$ in a similar way. However, all the axionic parts of T_i remain massless at this stage.

3.4.2 Analysis and results

Let us begin with our discussions by the setup of our potential. By the existence of flux-induced superpotential, all the complex structure moduli and dilaton field are stabilized. After the stabilization of complex structure moduli, the total scalar potential with the α'-correction becomes

$$\begin{aligned} V \;\; \simeq \;\; & \frac{3\xi}{4e^{K(S,U)/2}W}(\hat{F}^T)^3 + \frac{1}{64\pi^2}\left[a_1\left(c^2 - \left(\hat{F}^T\right)^2\right)^2 \ln\left(c^2 - \left(\hat{F}^T\right)^2\right)\right. \\ & \left. - a_2\left(\hat{F}^T\right)^4 \ln\left(a_3\left(\hat{F}^T\right)^2\right)\right], \end{aligned} \tag{3.67}$$

with

$$\hat{F} \equiv \frac{|F^T|}{(T+\bar{T})}, \tag{3.68}$$

as shown in eq.(3.64). In the case of single Kähler modulus with the Kähler potential $K = -3\ln\left(T+\bar{T}\right)$, the modulus kinetic term is given by

$$\begin{aligned}\mathcal{L} &= K_{T\bar{T}}\partial^{\mu}T\partial_{\mu}\bar{T} \\ &= -\frac{3}{(T+\bar{T})^2}\partial^{\mu}T\partial_{\mu}\bar{T} \\ &= -\frac{1}{2}\left[\partial^{\mu}\hat{\sigma}\partial_{\mu}\hat{\sigma}\right]-\frac{3}{4\sigma^2}\left[\partial^{\mu}\hat{\tau}\partial_{\mu}\hat{\tau}\right],\end{aligned} \tag{3.69}$$

where $T = 1/\sqrt{2}(\sigma + i\tau)$ and the real part of Kähler modulus is now canonically normalized as

$$\hat{\sigma} = \sqrt{\frac{2}{3}}\ln\sigma. \tag{3.70}$$

Thus, the F-term of the Kähler modulus is given by

$$\hat{F} \equiv \frac{|F^T|}{(T+\bar{T})} \simeq \frac{e^{K(S,U)/2}\bar{W}}{(T+\bar{T})^{3/2}} = \frac{e^{K(S,U)/2}\bar{W}}{\left(\sqrt{2}e^{\sqrt{\frac{2}{3}}\hat{\sigma}}\right)^{3/2}}. \tag{3.71}$$

In our model, $\hat{\sigma}$ in eq.(3.71) is identified with the inflaton.

We now discuss the inflation dynamics in our scenario, and let us introduce the following re-parameterization for convenience

$$c \equiv c_1, \qquad e^{K(S,U)/2}W \equiv c_2. \tag{3.72}$$

Futher for simplicity, we take $\xi = 1$. In what follows we will search the parameter sets (a_1, a_2, a_3, c_1, c_2), and investigate whether the inflation could succussesfuly occur. Then, the scalar potential is now given by eqs.(3.67), (3.72) and (3.71).

In order to achieve successful inflation and the observed values of the vacuum energy density, first we fix the parameter c_2. We choose reasonable parameters, then the typical form of the scalar potential is given, shown in Fig. 3.23. One can find that the slow roll conditions are satisfied in some parameter regions. Here, we propose the reasonable sample values of the parameters in Table 3.4, focusing on a theoretical consistency with the original framework in this section 3.4.1.

In the case that there are some uplifting terms V_0 in the original potential eq.(3.67), we also consider the successful inflation scenarios. For instance, the case for V_0 is constant, the results are given in Table 3.5.

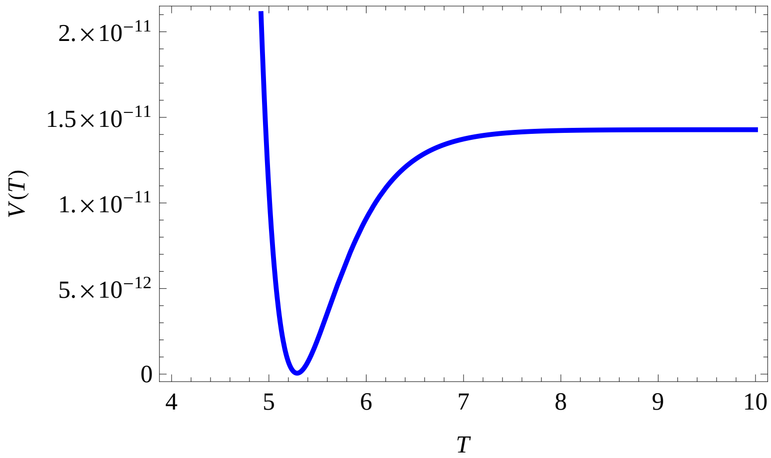

Figure 3.23: - A canonically normalized potential which is given by eqs.(3.67), (3.72) and (3.71), while the original one is already shown in Figure. 3.22. We put the parameters as ($a_1 = 1$, $a_2 = 1$, $a_3 = 1$, $c_1 = 1.01$, $c_2 = 250$).

r	n_s	α_s
$[5.21 \times 10^{-4}, 5.37 \times 10^{-4}]$	$[0.9611, 0.9674]$	$[-1.01 \times 10^{-5}, -5.93 \times 10^{-6}]$

Table 3.4: The parameter sets ($a_1 = 0.459$, $a_2 = 0.459$, $a_3 = 1$, $c_1 = 1 + 10^{-8}$, $c_2 = 0.379$) and inflationary predictions. The left and right values correspond to $N = 50$ and $N = 60$, respectively, and $P_\xi = 2.20 \times 10^{-9}$ for $N = 55$.

In another case, one can assume the D-term up-lifting term

$$V_0 = \frac{a_4}{(T + \bar{T})^\rho}, \tag{3.73}$$

where a_4 is a free parameter, and ρ is the modular wight. Also, in this case, we found that inflation occurs successfully. We exhibit the results in Table 3.6. In our analysis, we show only $\rho = 3$ case, while we have to check other cases. So far, we found for $\rho = 2$, the inflation could not occur due to the difficulty of realizing a flat potential.

Here, we just show reasonable parameter sets (a_1, a_2, a_3(, a_4), c_1, c_2), and investigated whether the inflation could succussfully occur. As a result, so far, in any case, we can find suitable parameters which do not conflict with observable data.

In such the scenario discussed this section, the string axiverse scenario may highly depend on details. Such an analysis is beyond our scope of this section. Therefore, the detail discussion of moduli phenomenology will be left for future work.

r	n_s	α_s
$[5.37 \times 10^{-4}, 3.74 \times 10^{-4}]$	$[0.9604, 0.9669]$	$[-1.06 \times 10^{-5}, -6.18 \times 10^{-6}]$

Table 3.5: The parameter sets ($a_1 = 1.45$, $a_2 = 1.45$, $a_3 = 1$, $c_1 = 1$, $c_2 = 0.00675$, $V_0 = 1.45 \times 10^{-11}$) and inflationary predictions. The left and right values correspond to $N = 50$ and $N = 60$, respectively, and $P_\xi = 2.20 \times 10^{-9}$ for $N = 55$.

r	n_s	α_s
$[5.37 \times 10^{-4}, 3.74 \times 10^{-4}]$	$[0.9604, 0.9669]$	$[-1.06 \times 10^{-5}, -6.18 \times 10^{-6}]$

Table 3.6: The parameter sets ($a_1 = 0.0459$, $a_2 = 0.0459$, $a_3 = 1$, $a_4 = 5.82 \times 10^{-5}$, $c_1 = 1 + 10^{-7}$, $c_2 = 12.1$, $\rho = 3$) and inflationary predictions. The left and right values correspond to $N = 50$ and $N = 60$, respectively, and $P_\xi = 2.20 \times 10^{-9}$ for $N = 55$.

3.5 Conclusion

We have studied the axion inflation model proposed recently within the framework of type IIB superstring theory with a particular emphasis on the sub-Planckian axion decay constant, $0.01 \lesssim f \lesssim 1.0$. The axion potential with such a sub-Planckian decay constant possesses many flat plateaus and the small field inflation can be realized with a sufficient number of e-folds.

In section 3.2, A notable feature of our scenario with a small decay constant f is the low inflation energy scale $V_{inf} \propto f^4$ (eq. (3.12)). The implications of the consequent low reheating temperature in our string axion inflation scenarios were discussed including the dark matter abundance, gravitino/moduli problem and the isocurvature fluctuations of the QCD axion. More detailed studies would be of great interest where we combine concrete mechanism for the moduli stabilization/uplifting, fix the mass scale of light moduli, choose a candidate for dark matter, and embed the QCD axion in superstring theory. We leave such detailed studies through the concrete models and their generalization for the next section.

We have studied one concrete potential which is derived from superstring theory. The shift symmetry of axion is violated by quantum effects inducing the axion potential. Such an axion potential consists of the mixture of polynomial functions and sinusoidal functions with the periodicity $\phi \sim \phi + 2\pi/f$, represented as $V(\phi^m, \cos(\phi/f), \sin(\phi/f))$. Similar but different forms including sinusoidal functions could be derived from another setup different from our choice in superstring theory. For a small decay constant $f \ll 1$, such a potential can have many bumps and plateaus with the size of the flat regime $f/(2\pi)$, and the small field inflation can be realized on one of the plateaus.

We expect our concrete examples discussed in our paper can capture the generic features for a wider class of axion inflation consisting of the sinusoidal and polynomial terms with a sub-Planckian axion decay constant. For instance, let us assume that the sinusoidal parts are dominant in some derivatives of the potential. We then would find $V^{(n+1)} \sim V^{(n)}/f$ with $n \geq n_0$ for a certain value n_0, where $V^{(n)}$ denotes the n-th derivative [1]. Analogous to Eq. (3.10), we can then make a similar Ansatz, $\eta \sim \Delta\phi f^{-p}$. Here, p would depend on the form of the potential, e.g. n_0, while $p = 2$ in our model presented in this section. This would lead to $r \sim 10^{-6} \times f^{2p}$ when the tensor-to-scalar ratio is small $r < \mathcal{O}(10^{-2})$ and we can estimate $2\eta \approx n_s - 1 \approx 0.03$. In such a model analogous to our discussion in this section, the inflation energy scale and Hubble parameter could have the power law dependence on f and hence become rapidly small as f becomes small. As a consequence, the reheating temperature would become small too, although its precise value depends on the detailed reheating processes such as couplings between the inflaton and light modes. We would also be able to put the tight lower bound on f from the BBN so that $T_{\text{reh}} > \mathcal{O}(1)$ MeV. Confirming such a generalization of our study is quite fascinating, and we have planned to present the analysis extending our studies here for a wider class of axion inflation models which can be explicitly derived from superstring theory.

In section 3.3, We have discussed the general class of small-field axion inflation which is the mixture of polynomial and sinusoidal functions with an emphasis on the small axion decay constant compared with the Planck scale. In contrast to the large-field axion inflation, such as the natural inflation (18) and axion monodromy inflation (36), the small-field axion inflation predicts that the small amount of primordial gravitational wave and low inflation scale. This class of inflation models is motivated by the weak gravity conjecture which prohibits the trans-Planckian axion decay constant and the constraint from isocurvature perturbation due to the QCD axion. When the axion decay

[1] $V^{(n+1)} \sim V^{(n)}/f$ can well happen for a higher derivative of the potential including the sinusoidal terms because a polynomial term vanishes at a sufficiently large n

constants and parameters in the scalar potential satisfy the certain conditions leading to the successful small-field axion inflations as discussed in sections 3.3.1, 3.3.2, we find that the cosmological observables are written in terms of the axion decay constants in a systematic way.

In section 3.4, we have studied a new type of moduli potential and stabilization. In the model with Kähler moduli, this model has the flat direction along both $\mathrm{Re}(T)$ and $\mathrm{Im}(T)$ at the tree level. The SUSY vacuum and SUSY breaking vacuum are degenerate, but the SUSY vacuum corresponds to the decompactification limit $\mathrm{Re}(T) \to \infty$. In this model, the modulus F term depends only on $\mathrm{Re}(T)$. The real part $\mathrm{Re}(T)$ can be stabilized by inclusion of α' corrections and loop effects due to $\mathrm{Re}(T)$-dependent gaugino and sfermion masses. However, the axion $\mathrm{Im}(T)$ remains massless at this stage. We extend the model with the single Kähler modulus to the inflation. The result is that it is possible if some parameters are tuned even in the case for adding the p-lifting terms. Also, in this model, one of the light axions could derive the cosmological inflation if a proper potential is generated. Moreover, these axions would be interesting from the viewpoint of a string axiverse. Such axion phenomenology would be studied elsewhere.

Part II

SUPERSYMMETRY AND COSMOLOGY

4

Cosmological aspects of Supersymmetry

In this chapter, we collectively review of Supersymmetry, which is attractive from both theoretical and phenomenological point of view. We also remark on some aspects of Cosmology in the context of Supersymmetry field theory. Note that here, we do not concern about a concrete SUSY breaking mediation model and its breaking scale, just discuss the implications of cosmology for supersymmetry, and vice versa.

4.1 Supersymmetry

Since there are several problems in the standard model of high-energy physics, Many scientists actively work for the resolution. Naively, we suppose that the new physics beyond the standard model based on (spontaneously broken) symmetries, and it would describe a unified picture of those symmetries from the point of view of simplicity and minimality. In the following, we introduce the supersymmetry as a new physics and its motivations.

As we mentioned, the standard model can reproduce the experimental results as well as expected. However, such results are only described under the around TeV scale. This fact suggests that the standard model as a weak scale have to be extended in order to describe the higher energy scale. Also, from viewpoint of Planck scale ($M_p = 2.4 \times 10^{18}$) theory, we can naively expect the new physics in the Tev scale, discussing some effective theory as a Planck scale theory. In this sense, supersymmetry also seems to be a fundamental theory beyond the standard model. The supersymmetry is motivated due to the following reasons:

- solution to the gauge hierarchy problem,
- suggests the unification of gauge couplings,
- provides the candidate of the dark matters.

Not only for the above theoretical powerful motivations, but also for the existence of the experimental hints, the supersymmetry theory became the frontiers of the particle physics. Supersymmetry scenario is especially satisfying the solution to the hierarchy problems, which requires at least $\mathcal{O}(10^{-32})$ level of fine tunings among the parameters in the Higgs sector of the standard model. Indeed, supersymmetry assumed as a simple structure relaxes such the tunings. Hence, it is important to study from the theoretical predictions, and we have to test it by experiments to confirm phenomenologically. Unfortunately, so far [1] experimental signals for supersymmetry has never been confirmed. The breaking mechanism itself does not tell us where the supersymmetry breaking scale should be. Thus, the scale is to be set by phenomenological considerations.

The supersymmetry is a symmetry to transform a bosonic state into a fermionic state, and vice versa,

$$Q|\text{fermion}\rangle = |\text{boson}\rangle, \qquad Q|\text{boson}\rangle = |\text{fermion}\rangle. \tag{4.1}$$

Here, the operator Q generates such a transformation, whose complex object $Q^\dagger$ is also a symmetry generator. For realistic theories, like the standard model, this symmetry implies that the complex generators Q and $Q^\dagger$ must satisfy an algebra of anticommutation and commutation relations with schematic form

$$\{Q,\ Q^\dagger\} = P^\mu, \qquad \{Q,\ Q\} = \{Q^\dagger,\ Q^\dagger\} = 0, \qquad [P^\mu,\ Q] = [P^\mu,\ Q^\dagger] = 0, \tag{4.2}$$

where P^μ is the four-momentum generator of space-time translations. Since Q carry spin 1/2, it is clear that the supersymmetry must be a space-time symmetry. Note that the above relations are restricted by the Haag-Lopuzanski-Sohnius (68) extension of the Coleman-Mandula (69).

[1] at present: February 19, 2019

4.2 Minimal Supersymmetric Standard Model (MSSM) and its extension

We give a brief review of the minimal supersymmetric standard model (MSSM) which is the simplest extension of the standard model. For more detail, see Ref. (70).

In a supersymmetric extension of the standard model, the fundamental known particles become chiral and gauge supermultiplet, and must have superpartners with spin differing by 1/2. The squarks, sleptons, and gauginos present as the superpartners of quarks, leptons, and gauge boson, respectively. The field contents of MSSM are summarized in Table 4.1 and Table 4.2 (70). Note that when we extend the Higgs field to superfield, anomaly cancellation in the standard model appears again due to the new fermions, called a higgsino. In order to avoid this difficulty, we add another Higgs doublet superfield which has the opposite hypercharge. These Higgs fields are often denoted by H_u and H_d as a minimal extension of the standard model.

Names		spin 0	spin 1/2	$SU(3)_C, SU(2)_L, U(1)_Y$
squarks, quarks	Q	$(\tilde{u}_L, \tilde{d}_L)$	(u_L, d_L)	$(\mathbf{3}, \mathbf{2}, \frac{1}{6})$
	$\bar{u}$	$\tilde{u}_R^*$	$u_R^\dagger$	$(\bar{\mathbf{3}}, \mathbf{1}, -\frac{2}{3})$
	$\bar{d}$	$\tilde{d}_R^*$	$d_R^\dagger$	$(\bar{\mathbf{3}}, \mathbf{1}, \frac{1}{3})$
slepton, lepton	L	$(\tilde{\nu}, \tilde{e}_L)$	(ν, e_L)	$(\mathbf{1}, \mathbf{2}, -\frac{1}{2})$
	$\bar{e}$	$\tilde{e}_R^*$	$e_R^\dagger$	$(\mathbf{1}, \mathbf{1}, 1)$
Higgs, higssino	H_u	(H_u^+, H_u^0)	$(\tilde{H}_u^+, \tilde{H}_u^0)$	$(\mathbf{1}, \mathbf{2}, +\frac{1}{2})$
	H_d	(H_d^0, H_d^-)	$(\tilde{H}_d^0, \tilde{H}_d^-)$	$(\mathbf{1}, \mathbf{2}, -\frac{1}{2})$

Table 4.1: Denote the chiral supermultiplets in the standard model. All fermion fields are defined in terms of the two-component left-handed spinors. Note that tilde, like as $\bar{u}$, $\bar{d}$, $\bar{e}$ indicate the superpartners of the corresponding standard model fields, do not have meanings of its conjugate. There are 3 families in the quarks and leptons.

In the MSSM, under the gauge invariance and the R-parity, the superpotential is given as

$$W_{\text{MSSM}} = \bar{u}\mathbf{y_u}QH_u - \bar{d}\mathbf{y_d}QH_d - \bar{e}\mathbf{y_e}LH_d + \mu H_u H_d \tag{4.3}$$

Names	spin 1/2	spin 1	$SU(3)_C, SU(2)_L, U(1)_Y$
gluino, gluon	$\bar{g}$	g	$(\mathbf{8}, \mathbf{1}, 0)$
wino, W bosons	$\tilde{W}^{\pm}, \tilde{W}^0$	$W^{\pm}, W^0$	$(\bar{\mathbf{1}}, \mathbf{3}, 0)$
bino, B boson	$\tilde{B}^0$	B^0	$(\bar{\mathbf{1}}, \mathbf{1}, 0)$

Table 4.2: Gauge supermultiplets in the MSSM.

with $A \cdot B \equiv A_\alpha B_\beta \epsilon^{\alpha\beta}$ [1], and $\mathbf{y_u}$, $\mathbf{y_d}$, and $\mathbf{y_e}$ are dimensionless Yukawa couplings. The last term μHH is the so-called μ-term, where μ has mass dimension one, and it is the only dimensionful parameter in the MSSM superpotential. The μ-term corresponds to the Higgs mass term in the standard model, written as,

$$H_u = \begin{pmatrix} H_u^+ \\ H_u^0 \end{pmatrix}, \quad H_d = \begin{pmatrix} H_d^0 \\ H_d^- \end{pmatrix} \tag{4.4}$$

Note that the holomorphy of the MSSM sperpotential requires both H_u and H_d. This is another reason why we need at least two Higgs doublets in the MSSM superpotential.

A realistic phenomenological model must have supersymmetry breaking because from a theoretical point of view we expect if it exists, superpartners of standard model particles are massless. Therefore, in addition to being supersymmtric, the MSSM also contains the soft supersymmetry breaking terms under the gauge invariance and the R-parity;

$$\begin{aligned} \mathcal{L}_{\text{soft}} = &-\frac{1}{2}(M_3\tilde{g}\tilde{g} + M_2\tilde{W}\tilde{W} + M_1\tilde{B}\tilde{B} + h.c.) \\ &- (\tilde{\bar{u}}\mathbf{a_u}\tilde{Q}H_u - \tilde{\bar{d}}\mathbf{a_d}\tilde{Q}H_d - \tilde{\bar{e}}\mathbf{a_e}\tilde{Q}H_d + h.c.) \\ &- \tilde{Q}^\dagger\mathbf{m_Q}^2\tilde{Q} - \tilde{L}^\dagger\mathbf{m_L}^2\tilde{L} - \tilde{\bar{u}}^\dagger\mathbf{m_{\bar{u}}}^2\tilde{\bar{u}}^\dagger - \tilde{\bar{d}}^\dagger\mathbf{m_{\bar{d}}}^2\tilde{\bar{d}}^\dagger - \tilde{\bar{e}}^\dagger\mathbf{m_{\bar{e}}}^2\tilde{\bar{e}}^\dagger \\ &- m_{H_u}^2 H_u^* H_u - m_{H_d}^2 H_d^* H_d - (bH_uH_d + h.c.) \end{aligned} \tag{4.5}$$

where $M_{1,2,3}$ are bino, wino, gluino, mass terms, $a_{u,d,e}$ are 3-point coupling of scalars, $m^2_{Q,L,\bar{u},\bar{d},\bar{e}}$ are squark and slepton mass terms, m_{H_u,H_d}, b are contributions from SUSY breaking to Higgs potential respectively. This is a generic soft SUSY breaking Lagrangian, and parameters in the above eq.(4.5) introduce new sources of flavor and CP violation, which are restricted by low-energy precision experiments (71). Since

[1] The convention of the supersymmetry notation is defined in Appendix A.

supersymmetry should be an exact symmetry that is broken spontaneously, the underlying model also supersymmetric Lagrangian, but vacuum state is not. Therefore, we naively suppose that the supersymmetry is hidden at low energy scale, some kind of mechanism passes down, so-called the mediation mechanism. Although many models of spontaneous SUSY breaking have been proposed, we do not mention any of them in this thesis.

Including the soft SUSY breaking terms, eq.(4.5), MSSM yields the scalar potential, and its vacuum corresponds to the ground state of the theory. Finally, in the following section, let us discuss the Higgs scalar potentials and standard model Higgs mass in the same manner of the electroweak symmetry breaking mechanism. Here, we assume that only the Higgs bosons in the MSSM have the VEVs, on the other hand, especially, squarks and sleptons do not get

VEVs because they have large positive squared masses. Then, the Higgs scalar potential in the MSSM is given as

$$\begin{aligned} V_{\text{Higgs}} &= \left(|\mu|^2 + m_{H_u}^2\right)\left(|H_u^0|^2 + |H_u^+|^2\right) + \left(|\mu|^2 + m_{H_d}^2\right)\left(|H_d^0|^2 + |H_d^-|^2\right) \\ &+ \left[b(H_u^+ H_d^- - H_u^0 H_d^0) + h.c.\right] \\ &+ \frac{g_1^2 + g_2^2}{8}\left(|H_u^+|^2 + |H_u^0|^2 - |H_d^0|^2 - |H_d^-|^2\right)^2 + \frac{g_2^2}{2}\left|H_u^0 H_d^{-\dagger} + H_u^+ H_d^{0\dagger}\right|^2, \end{aligned} \tag{4.6}$$

where g_1, g_2 are the coupling constants of $U(1)_Y$ and $SU(2)_L$, respectively. Here, we demand that a minimum of the potential breakdown electroweak symmetry to electromagnetism ($SU(2)_L \times U(1)_Y \to U(1)_{EM}$). In this case, we can rotate away from a possible VEV for one component of one of the scalar fields by using the $SU(2)_L$ gauge transformation. As a result, one can always take $\langle H_u^+ \rangle = 0$ at the minimum of potential without loss of generality. Further, we can take $\langle H_d^- \rangle = 0$ due to satisfing the stationary condition, $\partial V / \partial H_u^+ = 0$. Then, after these two conditions, $H_u^+ = H_d^- = 0$ are set, we reduce the eq.(4.6), and only consider the following potential consisting of only the neutral scalar component fields,

$$\begin{aligned} V_{\text{Higgs}} &= \left(|\mu|^2 + m_{H_u}^2\right)|H_u^0|^2 + \left(|\mu|^2 + m_{H_d}^2\right)|H_d^0|^2 \\ &- \left[b H_u^0 H_d^0 + h.c.\right] + \frac{g_1^2 + g_2^2}{8}\left(|H_u^0|^2 - |H_d^0|^2\right)^2. \end{aligned} \tag{4.7}$$

The only b-term depends on the phase of the field, but we can redefine the phases of H_u^+ or H_d^- such that the b is real and positive.

When the potential eq.(4.7) has a minimum, parameters of it are restricted. Here, we write the vev of the Higgs fields as

$$\langle H_u^+ \rangle = v_u, \qquad \langle H_d^- \rangle = v_d. \tag{4.8}$$

These vevs are related to the known Z boson mass m_Z and the electroweak gauge couplings

$$v_u^2 + v_d^2 = v^2 = \frac{2m_Z^2}{g_1^2 + g_2^2} \simeq (174\text{GeV})^2. \tag{4.9}$$

Conventionally, the ratio of the vevs is denoted by

$$\tan\beta \equiv \frac{v_u}{v_d}, \qquad \left(0 < \tan\beta < \frac{\pi}{2}\right), \tag{4.10}$$

leading to

$$v_u = v\sin\beta, \qquad v_d = v\cos\beta. \tag{4.11}$$

The W and Z boson mass are given by

$$m_W = \frac{1}{2}g_2^2 v^2, \qquad m_Z = \frac{1}{2}(g_1^2 + g_2^2)v^2, \tag{4.12}$$

which are identical to the standard model case.

The Higgs scalar fields in the MSSM consist of eight real, scalar degree of freedom. When the electroweak symmetry is broken in the potential eq.(4.6), three of them would be eaten by Z^0, $W^\pm$ as Nambu-Goldstone bosons. The remaining five Higgs scalar masses consist of two CP-even neutral scalars h^0, H^0, one CP-odd neutral scalar A^0, and a charge ± 1 scalar $H^\pm$,

$$\begin{aligned} m_{A_0}^2 &= 2b\csc(2\beta) \\ m_{H^\pm}^2 &= m_{A_0}^2 + m_W^2 \\ m_{H_0}^2 &= \frac{(m_{A_0}^2 + m_Z^2) + \sqrt{(m_{A_0}^2 + m_Z^2)^2 - 4m_{A_0}^2 m_Z^2 \cos^2 2\beta}}{2} \\ m_{h_0}^2 &= \frac{(m_{A_0}^2 + m_Z^2) - \sqrt{(m_{A_0}^2 + m_Z^2)^2 - 4m_{A_0}^2 m_Z^2 \cos^2 2\beta}}{2} \end{aligned} \tag{4.13}$$

which are calculated by taking account of the mass matrix of Higgs scalar. From eq.(4.13), we can find that the mass of the lighter CP-even Higgs boson m_h is bounded at tree-level,

$$m_{h^0} \leq m_Z|\cos(2\beta)|. \tag{4.14}$$

This fact suggests that the lightest Higgs boson of the MSSM is smaller than the Z boson mass at tree-level, which would be disfavored by current experiment results, originated from the quartic coupling of the MSSM Higgs potential as seen in the eq.(4.7). However, quantum corrections drastically change this situation (72, 73, 74, 75, 76). The largest contribution is typically come from stop loops due to the large Yukawa coupling. Including such the correction, the resultant Higgs mass at one-loop level is given by

$$\Delta(m_{h^0}^2) = \frac{3}{4\pi^2} v^2 y_t^4 \sin\beta \ln\left(\frac{m_{\tilde{t}_1} m_{\tilde{t}_2}}{m_t^2}\right) \simeq \frac{(90\text{ GeV})^2}{\sin^2\beta}, \tag{4.15}$$

where m_t is the top mass, and $m_{\tilde{t}_{1,2}}$ are the stop mass. Note that we cannot take $\sin\beta$ to be too small otherwise, the top Yukawa coupling will blow up at a relatively low scale. From the above calculation, one finds large enough 126 GeV Higgs mass when the stop mass is sufficiently large. This shows that m_h can exceed the experimental bounds. Note that including all of the sparticle that can contribute to m_h^2 in loops, one can obtain an interesting bound

$$m_{h^0} \lesssim 135\text{ GeV} \tag{4.16}$$

in the MSSM (70) (see also the references thereinn). By adding extra supermultiplet to the MSSM, this bound can be made even weaker.

4.3 Cosmological aspects of supersymmetry

In order to construct realistic cosmological models, it is important to survey them depended on the supersymmetry. Here, we want to discuss the implications of cosmology for supersymmetry, and vice versa. We selectively include that motivation for the next-to-minimal supersymmetric standard model (NMSSM) and the domain wall problems in the NMSSM in section 4.3.1 and section 4.3.2, and about a baryogenesis and itself from the Affleck-Dine mechanism in section 4.3.3 and section 4.3.4.

4.3.1 Next-to-minimal supersymmetric standard model (NMSSM)

As we mentioned above, the MSSM has phenomenologically quite fascinating features, and it is predicted as a new physics in TeV scale. However, from theoretical points of view, actually, the MSSM includes a serious problem; μ-problem, which originates from the Higgs mass term in the MSSM superpotential. In order to reproduce a Higgs VEV of order 174 GeV without cancellation between $|\mu|^2$ and soft mass terms, naively we expect that μ should be rough of order 10^2 - 10^3 GeV. Then, why should $|\mu|^2$ be small or why should it be rough of the same order of soft mass terms? This is the μ-problem.

There are various models which solve the μ-problem, the simplest extension of the particle contents of MSSM is proposed (77), (78, 79, 80, 81, 82, 83, 84, 85, 86), adding a new gauge singlet chiral supermutiplet. This model is often called NMSSM. Generally, in the NMSSM the new superpotential and Lagrangian is invariant under discrete symmetry, Z_3-symmetry to extract dimensionful terms in the NMSSM superpotential. For every chiral superfield, we impose

$$\Phi \to e^{2\pi i/3}\Phi, \tag{4.17}$$

and all gauge and gaugino fields are inert. Then, we could write down the renormalizable NMSSM superpotential;

$$W_{\mathrm{NMSSM}} = \lambda S H_u H_d + \frac{\kappa}{3} S^3 + W_{\mathrm{Yukawa}} \tag{4.18}$$

where κ and λ are dimensionless couplings. After the Z_3-symmetry is broken spontaneously and a new singlet S get a VEV, $\langle S \rangle \equiv s$, an effective μ-term for $H_u H_d$ will arise as

$$\mu_{\mathrm{eff}} = \lambda s. \tag{4.19}$$

It is determined by the dimensionless coupling and the soft mass terms, which then solves the μ-problem of the MSSM. The detail of NMSSM and μ-problem is discussed in the next chapter 5.

4.3.2 Domain wall problem

In the following, let us review the domain wall solution in the Z_3 symmetric NMSSM. We already know the Z_3-symmetry prohibit the dimensionful parameters in the superpotential and Lagrangian in the NMSSM. However, there is a cosmological problem; domain wall problem. Generally, discrete symmetries can generate domain wall problems, once they are spontaneously broken. In the early universe, domain walls in the NMSSM are generated which can dominate the energy density of the universe, creating unfavorable large anisotropies of the cosmic microwave background and spoiling successful Big-Bang nucleosynthesis (87). Subsequently solutions of this problem have been proposed in (88, 89, 90), hereafter, we do not pursue these solutions and just review about the domain wall solution (91).

Again, discrete symmetries can generate domain wall. Then, we consider a following Lagrangian which has Z_N discrete symmetries for a complex scalar field

$$\mathcal{L} = (\partial_\mu \phi)^\dagger (\partial^\mu \phi) - \frac{1}{4}\lambda(\phi^\dagger \phi - \eta^2)^2 + 2\frac{m^2\eta^2}{N^2}(\cos N\theta - 1), \tag{4.20}$$

where N is an integer, $\eta = \langle \phi \rangle$. At a low-energy scale, we assume that $\phi = \eta e^{i\theta}$, leading to an effective Lagrangian or θ as

$$\begin{aligned} \mathcal{L}_\theta &= \eta^2 (\partial_\mu e^{i\theta})^\dagger (\partial^\mu e^{i\theta}) - \frac{1}{4}\lambda(\eta^2 - \eta^2)^2 + 2\frac{m^2\eta^2}{N^2}(\cos N\theta - 1) \\ &= \eta^2 (\partial_\mu \theta)^2 + 2\frac{m^2\eta^2}{N^2}(\cos N\theta - 1). \end{aligned} \tag{4.21}$$

The potential minimum in this potential exists at $\theta = \frac{2\pi n}{N}$ (with $n = 0, 1, \cdots, N-1$, and we can see these vacua are separated by the domain walls. Such a Domain wall solution between vacua is calculated as follows. From eq.(4.21), equation of motion for θ is given

$$\begin{aligned} \eta^2 \partial_\mu \partial^\mu \theta + 2\frac{m^2\eta^2}{N^2} \cdot N \sin N\theta &= 0 \\ \frac{d^2\theta}{dz^2} - \frac{m^2}{N}\sin N\theta &= 0. \end{aligned} \tag{4.22}$$

Here we assume that the domain wall is vertical to z-axis and is stationary, or time independent. This equation form relates to the sine-Gordon equation for $N = 1$. We solve the eq.(4.22), then,

$$\begin{aligned} \frac{d\theta}{dz} \cdot \frac{d^2\theta}{dz^2} - \frac{m^2}{N}\frac{d\theta}{dz} \cdot \sin N\theta &= 0 \\ \left(\frac{d\theta}{dz}\right)^2 &= -\frac{2m^2}{N^2}\cos N\theta + C_1. \end{aligned} \tag{4.23}$$

Now we chose $\theta \to 0,\ \frac{2\pi}{N}$ at $z \to -\infty,\ +\infty$,

$$C_1 = \frac{2m^2}{N^2}. \tag{4.24}$$

Therefore, we find

$$\begin{aligned} \left(\frac{d\theta}{dz}\right)^2 &= \frac{2m^2}{N^2}(1 - \cos N\theta) \\ \frac{d\theta}{\sin\left(\frac{N\theta}{2}\right)} &= \pm\frac{2m}{N}dz. \end{aligned} \tag{4.25}$$

By integrating above equation, the left hand side of it becomes as

$$\begin{aligned}(L.H.S) &= \int d\theta \frac{1}{\sin\left(\frac{N\theta}{2}\right)} \\ &= \frac{1}{N}\log\left(\tan^2\left(\frac{N\theta}{4}\right)\right) + C_2 \end{aligned} \tag{4.26}$$

and right hand side as

$$\begin{aligned}(R.H.S) &= \pm\int dz \frac{2m}{N} \\ &= \pm\frac{2m}{N}z + C_3. \end{aligned} \tag{4.27}$$

Then, we obtain the equation of motion of θ for z-axis

$$\begin{aligned}\frac{1}{N}\log\left(\tan^2\left(\frac{N\theta}{4}\right)\right) &= \pm\frac{2m}{N}z + C_4 \\ \theta &= \frac{4}{N}\arctan\left(e^{\pm m(z-z_0)}\right), \end{aligned} \tag{4.28}$$

where z_0 is a constant of integration. This is the domain wall solution.

Further, we define the tension (surface energy density) of domain wall σ, which characterize the domain wall qualitativety, related to the product of energy density and thin of domain wall,

$$\sigma = \int dz\ \rho_{DW} = \int dz\ \left((\partial_\mu\phi)^\dagger(\partial^\mu\phi) - V(\phi)\right) = 2\int dz\ \left|\frac{d\phi(z)}{d\theta}\right|^2. \tag{4.29}$$

Remaining

$$\begin{aligned}\left|\frac{d\phi(z)}{d\theta}\right|^2 &= \eta^2\left(\frac{d\theta}{dz}\right)^2 \\ &= \left(\frac{2m\eta}{N}\right)^2 \frac{1}{\cosh^2\left(m(z-z_0)\right)}, \end{aligned} \tag{4.30}$$

and then, we get

$$\begin{aligned}\sigma &= 2\left(\frac{2m\eta}{N}\right)^2 \int_{-\infty}^{\infty} dz \frac{1}{\cosh^2\left(m(z-z_0)\right)} \\ &= \frac{16m\eta^2}{N^2}. \end{aligned} \tag{4.31}$$

Above general results is used in chapter 5.

Our study related to this subsection is summarized in chapter 5, see it.

4.3.3 Baryon asymmetry

The baryon asymmetry of the universe is one of the intriguing puzzles in our universe. We have shown our attitude toward the inflation and proposed the concrete our models. Depending on its motivation, one of the most important points of the inflation model is that dilute unwanted relics, i.e. gravitino and moduli which contribute too generous to the present energy density leading to unsuccessful standard cosmology. However, inflation has serious negative parts: it also dilutes the baryon asymmetry in our understanding of the universe. Thus, the baryon asymmetry might be washed out by the inflation, even in the case of the lepton-number violation through the sphaleron processes (once the net lepton number is generated, it is transferred into the baryon number via the sphaleron process). So, the baryogenesis (leptogenesis) is phenomenologically interesting, and we eagerly desire the baryogenesis (leptogenesis) scenario for the great triumph of particle cosmology.

Compared to particles or matters, there are few antiparticles (antimatter) on large scale, around 10 Mpc at least, and this fact suggests that some mechanism of baryogenesis work on between particles and antiparticles during cosmological evolution. The baryon number of the universe may be explained as follows. When the nucleosynthesis begin to occur in the early universe, with the expansion of the universe, the number density of baryons changes as $n_{\rm b} \propto a^{-3} \propto T^3$, where T denotes a temperature of the universe. The number density of baryons with a temperature T is given as

$$n_{\rm b} = n_{\rm b}^{(0)} \left(\frac{T}{T_0}\right)^3 = \Omega_{\rm b}^{(0)} \frac{\rho_0}{m_{\rm p}} \left(\frac{T}{T_0}\right)^3, \qquad (4.32)$$

where $m_{\rm p}$ is proton mass, $\Omega_{\rm b}^{(0)} = m_{\rm p} n_{\rm b}^{(0)}/\rho_0$, ρ_0 is the average energy density of the universe, and (0) means the current values. Since the number density of photons is provided as $n_\gamma = 2\zeta(3)T^3/\pi^2$, the ratio $n_{\rm b}/n_\gamma$ is kept a constant,

$$\eta_{\rm b} \equiv \frac{n_{\rm b}}{n_\gamma} = \frac{\pi^2}{2\zeta(3)} \frac{\rho_0}{m_p} \frac{\Omega_{\rm b}^{(0)}}{T_0^3}. \qquad (4.33)$$

With $m_p = 938$ MeV, $T_0 = 2.725$ K, and current critical density $\rho_0 = 1.878 \times 10^{-26} h^2$ kg m^{-3}, we can obtain easily

$$\begin{aligned} \eta_{\rm b} &= 2.7 \times 10^{-8}\ \Omega_{\rm b}^{(0)} h^2 \\ &\simeq 5.9 \times 10^{-10}. \end{aligned} \qquad (4.34)$$

Here, from the analysis of the anisotropy and polarization of cosmic microwave background data provided by WMAP collaboration(92), we obtain $\Omega_{\mathrm{b}}^{(0)} h^2 = 0.0455 \pm 0.00028$. Also, the ratio n_{b}/s is kept fixed unless the baryon number and entropy are created. The entropy in a temperature T is given as $s = 2\pi^2 g_* T^3/45$, and this leads to

$$\begin{aligned} \frac{n_{\mathrm{b}}}{s} = \frac{45\zeta(3)}{\pi^4 g_*}\eta_{\mathrm{b}} &= 3.8 \times 10{-}9\ \Omega_{\mathrm{b}}^{(0)} h^2 \\ &\simeq 8.4 \times 10^{-11}, \end{aligned} \tag{4.35}$$

where $g_*^{(0)} = 2 + \frac{7}{8} \times 6 \times \frac{4}{11} = 3.91$. Therefore, naively, we need the baryon asymmetry around $n_{\mathrm{b}}/s \sim 10^{-10}$ to explain our present universe.

In order to generate the baryon asymmetry of the universe, the three conditions should be satisfied, which have been pointed out by Sakharov (93); (i) violating baryon (or lepton) number, (ii) violating C and CP, and (iii) dropping out of thermal equilibrium in the early universe.

The leptogenesis (94) is known as one of the most attractive and the relatively simple ways to realize the Sakharov's conditions, and baryon number is generated via the electroweak sphaleron process at high-temperature (95). Then, the sphaleron effect converts lepton number n_{L} to baryon asymmetry

$$\frac{n_{\mathrm{B}}}{s} \sim c_{\mathrm{sph}} \frac{n_{\mathrm{L}}}{s} \tag{4.36}$$

with $c_{\mathrm{sph}} \sim -8/23$ (96, 97) at higher temperature than the electroweak scale in SUSY theories. In our study (chapter 6), we assume lepton asymmetry is originated from a lepton current caused by a large VEV of left- (and right-) handed sneutrino, and such an asymmetry generates the present baryon asymmetry eq.(4.35) which is observed today from CMB data (98).

4.3.4 Affleck-Dine mechanism

As mentioned above, in order to reproduce the baryon asymmetry, we need some interactions which violate the baryon number, or lepton number in the Lagrangian we assumed. If we put the R-parity in a model, there are not such violating interaction, and we have to introduce the non-renormalizable interactions, which seems to be a little complicated and there need the concrete higher scale theory than the electroweak scale which we can observe by some experiments. However, today we know that there exists the neutrino oscillation, and this fact suggests the lepton number violation, leading to baryon asymmetry in a minimal assumption within the framework of supersymmetry. Actually, some studies on the Affleck-Dine mechanism(64, 65) using the Lepton number violation are proposed (99), and in that paper, we can explain that the baryon asymmetry is naturally realized by so-called the Affleck-Dine Leptogenesis.

Here, let us review the Affleck-Dine mechanism (leptogenesis) depending on the LH_u directions. This mechanism is one of the most beautiful scenarios, and the thermal leptogenesis that produces a lepton asymmetry from thermally produced right-handed (s)neutrinos. When the produced right-handed (s)neutrinos are out of equilibrium, finally they decay asymmetrically into leptons and anti-leptons, and thus it generates a net lepton number. In this section, we will a review on the Refs.(65), (99) and references therein. Note that in this review here, we do not introduce the right-handed neutrinos and thermal correction to the effective potentials, for simplicity.

We consider the minimal superpotential within the framework of MSSM. Introducing the effective dimension-five operator in the superpotential, we start wtih following superpotential

$$W = W_{\rm MSSM} + \frac{1}{2M}(LH_u)(LH_u), \tag{4.37}$$

where $m_\nu = v_u^2/M$, $v_u = \langle H_u \rangle = (174~\text{GeV})~\sin\beta$. The second term is necessary to produce the lepton number violation in this model.

There are some flat directions in the MSSM (100). Especially, the LH_u flat direction is one of the most extensively studied. Under the $SU(2)$ gauge transformation, it is parametarized with a complex scalar field ϕ as follows;

$$L = \frac{1}{\sqrt{2}}\begin{pmatrix} \phi \\ 0 \end{pmatrix}, \qquad H_u = \frac{1}{\sqrt{2}}\begin{pmatrix} 0 \\ \phi \end{pmatrix}, \tag{4.38}$$

where L and H_u denote the scalar components of the superfields. In the following, we call ϕ AD-field. Along this flat direction $L = H_u = \phi/\sqrt{2}$, the potential is given by

$$V_F = m^2|\phi|^2 + A\left(\phi^3 + \phi^{*3}\right) + \frac{1}{4M^2}|\phi|^6. \tag{4.39}$$

The last term is F-term potential come from the eq.(4.37), while the first and second term represents soft SUSY breaking terms.

We want to consider the evolution of flat direction of the AD-field. Although this direction is flat before the primordial inflation, it can have a large initial amplitude necessary for this model. During the inflation, the Hubble parameter is almost constant. Within the framework of supergravity, generally, there is a possible negative Hubble mass squared in the scalar potential,

$$V_H = -c|\phi|^2 H^2 \tag{4.40}$$

which is due to the non-zero energy in the early universe parameterized the Hubble parameter H (See Appendix C.3). Here we assume that A, c are $\mathcal{O}(1)$ coefficients depending on a model of the supergravity.

In this era, the AD-field quickly settle down to one of the minima of the scalar potential, eq.(4.39). After AD-field is fixed at a minimum, the Hubble parameter varies in time as $H = 2/(3t)$ with the inflation ends. The AD-field will start coherent oscillation since the negative Hubble mass term is decreased, and effective masses dominate the scalar potential. In such a case, the phase of the AD-field is decided by almost the phase of A-term. The phase direction of AD-field is kicked, and then, Lepton asymmetry is generating through the evolution of AD-field at the time $H \simeq m$, as a result. Based on the discussion here, minimizing

$$V = -cH^2|\phi|^2 + \frac{1}{M^2}|\phi|^6, \tag{4.41}$$

we can estimate the amplitude of the AD-field at the end of inflation,

$$|\phi|^2 \sim M^2 H_{\mathrm{inf}}^2. \tag{4.42}$$

It turns out that the initial value of the AD-field depend on only M and H at the end of inflation.

After the AD-field is destabilized, and given the above initial condition, the equation of motion of AD-field ϕ is written as

$$\ddot{\phi} + 3H\dot{\phi} + V_{\phi^*} = 0. \tag{4.43}$$

The AD-field start coherent oscillation at eq.(4.42), since the negative Hubble mass term is decerésed and effective mass dominated in the scalar potential. After the reheating ends, Lepton asymmetry at this time is easily given as [1],

$$\frac{n_L}{s} \sim \frac{AMT_{reh}}{H_{\mathrm{osc}} M_{pl}^2}\delta_{eff}, \qquad \text{where} \qquad \sin\delta_{eff} = (arg(A))\,. \tag{4.44}$$

[1] We define the ϕ number density and show a concrete evolution of ϕ at the early universe in Appendix C.1

Here we utilize $s_{reh} \sim T_{reh}^3$, $H_{\rm osc}^2 M_{pl}^2 \sim T_{reh}^4$ and assume $H_{\rm osc} \sim m$, and $c \sim 1$, $\delta_{eff} \sim \mathcal{O}(1)$.

By the effects of the sphaleron, the above Lepton asymmetry is partially converted to the Baryon asymmetry. Especially, in the MSSM, we take (96, 97)

$$\frac{n_{\rm B}}{s} = \frac{8}{23}\left|\frac{n_{\rm L}}{s}\right|. \tag{4.45}$$

Then, finally we can obtain the Bryon asymmetry as

$$\frac{n_B}{s} \sim 6 \times 10^{-11} \left(\frac{m_\nu}{10{\rm meV}}\right)^{-1} \left(\frac{m}{1{\rm TeV}}\right)^{-1} \left(\frac{A}{1{\rm TeV}}\right) \left(\frac{T_{reh}}{10^{10}{\rm GeV}}\right). \tag{4.46}$$

Since the lepton number is inversely proportional to the mass of the neutrino, so far we have considered only a lightest neutrino mass m_ν.

Our study related to this subsection is summarized in chapter 6.

5

Entropy production by domain wall decay in the NMSSM

In this chapter, we consider domain walls in the Z_3 symmetric NMSSM. The spontaneous Z_3 discrete symmetry breaking produces domain walls, and the stable domain walls are problematic. Thus, we assume the Z_3 symmetry is slightly, but explicitly broken and the domain walls decay. Such a decay causes a large late-time entropy production. We study its cosmological implications on unwanted relics such as moduli, gravitino, LSP, and axion. Note that this chapter is based on our works (c).

5.1 Introduction

Supersymmetric extension of the standard model (SM) is one of the candidates for TeV-scale physics, because supersymmetry (SUSY) can stabilize a large hierarchy. The minimal supersymmetric standard model (MSSM) is quite interesting because of its minimality, and various phenomenological aspects have been studied. However, from a theoretical point of view, it has a serious problem. The MSSM includes supersymmetric mass terms of Higgs superfields, H_u and H_d i.e. the so-called μ-term, $\mu H_u H_d$, in the superpotential. It must be comparable with soft SUSY breaking masses in order to realize successfully the electroweak symmetry breaking. However, the μ-term and soft SUSY breaking terms, in general, have origins different from each other. Why are these comparable to each other? That is the so-called μ-problem (101).

5. ENTROPY PRODUCTION BY DOMAIN WALL DECAY IN THE NMSSM

The next-to-minimal supersymmetric standard model (NMSSM) is an extension of the MSSM by adding a singlet superfield S (78) [1]. Then, the NMSSM superpotential has $\lambda S H_u H_d$. Also, we impose the Z_3 symmetry, which forbids dimensionful parameters in the superpotential. Dimensionful parameters appear only as soft SUSY breaking parameters. Thus, vacuum expectation values (VEVs) of Higgs and singlet fields are determined by soft SUSY breaking terms. That is, the μ-problem is solved, and the effective μ-term is generated as $\mu = \lambda\langle S\rangle$.

In the NMSSM, the Higgs sector, as well as the neutralino sector, has a richer structure than one in the MSSM, because of inclusion of the singlet superfield S. Also, the NMSSM can raise the SM-like Higgs boson mass. At any rate, heavier superpartner masses such as $\mathcal{O}(1) - \mathcal{O}(10)$ TeV may be favorable. We may need fine-tuning to realize a little hierarchy between the electroweak scale and SUSY breaking scale. However, such a fine-tuning can be improved in a certain mediation mechanism, e.g. in the TeV-scale mirage mediation scenario (102) [2].

The Z_3 symmetry is important to forbid dimensionful parameters in the superpotential and to solve the μ-problem. However, it is problematic. VEVs of the Higgs scalar and singlet break spontaneously the Z_3 symmetry. In general, when a discrete symmetry is spontaneously broken, domain walls appear. They would dominate the energy density of the Universe and change the standard cosmology drastically. Thus, the exact Z_3 symmetry and the stable domain walls are problematic (107). See for the NMSSM (108) .

Here, we assume that the Z_3 symmetry is broken explicitly (e.g. by the hidden sector dynamics (109)), but its breaking size is much smaller than the electroweak scale. Then, the domain walls are unstable. They may dominate the energy density of the Universe at a certain period but decay. It has important effects on thermal history [3]. In this chapter, we study implications of unstable domain walls in the NMSSM. In general, SUSY models have other problems due to moduli, gravitino and the lightest superparticle (LSP). For example, in the gravity mediation scenario, moduli and gravitino masses would be comparable with masses of superpartners in the visible sector. When those are of $\mathcal{O}(1) - \mathcal{O}(10)$ TeV, they affect successful big bang nucleosynthesis

[1] See for a review Ref. (77).

[2] See for phenomenological aspects of MSSM in the TeV-scale mirage mediation scenario (103) and for generic mirage mediation (104, 105, 106).

[3] See e.g. Ref. (110).

(BBN), that is, the so-called moduli-problem and gravitino problem. They could be diluted by the decay of domain walls (60). Furthermore, even if the moduli and gravitino are heavier than superpartners in the visible sector, that would lead to another problem. Indeed, in the mirage mediation mechanism (104), the gravitino is heavier by $\mathcal{O}(8\pi^2)$ than superpartners in the visible sector, and the modulus is also heavier by $\mathcal{O}(8\pi^2)$ than the gravitino. In such a case, the moduli decay into the gravitino with a large rate and the gravitino decays into the LSP. This overproduces non-thermally the LSP (111). We need to dilute the moduli, gravitino and the LSP. Also, in some other scenarios, the LSP such Bino-like neutralino has a large thermal relic density. The decay of domain walls, which was mentioned above, can produce a large entropy and dilute moduli and dark matter candidates in the NMSSM.

This chapter is organized as follows. In section 5.2, we study the domain wall solution in the NMSSM. In section 5.3, we study cosmological evolution of unstable domain walls. In sections 5.4 and 5.5, we study implications of the domain wall decay in two scenarios. Section 5.6 is devoted to conclusion and discussion.

5.2 Domain wall solution in the NMSSM

5.2.1 Domain wall solution in the Z_3 symmetric NMSSM

We briefly review a domain wall solution of the Higgs potential in the Z_3 symmetric NMSSM [1]. We adopt the convention for H_u, H_d and S that the superfield and its lowest component are written in the same letter. The superpotential terms including only H_u, H_d and S are written as

$$W_{\text{Higgs}} = \lambda S H_u H_d + \frac{\kappa}{3} S^3, \tag{5.1}$$

where the Z_3 symmetry is imposed as mentioned. The scalar potential is written by

$$V_{\text{Higgs}} = \sum_{\phi_i = H_u, H_d, S} \left| \frac{\partial W}{\partial \phi_i} \right|^2 + V_D + V_{\text{soft}}, \tag{5.2}$$

[1] The full scalar potential includes superpartners of quarks and leptons, and it has several unrealistic vacua. We assume that taken SUSY breaking parameters in the full potential satisfy the condition to avoid such unrealistic vacua. (See e.g., Ref. (112) and references therein.)

where V_D is the D-term potential due to $SU(2) \times U(1)_Y$ and $V_{\rm soft}$ denotes the soft SUSY breaking terms,

$$V_{\rm soft} = m_{H_u}^2 |H_u|^2 + m_{H_d}^2 |H_d|^2 + \frac{1}{3}\kappa A_\kappa S^3 + \lambda A_\lambda H_u H_d S + h.c. \tag{5.3}$$

Only the neutral components develop their VEVs, and their scalar potential is written explicitly by

$$\begin{aligned} V_{\rm Higgs} &= \left|\kappa S^2 - \lambda H_u^0 H_d^0\right|^2 + m_{H_u}^2 |H_u^0|^2 + m_{H_d}^2 |H_d^0|^2 + m_S^2 \left|S\right|^2 + \left|\lambda\right|^2 \left|S\right|^2 (|H_d^0|^2 + |H_u^0|^2) \\ &\quad + \frac{g^2 + g'^2}{8} \left(|H_u^0|^2 - |H_d^0|^2\right)^2 + \frac{1}{3}\kappa A_\kappa S^3 - \lambda A_\lambda H_u^0 H_d^0 S + h.c., \end{aligned} \tag{5.4}$$

where g and g' are the $SU(2)$ and $U(1)_Y$ gauge couplings, respectively. Here, we assume that all of λ, κ, A_λ and A_κ are real.

The potential minima are obtained by analyzing the stationary conditions,

$$\frac{\partial V_{\rm Higgs}}{\partial H_u^0} = \frac{\partial V_{\rm Higgs}}{\partial H_d^0} = \frac{\partial V_{\rm Higgs}}{\partial S} = 0, \tag{5.5}$$

and these VEVs lead to the successful electroweak symmetry breaking, where the effective μ term is obtained as $\mu = \lambda\langle S\rangle$. Since the scalar potential has the Z_3 symmetry, three vacua are degenerate,

$$\left(\langle S\rangle, \langle H_u^0\rangle, \langle H_d^0\rangle\right) = \left(v_s e^{2\pi i m/3}, v_u e^{2\pi i m/3}, v_d e^{2\pi i m/3}\right), \tag{5.6}$$

with $m = 0, 1, 2$, where all v_s, v_u and v_d are real with $v = \sqrt{v_u^2 + v_d^2} \simeq 174$ GeV. One of three degenerate vacua is selected in the vacuum, and then the Z_3 symmetry is broken spontaneously. Then, the domain walls are generated.

First, we study the domain wall solution (91). We fix field values of radial directions of S, H_u and H_d, and discuss a field equation for the phase degree of freedom ϕ,

$$\left(S, H_u^0, H_d^0\right) = \left(v_s e^{\mathrm{i}\phi}, v_u e^{\mathrm{i}\phi}, v_d e^{\mathrm{i}\phi}\right). \tag{5.7}$$

The potential of ϕ can be obtained from $V_{\rm Higgs}$ as

$$V(\phi) \;=\; -2\left(\frac{1}{3}\left|\kappa A_\kappa v_s^3\right| + \lambda A_\lambda v_s v_u v_d\right)\cos(3\phi) + V_0, \tag{5.8}$$

where V_0 denotes ϕ-independent terms. The first term would be dominant when $A_\kappa \sim A_\lambda$, $\lambda \sim \kappa$ and $v_s^2 \gg v_u v_d$. Also, the kinetic term of ϕ is written by

$$\mathcal{L}_{\rm kinetic}(\phi) \;=\; \eta^2 (\partial_\mu \phi)(\partial^\mu \phi), \tag{5.9}$$

with $\eta^2 = v_s^2 + v_u^2 + v_d^2$.

For simplicity, we consider a planar domain wall orthogonal to the z-axis, $\phi(z)$. Then, the field equation,

$$\partial_\mu \frac{\partial \mathcal{L}_{\text{kinetic}}}{\partial_\mu(\partial\phi)} + \frac{\partial V_{\text{VEV}}}{\partial \phi} = 0, \tag{5.10}$$

can be written by

$$\frac{\mathrm{d}^2\phi}{\mathrm{d}z^2} - \frac{1}{3B^2}\sin(3\phi) \quad = \quad 0, \tag{5.11}$$

with

$$\left(\frac{1}{B}\right)^2 = \frac{9\left(|\frac{1}{3}\kappa A_\kappa v_s^3| + \lambda A_\lambda v_s v_u v_d\right)}{\eta^2}. \tag{5.12}$$

The first term in the numerator of the left hand side of eq. (5.12) is dominant when $v_s^2 \gg v_u v_d$. We set the boundary condition such that $\phi = 2\pi n/3$ at $z \to -\infty$ and $\phi = 2\pi(n+1)/3$ at $z \to +\infty$ with $n = 0, 1, 2$. By solving the above field equation with this boundary condition, the domain wall solution is derived as

$$\phi \quad = \quad \frac{2n\pi}{3} + \frac{4}{3}\arctan\left(\mathrm{e}^{\pm\frac{1}{B}(z-z_0)}\right), \tag{5.13}$$

where B corresponds to the width of the domain wall. Figure 5.1 shows this solution for $n = 0$.

Now, we can estimate the domain wall tension

$$\begin{aligned}\sigma &= \int dz \rho_{\text{wall}}(z) = \int dz \left(\left|\frac{\mathrm{d}S}{\mathrm{d}z}\right|^2 + \left|\frac{\mathrm{d}H_u^0}{\mathrm{d}z}\right|^2 + \left|\frac{\mathrm{d}H_d^0}{\mathrm{d}z}\right|^2 + V(\phi)\right) \\ &= \frac{16}{9}\frac{\eta^2}{B}.\end{aligned}$$

Thus, we can estimate

$$\sigma \simeq \frac{16}{3\sqrt{3}} v_s^2 \sqrt{\kappa A_\kappa v_s} = \frac{16}{3\sqrt{3}}\frac{\mu^2}{\lambda^2}\sqrt{\frac{\kappa}{\lambda}A_\kappa \mu}, \tag{5.14}$$

for $v_s^2 \gg v_u v_d$. The size of μ is of the SUSY breaking scale [1]. The couplings λ and κ must be of $\mathcal{O}(0.1)$ or less at the electroweak scale such that they do not blow up below a high energy scale such as the GUT or Planck scale. Thus, the size of $\sigma^{1/3}$ would be of the SUSY breaking scale or larger. Figure 5.2 shows an example of $\rho_{DW}(z)$.

[1] When μ is much larger than the electroweak scale, we have the fine-tuning problem to derive the Z-boson mass m_Z from $m_{H_u}^2, \mu$, and $m_{H_d}^2$. However, in a certain mediation such as the TeV-scale mirage mediation contributions due to μ and $m_{H_d^2}$ cancel each other in m_Z, and m_Z is independent of μ. Without severe fine-tuning μ can be larger than the electroweak scale, e.g. $\mu = \mathcal{O}(1)$TeV (102).

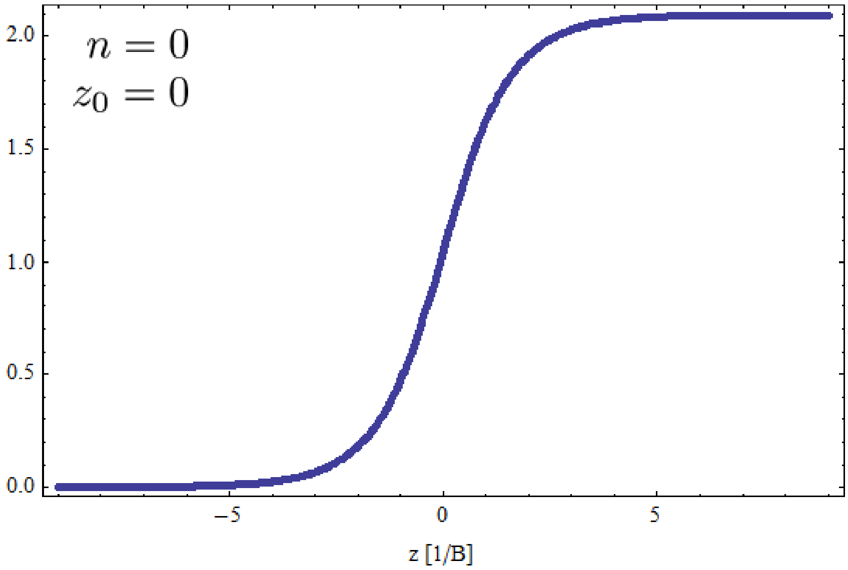

Figure 5.1: - The phase of scaler field$(S(z), H_u(z), H_d(z))$ of planer domain wall solution. Here we take $n = 0$, $z_0 = 0$, and normalize z-axis by $1/B$ (eq. (5.12)).

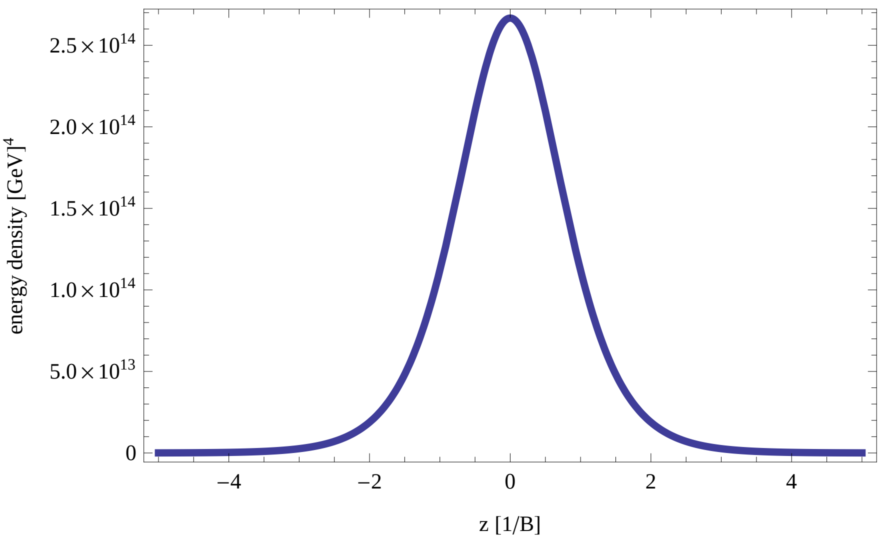

Figure 5.2: - Spatial configuration of a domain wall energy density for $\lambda = \kappa = 0.01$, $A_\lambda = A_\kappa = 10$ TeV, $\mu = 1$ TeV, $\tan\beta = 10$. The z-axis is normalized by $1/B$.

5.2.2 Decaying domain wall by Z_3 breaking

Formed domain walls are stretched by the cosmic expansion and smoothed by interactions with particles in the background thermal plasma. The energy density of domain walls ρ_{DW} and its pressure p_{DW} can be read from the averaged energy-momentum tensor of domain walls. The equation of state of domain walls is given by

$$p_{DW} = \left(v^2 - \frac{2}{3}\right)\rho_{DW}, \tag{5.15}$$

with v being the averaged velocity of walls (113). The dynamics depend on v. In one extremal limit, non-relativistic limit or static limit with $v = 0$, the energy density behaves

$$\rho_{DW} \propto a^{-1}, \tag{5.16}$$

where $a(t)$ is the scale factor of the Universe. Such domain wall network is sometimes referred to as "frustrated domain wall". Such a frustrated domain wall dominated Universe causes acceralating expansion because of $w = p/\rho = -2/3 < -1/3$. On the other hand, for $v^2 \geq 1/3$ where $w \geq -1/3$ is realized, the cosmic expansion is not accelerating.

In fact, the dynamics of domain walls have been investigated and many detailed numerical simulations show that the dynamics of domain wall network is relaxed at a late time to the so-called scaling regime, where the typical length scale ξ of the system stays of the Hubble radius H^{-1} (114, 115, 116, 117, 118, 119). Then, the energy density of domain walls also scales as (119)

$$\rho_{DW} \simeq \frac{\sigma}{t}. \tag{5.17}$$

The energy density of domain wall decreases slower than any other "matter" or radiation in the scaling solution [1]. Thus, at some point, the energy density of domain walls dominates that in the Universe. This is the domain wall problem (107).

Thus, the stable domain wall in the Z_3 symmetric NMSSM is problematic (108). Here, we consider a tiny but explicit breaking of the Z_3 discrete symmetry so that domain walls might have a long lifetime but finally decay. In fact, the decay of domain

[1] In the static limit $v = 0$, it is further slower.

walls after domain wall domination has an interesting cosmological implication, namely the dilution of unwanted relics by late time entropy production (60).

Few numerical detailed studies on the dynamics of the domain walls network in a domain wall dominated Universe has been done. Hence, the domain wall dynamics in a domain wall dominated Universe after its scaling behavior is uncertain. One likely possibility is that the scale of the system remains of the order of the Hubble radius as in the scaling regime after domain wall domination too. This can be realized for the equation of the state $w \simeq -1/3$. Thus, in most of the following analysis, we assume this. On the other hand, there is another possibility that the dynamics after the domination would be frozen as suggested in Ref. (117), where $\xi \propto a(t)$ and $\rho \propto a(t)^{-1}$ are realized as in the non-relativistic limit. We briefly discuss results for this latter case too.

Before closing this subsection, here we briefly note some examples of the Z_3 symmetry breaking in the literature for information. In Ref. (90), Panagiotakopoulos and Tamvakis proposed adding extra symmetries which consistently allows inducing a tiny enough tadpole term

$$\Delta V \sim \frac{1}{(16\pi^2)^n} m_{SUSY}^3 (S + S^*), \tag{5.18}$$

where m_{SUSY} is a soft SUSY breaking mass and n is a power of loop inducing this term, in the scalar potential and the degeneracy of vacua is resolved. Hamaguchi et al proposed another solution by introducing hidden QCD theory, where the Z_3 symmetry becomes anomalous and is broken by quantum effects (109). In such a minor extension of Z_3 symmetric NMSSM, the domain walls become unstable. Since the size of the Z_3 breaking term is highly model dependent and the main purpose is to study the cosmological effects of late time domain walls decay, the decay rate of a domain wall Γ_{DW}, which also parameterize the size of the Z_3 symmetry breaking, is treated as a free parameter. Throughout this paper, in order to connect successful BBN, we take the domain wall decay temperature T_d of a few MeV. We note that the lower bound of the rehearting temperature by late decay objects is about a few MeV (120, 121, 122).

5.3 Cosmological evolution of unstable domain wall

When doublet and/or singlet Higgs fields develop the VEVs, domain walls are formed. For the temperature T_i, the initial energy density of domain walls is estimated as

$$\rho_{DW,i} \sim \sigma H_i. \tag{5.19}$$

As mentioned above, after certain dynamics, the domain wall network would be relaxed to be in the scaling solution. In the scaling regime, the energy density of domain walls is given by

$$\rho_{DW} \simeq \sigma H. \tag{5.20}$$

On the other hand, several domain walls must be inside the horizon not to lead to the old inflation and inhomogeneous Universe until its decay. That requires $T_d^4 > \sigma \Gamma_{DW}$, i.e.

$$T_d^2 \gtrsim \frac{\sigma}{M_P}. \tag{5.21}$$

This is rewritten as

$$T_d \gtrsim 1\,\mathrm{MeV} \left(\frac{\sigma^{1/3}}{10\,\mathrm{TeV}} \right)^{3/2}. \tag{5.22}$$

5.3.1 Matter-dominated era to domain wall dominated era

The first case we consider is that at the domain wall formation time H_i^{-1}, the Universe is dominated by the energy density of a matter ρ_M such as a long-lived coherent oscillating moduli field. In the scaling solution of the domain wall, the energy density of domain walls relative to that of the background increases and eventually dominates the Universe. The domain wall energy density becomes equal to one of the matter at H_{eq}^{-1}, which is estimated with eq. (5.20) as

$$H_{eq} \simeq \frac{\sigma}{3M_P^2}, \tag{5.23}$$

where M_P is the reduced Planck mass. The condition that domain walls indeed dominate the Universe before those decay is expressed as

$$H_{eq} > \Gamma_{DW}. \tag{5.24}$$

After H_{eq}, the domain walls dominate the energy density.

At the domain wall decay time Γ_{DW}^{-1}, the ratio of these energy densities is estimated as

$$\left.\frac{\rho_M}{\rho_{DW}}\right|_{\Gamma_{DW}} = \left(\frac{\Gamma_{DW}}{H_{eq}} \right), \tag{5.25}$$

from $a \propto t$, where we assume $\rho_{DW} \propto a^{-2}$ during the domain wall domination between H_{eq} and Γ_{DW}. After the domain walls decay, the energy density of the matter is diluted as

$$\frac{\rho_M}{s} = \frac{3T_d}{4}\left(\frac{\Gamma_{DW}}{H_{eq}}\right) \simeq \frac{3T_d}{4}\left(\frac{\pi^2 g_*(T_d)T_d^4}{10}\frac{M_P^2}{\sigma^2}\right)^{1/2}, \tag{5.26}$$

for the case that the domain wall decays earlier than the matter does. Here, g_* is the number of relativistic degrees of freedom.

5.3.2 Radiation-dominated era to domain wall dominated era

Next, we discuss the case that domain walls are formed in radiation-dominated Universe. Both energy densities become comparable with each other at

$$H_{eq} \simeq \frac{\sigma}{3M_P^2}, \tag{5.27}$$

since domain walls are in the scaling solution. Assuming $\rho_{DW} \propto a^{-2}$ during the domain wall domination, at the domain wall decay time, we have

$$\left.\frac{\rho_R}{\rho_{DW}}\right|_{\Gamma_{DW}} = \left(\frac{\Gamma_{DW}}{H_{eq}}\right)^4, \tag{5.28}$$

$$\left.\frac{\rho_R}{s}\right|_{\Gamma_{DW}} = \frac{3T_d}{4}\left(\frac{\Gamma_{DW}}{H_{eq}}\right)^4. \tag{5.29}$$

Then, the entropy density ratio of after- to before-domain wall decay is given by

$$\Delta = \frac{s_{\text{after}}}{s_{\text{before}}} \simeq \frac{T_{eq}}{T_d}\left(\frac{H_{eq}}{\Gamma_{DW}}\right) \simeq \left(\frac{10\sigma^2}{\pi^2 g_*(T_d)T_d^4 M_P^2}\right)^{3/4}\left(\frac{g_*(T_d)}{g_*(T_{eq})}\right)^{1/4}, \tag{5.30}$$

for $\Delta \gg 1$. We can obtain an entropy production

$$\Delta \simeq 10\left(\frac{\sigma^{1/3}}{50\,\text{TeV}}\right)^{9/2}\left(\frac{2\,\text{MeV}}{T_d}\right)^3. \tag{5.31}$$

One might think that the tension of about 100 TeV looks somewhat too large. However, for instance, in the MSSM-like region of the NMSSM with $\lambda \sim \kappa \ll 1$ and $v_s \gg v$, the domain wall tension

$$\sigma \simeq \frac{16}{3}\sqrt{\frac{2}{3}}\kappa v_s^3, \tag{5.32}$$

can be of such an order with $\lambda \sim \kappa \sim 10^{-2}$ and $v_s \sim 100$ TeV. Those results in the effective μ term and the singlino mass of about 1 TeV. Figure 5.3 shows the entropy density ratio of after- to before- domain wall decay for $\lambda = \kappa = 0.01$, $T_d = 3$ MeV. The ratio increases as μ and A_κ increase.

Such a large late-time entropy production can dilute unwanted relics such as gravitino, overproduced LSP as well as the axion.

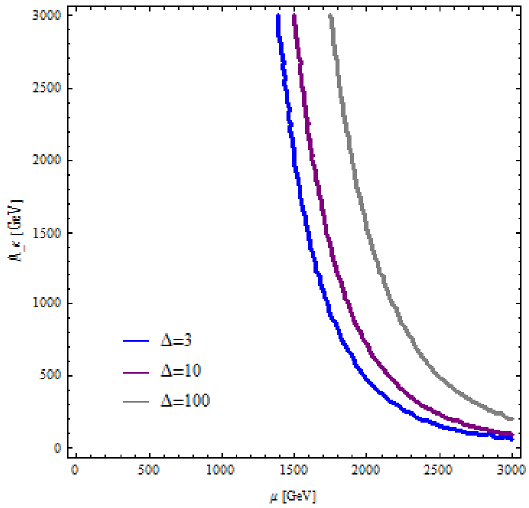

Figure 5.3: - The entropy density ratio Δ of after- to before- domain wall decay in radiation-dominated era to domain wall dominated era for $\lambda = \kappa = 0.01$, $T_d = 3$ MeV.

5.3.3 Non-relativistc domain wall during the domination

Here, we note resultant quantities if the domain wall energy density scales as a^{-1} during the domination.

5.3.3.1 Matter-dominated era to domain wall dominated era

At the domain wall decay time Γ_{DW}^{-1}, the ratio of these energy densities is estimated as

$$\left.\frac{\rho_M}{\rho_{DW}}\right|_{\Gamma_{DW}} = \left(\frac{\Gamma_{DW}}{H_{eq}}\right)^4, \tag{5.33}$$

from $H \propto a^{-1/2}$, where we assume $\rho_{DW} \propto a^{-1}$ during the domain wall domination between H_{eq} and Γ_{DW}. After the domain walls decay, the energy density of the matter is diluted as

$$\frac{\rho_M}{s} = \frac{3T_d}{4}\left(\frac{\Gamma_{DW}}{H_{eq}}\right)^4 \simeq \frac{3T_d}{4}\left(\frac{\pi^2 g_*(T_d)T_d^4}{10}\frac{M_P^2}{\sigma^2}\right)^2, \tag{5.34}$$

for the case that the domain wall decays earlier than the matter does.

5.3.3.2 Radiation-dominated era to domain wall dominated era

At the domain wall decay time, we have

$$\left.\frac{\rho_R}{\rho_{DW}}\right|_{\Gamma_{DW}} = \left(\frac{\Gamma_{DW}}{H_{eq}}\right)^6, \tag{5.35}$$

$$\left.\frac{\rho_R}{s}\right|_{\Gamma_{DW}} = \frac{3T_d}{4}\left(\frac{\Gamma_{DW}}{H_{eq}}\right)^6. \tag{5.36}$$

Assuming $\rho_{DW} \propto a^{-1}$ during the domain wall domination, the entropy density ratio of after- to before-domain wall decay is given by

$$\Delta = \frac{s_{after}}{s_{before}} \simeq \frac{T_{eq}}{T_d}\left(\frac{H_{eq}}{\Gamma_{DW}}\right)^4 \simeq \left(\frac{10\sigma^2}{\pi^2 g_*(T_d)T_d^4 M_P^2}\right)^{9/4}\left(\frac{g_*(T_d)}{g_*(T_{eq})}\right)^{1/4}, \tag{5.37}$$

for $\Delta \gg 1$. We can obtain an entropy production

$$\Delta \simeq 600\left(\frac{\sigma^{1/3}}{50\,\mathrm{TeV}}\right)^{27/2}\left(\frac{2\,\mathrm{MeV}}{T_d}\right)^9. \tag{5.38}$$

5.4 Cosmological evolution of unstabled domain wall

In this section, we study implications of the NMSSM domain wall decay to some relics in several models.

5.4.1 Thermal relic WIMP LSP such as singlino or sneutrino

WIMPs have been regarded as a promising dark matter candidate in our Universe. In the NMSSM, neutralino is the candidate (77). In a right-handed neutrino extended model, right-handed sneutrino also becomes a WIMP dark matter candidate (123).

Since the WIMP thermal relic abundance is inversely proportional to its thermal averaged annihilation cross section $\langle \sigma v \rangle$ as

$$\Omega_{WIMP} h^2 \simeq \frac{0.1\,\mathrm{pb}}{\langle \sigma v \rangle}, \tag{5.39}$$

too small annihilation cross section leads to overabundant WIMPs. The Singlino- or Bino-like neutralino, or right-handed sneutrino with small couplings is indeed such a case. The domain wall decay produces extra entropy with the dilution factor (5.30) and could regulate the WIMP relic abundance to be

$$\Omega_{WIMP} h^2 \frac{1}{\Delta} \simeq 0.1, \tag{5.40}$$

even for a small annihilation cross section $\langle \sigma v \rangle \ll 1$ pb.

5.4.2 The moduli problem in the mirage mediation scenario

Mirage mediation models appear free from the cosmological moduli problem because a moduli mass is quite large. However, nonthermally produced LSP through a decay chain by way of gravitino are in fact overabundant. Let us examine whether the domain wall decay dilutes those LSPs.

Moduli decay before the energy density of domain walls dominates the Universe, because the moduli decay rate

$$\Gamma_{moduli} \simeq \frac{m_{moduli}^3}{8\pi M_P^2}, \tag{5.41}$$

is larger than $H_{\rm eq}$ given by eq. (5.23) in the mirage mediation scenario. At $H \simeq \Gamma_{moduli}$, the moduli decay at a moduli dominated Universe produces gravitinos as

$$Y_{3/2} = \frac{n_{3/2}}{s} = B_{3/2} \frac{3T_D}{2m_{moduli}}, \tag{5.42}$$

with the branching ratio of moduli decay into gravitinos $B_{3/2} = \mathcal{O}(0.01) - \mathcal{O}(1)$ (111), and the Universe becomes radiation dominated. Here T_D is the decay temperature of the moduli field given by

$$3M_P^2 \Gamma_{moduli}^2 = \frac{\pi^2 g_*(T_D)}{30} T_D^4. \tag{5.43}$$

The entropy density ratio of after- to before-domain wall decay is given by eq. (5.30). Unstable gravitinos decay into LSP with $n_{3/2} = n_{LSP}$ due to R-parity conservation.

Usually, this leads to the overproduction of LSP whose abundance exceeds the dark matter abundance. After extra entropy production by the domain wall decay, the resultant final LSP abundance becomes

$$\frac{\rho_{LSP}}{s} \simeq \frac{3m_{LSP}T_D}{2m_{moduli}}\frac{B_{3/2}}{\Delta}, \tag{5.44}$$

in other words,

$$\Omega_{LSP}h^2 \simeq 4.2 \times 10^8 \frac{m_{LSP}T_D}{m_{moduli}}\frac{B_{3/2}}{\Delta}\ \mathrm{GeV}^{-1}. \tag{5.45}$$

In figure 5.4, we consider the case that the LSP is the dark matter, and plot $\Omega_{LSP}h^2 = 0.1$ by using (5.45). The input parameters are $\lambda = \kappa = 0.01$, $T_d = 3$ MeV, $m_{\mathrm{LSP}} = 100$ GeV, $m_{\mathrm{moduli}} = 1000$ TeV.

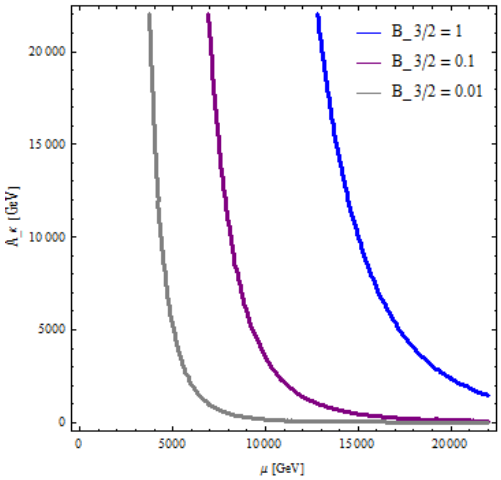

Figure 5.4: - The required branching ratio contour to keep $\Omega_{LSP}h^2 = 0.1$ in the mirage mediation scenario for $\lambda = \kappa = 0.01$, $T_d = 3$ MeV, $m_{\mathrm{LSP}} = 100$ GeV, $m_{\mathrm{moduli}} = 1000$ TeV. Above each curve, the relic abundance is smaller than $\Omega_{LSP}h^2 = 0.1$.

5.4.3 The decay constant of the QCD axion

Finally, we comment on the QCD axion, a, with the decay constant f_a. After the QCD transition, axions are produced by coherent oscillation, so-called misalignment mechanism, and a good candidate for dark matter because its lifetime is much longer than the age of the Universe. Its abundance is proportional to $f_a^{7/6}$ (124). The condition $\Omega_a \lesssim \Omega_{DM}$ is rewritten as

$$f_a \lesssim 10^{12}\,\text{GeV}. \tag{5.46}$$

f_a, which is larger than (5.46), corresponds to the overproduction of axions. Again, the domain wall decay can dilute the axion abundance for such a larger f_a (60).

For example, with the dilution (5.30) by the domain wall decay, the bound on f_a is relaxed as

$$f_a \lesssim 10^{16}\,\text{GeV}, \tag{5.47}$$

for $\sigma^{1/3} = 300$ TeV and $T_d = 2$ MeV.

The GUT scale axion decay constant is allowed, which is remarkable. In superstring theory, the natural decay constant of axionic parts in closed string moduli would be of the order of the GUT scale or string scale (27) [1]. Such stringy axions with larger decay constant can be the QCD axion.

Further, the dilution of axion implies that, in our scenario, the decay constant of the QCD axion can be larger like the GUT scale and Planck scale (60). That is important from the viewpoint of superstring theory because the decay constants of the axions from closed string moduli are usually as large as the GUT scale or string scale. We would study such possibility elsewhere.

5.5 Cosmological inmplication for $w = -1/3$ domain walls

In this section, we study implications of the NMSSM domain wall decay with $w = -1/3$ for the moduli problem within the gravity mediation scenario.

Now, let us study the dilution of moduli to avoid the moduli problem. After inflation, the moduli would start to oscillate and dominate the energy density of the Universe. They may decay during or after the BBN and change the success of BBN. In order to avoid such a situation, the energy density of moduli must satisfy

$$\frac{\rho_{moduli}}{s} \lesssim c \cdot 3.6 \times 10^{-9}\,\text{GeV}, \tag{5.48}$$

[1] Even larger decay constants can be obtained in a certain situation (see e.g., Ref. (125)).

where $c \sim 10^{-2} - 10^{-4}$ for 10 TeV moduli mass depending on the coupling between the moduli and the gauge field (126). We use $c = 10^{-3}$ in the following analysis.

The decay of domain walls can dilute the moduli density, which is given as

$$\frac{\rho_{moduli}}{s} \simeq \frac{3T_d}{4}\left(\frac{\pi^2 g_*(T_d)T_d^4}{10}\frac{M_P^2}{\sigma^2}\right)^2, \tag{5.49}$$

as derived in eq. (5.34). It depends on only T_d and tension σ, which depends on λ, κ, A_κ and μ. Imposing the constraint (5.48) on the resultant abundance (5.49), we find

$$\sigma^{1/3} \gtrsim 220\,\mathrm{TeV}\left(\frac{10^{-3}}{c}\right)^{1/12}\left(\frac{T_d}{3\,\mathrm{MeV}}\right)^{3/4}, \tag{5.50}$$

where $g(T_d) = 10$ is used.

Figure 5.5 shows the constraints (5.48) with (5.49) for $\lambda = \kappa = 0.01$, $T_d = 3$ MeV. The shaded region is excluded by the constraint.

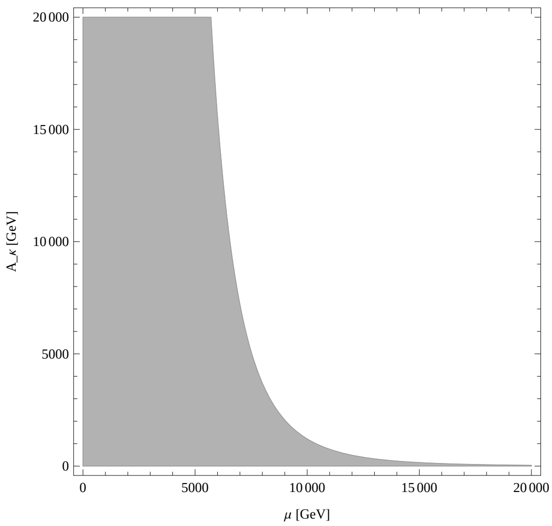

Figure 5.5: - The bound of the moduli abundance in gravity mediation scenario for $\lambda = \kappa = 0.01$, $T_d = 3$ MeV. The yellow region is allowed in the (μ, A_κ) plane.

5.6 Conclusion and discussion

We have studied the cosmological implication of unstable domain walls in the NMSSM. The spontaneous breaking of the Z_3 discrete symmetry in the NMSSM causes the cosmological domain wall problem. We consider that the Z_3 symmetry is slightly but explicitly broken and the domain walls decay with the decay temperature T_d. The domain walls easily dominate the density of the Universe and its decay causes a late-time entropy production, depending on its tension σ and T_d. Such entropy production has significant implications in thermal history. They can dilute unwanted relics such as moduli, gravitino, LSP, and axion.

We have shown that T_d of several MeV dilute various relics in several scenarios. Those include thermal WIMP LSP in gravity mediation model, nonthermally produced LSP in mirage mediation and misalignment produced cold axion in Peccei-Quinn extended models. If the energy density of the domain wall network decreases as $\rho_{DW} \propto a^{-1}$ during domain wall domination, cosmological moduli problem in gravity mediation also might be relaxed.

Note that, again, in order to dilute sufficiently the moduli density, the SUSY breaking scale would be several TeV or larger, and the size of μ would be 500 GeV or larger. Such a large SUSY breaking mass would be enough to realize the 125 GeV Higgs mass. However, when μ is large like 500 GeV, we need fine-tuning to derive the Z-boson mass from μ and soft Higgs masses. In the TeV-scale mirage mediation, μ and m_{H_d} are canceled each other, and severe fine-tuning would not be required (102).

6

Affleck-Dine leptogenesis

In this chapter, we propose a model of Affleck-Dine mechanism (64) for the leptogenesis which is realized in the supersymmetric standard model with right-handed Dirac neutrino. In this model, the baryon number can be explained through the leptogenesis and sphaleron process, and we have pointed out that a sufficient amount of baryon asymmetry can be generated in our model. We also discuss the amounts of the dark matter abundance and cosmological consequences.

6.1 Introduction

The origin of the baryon asymmetry is one of the interesting puzzles in our universe (127), and recently its existence is confirmed from Cocmic Microwave Backgraound (CMB) data (98). The baryon number asymmetry is given in terms of the ratio of the baryon density n_B to entropy density s of the universe as (128)

$$\frac{n_B}{s} \simeq (8.7 \pm 0.3) \times 10^{-11}. \tag{6.1}$$

In order to generate such an asymmetry of the universe, it is known that three Sakharov's conditions should be satisfied (93): violating baryon number, violatineg C and CP, and dropping out of thermal equilibrium in the early univese.

While several ideas have been proposed to prodused a baryon number by using the baryon number violation interaction, the leptogensis not only may be attractive and simple ways to realize the Sakharov's conditions, but also provides a different mechanism for generating baryon asymmetry. In such a case, instead of baryon asymmetry, a lepton asymmetry is generated in the early universe by lepton number violation and CP violation phase produced by right-handed neutrinos. Such a lepton number is partially converted into a baryon number via sphaleron process at high temperature, and the relation between the lepton number density n_L and final baryon asymmetry is expressed as

$$\frac{n_B}{s} = c_{\rm sph}\frac{n_L}{s} \tag{6.2}$$

with $c_{\rm sph} \sim -8/23$ in the minimal supersymmetric standard moddel (96, 97).

There are lots of attractive baryogenesis scenario in SUSY model. In this study, we focus on the Affleck-Dine leptogenesis mechanism based on SUSY theories for the baryogenesis scenario, where the difference of CP phase of the soft SUSY breaking A-term plays an important role to generate an amount of baryan asymmetry. Since we know that the heavy right-handed neutrinos also provide an attractive solution of the origin of the baryon asymmetry by leptogenesis, here, we apply Affleck-Dine mechanism based on a famous flat direction LH_u (129) to our model which develops large values due to a negative effective mass induced by the right-handed sneutrino condensate through the Yukawa coupling of the right-handed neutrino. Also, we utilize the D-flat directions, and consider the thermal collection with the F- and D-term scalar potential which induces a negative effective mass given by the right-handed sneutrino condensate. Due to the negative Hubble mass square of a right-handed sneutrino, minima of the potential of the right-handed sneutrino largely deviates from the origin. We will see its details in the following sections.

The remaining parts are organized as follows. In section 6.2, we address the model and the flat direction considered here. In section 6.3, we estimate the baryon number asymmetry generated through the evolution of this flat direction in our framework, and we consider the cosmological implications in section 6.4. At last, We summarized this study in section 6.5.

6.2 Model

6.2.1 Potential

Hereafter, we study a concrete leptogenesis scenario, which greatly depends on the form of the neutrino sector. In our model, we assume the lepton asymmetry is produced through the A-term of the sneutrino Yukawa term by Affleck-Dine mechanism, surveying the minimum of supergravity arose from effective potential during inflation and after inflaton slow-roll down to its global minimum if there exists negative Hubble induced masses for left and right sneutrinos.

We extend the minimal supersymmetric standard model (MSSM) with including right-handed Dirac neutrinos, N [1]. This model is described by generic MSSM superpotential plus ordinary MSSM sector, then the relevant superpotential is given by

$$W = W_{\mathrm{MSSM}} + yL \cdot H_u N \tag{6.3}$$

where L, H_u are the lepton doublet, and up-type Higgs doublet superfields respectively, and the dot stands for $SU(2)$ anti-symmetric product. Observed small neutrino masses are due to quite small Yukawa couplings, $y \sim \mathcal{O}(10^{-13})$.

The scalar potential in supergravity is expressed as

$$V = e^K \left(W_i (K^{-1})^i_j W^j - 3|W|^2 \right) + \mathrm{D-terms}, \tag{6.4}$$

with $W_i = \partial_{\Phi_i} W + W K_i$, $K_i = \partial_{\Phi_i} K$, where K is the Kahler potential and $(K^{-1})^i_j$ is the inverse of the Kahler metric matrix $\partial^2_{\Phi_i \bar{\Phi}^j} K$. The LH_u D-flat direction is parameterized by a complex scalar field ϕ as

$$\tilde{L} = \frac{1}{\sqrt{2}} \begin{pmatrix} \phi \\ 0 \end{pmatrix}, \quad H_u = \frac{1}{\sqrt{2}} \begin{pmatrix} 0 \\ \phi \end{pmatrix}, \tag{6.5}$$

where $\tilde{L}$, H_u are the scalar component of each superfields. Both LH_u flat direction ϕ and right-handed sneutrino $\tilde{N}$ are slightly lifted by soft SUSY breaking terms

$$V_{\mathrm{soft}} = m_\phi^2 |\phi|^2 + m_{\mathrm{N}}^2 |\tilde{N}|^2 + \left(y A_N \phi^2 \tilde{N} + c.c. \right). \tag{6.6}$$

Although in addition, there are neutrino Yukawa y suppressed F-term potential

$$V_{\text{F-term}} \supset |y|^2 \left(|\phi|^2 |\tilde{N}|^2 + \frac{1}{4} |\phi|^4 \right), \tag{6.7}$$

those terms are negligible in the effective scalar potential.

During and after the inflation, the energy density of the universe is dominated by inflaton field I. Through supergravity interaction with supersymmetry breaking W_I by

[1] we take the convention such that $N = \tilde{N} + \sqrt{2}\theta N^\dagger + \theta\theta F_N$.

its inflaton energy, the fields ϕ and $\tilde{N}$ acquire effective terms of the order of Hubble parameter as

$$V_{\rm inf} = H^2 \left(-c_{H1}|I|^2|\phi|^2 - c_{H2}|\tilde{N}|^2 + c_{H3}|\phi|^4 + c_{H3}|\tilde{N}|^4 + \cdots \right) + H \left(c_A y \phi^2 \tilde{N} + c.c. \right), \tag{6.8}$$

where H is the Hubble parameter at a giving time, ellipsis denote higher order terms, $c_{H1,2,3,4}$ are order unity real positive constants, and c_A is an order unity complex positive constant. Those terms generically arise from interaction terms in non-minimal Kahler potential couplings with an inflaton field I as

$$K = |I|^2 + |\phi|^2 + |\tilde{N}|^2 + c_1|I|^2|\phi|^2 + c_2|I|^2|\tilde{N}|^2 + \cdots . \tag{6.9}$$

A negative Hubble mass term with positive $c_{H1,2} \sim \mathcal{O}(1)$ to work the Affleck-Dine leptogenesis successfully is realized for $c_{H1,2} \gtrsim 1$ as we will assume. Note that we do not concern about specific inflation models.

In addition, after inflation, the field ϕ and $\tilde{N}$ recive the effects of thermal collections to the scalar potential for two-loop effects

$$V_{\rm thermal} = \sum_{f_i|\phi|<T} c_i f_i^2 T^2 |\phi|^2 + \sum_{f_i|\phi|>T} a_{\rm th} \alpha_s^2(T) T^4 \ln\left(\frac{|\phi|^2}{T^2}\right), \tag{6.10}$$

with T being the temperature of the thermal bath. The first term is a thermal-mass term induced by one-loop correction to the potential of light particles in the thermal bath. f_i denotes coupling constants of interaction between ϕ and particles. c_i are determined by the degree of freedom of these particles. The second thermal logarithmic term appears in two-loops level. α_s is strong coupling constant and a_{th} is estimated as $a_{th} \simeq 0.47T(R_i)$, where $T(R_i) = 1/2$ for the fundamental representation. Before the reheating completed, the temperature changes as

$$T \sim \left(H T_{\rm R}^2 M_p\right)^{1/4}, \tag{6.11}$$

where $T_{\rm R}$ is the reheating temperature after inflation.

Following the discussion, after the inflation, the relevant full effective scalar potential is given by [1]

$$V_{\text{eff}} \simeq m_\phi^2 |\phi|^2 + m_{\text{N}}^2 |\tilde{N}|^2 + \left(y A_N \phi^2 \tilde{N} + c.c. \right)$$
$$- c_{H1} H^2 |\phi|^2 - c_{H2} H^2 |\tilde{N}|^2 + T^4 \ln \left(\frac{|\phi|^2}{T^2} \right) + \cdots . \quad (6.12)$$

Then, we will examine the dynamics of this effective potential in section 6.3.

6.2.2 Asymmetric number density

The asymmetric under densities of lepton asymmetry carried by ϕ and $\tilde{N}$ are respectively given by

$$n_{\Delta\varphi} = i q_\varphi \left(\dot{\phi}^* \phi - \phi^* \dot{\phi} \right). \quad (6.13)$$

Here, φ is ϕ and $\tilde{N}$ with those charges $q_\phi = 1/2$, $q_{\tilde{N}} = -1$. Integrating the equation for the evolutikon of the asymmetry,

$$\dot{n}_{\Delta\varphi} + 3H n_{\Delta\varphi} = 2 q_\varphi \operatorname{Im} \left(\frac{\partial V}{\partial \varphi} \varphi \right) \quad (6.14)$$

obtained from eq.(6.13) and equation of motion:$\ddot{\varphi} + 3H\dot{\varphi} + V_{\varphi^*} = 0$, we obtain

$$n_{\Delta\varphi} = \frac{1}{a(t)^3} \int_{\varphi osc}^{t} 2 q_\varphi \, a(t')^3 \operatorname{Im} \left(\frac{\partial V}{\partial \varphi} \varphi \right) dt', \quad (6.15)$$

where the lower limit of integration φosc is the time when each φ field starts to oscillate.

The lepton number asymmetry $n_{\Delta\varphi}$ can be generated as since $H_{\text{osc},\phi} \leq H_{\text{osc,N}}$, the produced lepton number density $n_{\Delta\phi}$ would be diluted and be negligible compared to $n_{\Delta N}$ as the universe evolves. Then, we will focus on only the non-vanishing vev of $\tilde{N}$ which produces the lepton number asymmetry mainly.

6.3 Affleck-Dine leptogenesis from right-handed sneutrino decay

6.3.1 Initial conditions

During and soon after the inflation ends, the AD-fields ϕ and $\tilde{N}$ are settled in the minimum of the potential eq.(6.8) because the energy density of inflation denominates

[1] Besides, we could also obtain the F-term scalar potential V_F from eq.(6.3). However, in our model we assume dirac Yukawa coupling is very small, therefore we will neglect such the contribution to the effective scalar potential.

the universe. By solving stationary condition for the potential eq.(6.8), we find that ϕ and $\tilde{N}$ are stabilized with non-vanishing expectation values as

$$\phi \simeq \tilde{N} \simeq M_p, \tag{6.16}$$

due to the negative Hubble mass terms with order unity positive c_i.

6.3.2 Evolution of AD fields

After inflation, the energy density of the universe is dominated by that of coherent oscillating inflation. In oscillating inflation dominated universe, the Hubble parameter decreases as $H = 2/(3t)$. When the negative Hubble induced mass terms becomes small and negligible in the effective potential, ϕ and $\tilde{N}$ start oscillation with the initial amplitude, eq.(6.16).

Once the negative Hubble mass terms are negligible, firstly the field ϕ will start to oscillate due to the thermal log terms: $V \sim T^4 \ln\left(|\phi|^2/T^2\right)$. Then, $H_{\mathrm{osc},\phi}$ is estimated as $H^2_{\mathrm{osc},\phi} \sim T^4/|\phi|^2$, by using eq.(6.11), which can be rewritten as

$$H_{\mathrm{osc},\phi} \simeq \frac{T_R^2}{M_p}\left(\frac{M_p}{\phi}\right). \tag{6.17}$$

This value of Hubble parameter is the same as one at the time of the reheating $H_R \simeq T_R^2/M_p$. We find that for Planckian initial values eq.(6.16) ϕ starts oscilate when the reheating after inflation is completed. During ϕ oscillates by thermal log term after the reheating by inflaton decay, we find that, by cosmic virial theorem, the amplitude of ϕ scales as $|\phi|^2 \propto 1/a(t)^2$. Then, the amplitude of ϕ can be parameterized as

$$|\phi|^2 \simeq M_p^2 \frac{H}{H_R} \simeq M_p^3 \frac{H}{T_R^2}, \tag{6.18}$$

under the radiation dominated universe where we used eq.(6.16) and $H_{\mathrm{osc},\phi} \simeq H_R \simeq T_R^2/M_p$.

After that, the field $\tilde{N}$ will starts roll down to the origin secondly. In this case, $H_{\mathrm{osc},\tilde{\mathrm{N}}}$ is estimated as soft mass SUSY breaking term $V \simeq m^2_{\tilde{N}}|\tilde{N}|^2$, hence, we can roughly estimate as

$$H_{\mathrm{osc},\tilde{\mathrm{N}}} \simeq m_{\tilde{N}}. \tag{6.19}$$

The amplitude of ϕ and the temperature of radiation at this moment are estimated respectively as

$$|\phi|^2\big|_{H_{\rm osc,\tilde{N}}\simeq m_{\tilde{N}}} \simeq \frac{M_p^2}{T_R^2} M_p m_{\tilde{N}}, \tag{6.20}$$

$$T^2\big|_{H_{\rm osc,\tilde{N}}\simeq M_p} \simeq M_p m_{\tilde{N}}. \tag{6.21}$$

When $\tilde{N}$ starts to oscillate, the lepton number is generated through the AD mechanism, which is determined by the soft A-term SUSY breaking terms.

During $\tilde{N}$ oscillates, the effective mass matrix for the ϕ and $\tilde{N}$ is given as

$$\begin{pmatrix} \phi & \tilde{N}^* \end{pmatrix} \begin{pmatrix} m_\phi^2 + f^2T^2 + a\alpha^2 \frac{T^4}{\phi^2} & yA\phi \\ y^*A^*\phi^* & m_{\tilde{N}} \end{pmatrix} \begin{pmatrix} \phi^* \\ \tilde{N} \end{pmatrix}. \tag{6.22}$$

Due to a large value of ϕ, even with a small y, the mixing between ϕ and $\tilde{N}$,

$$\text{mixing} \simeq \frac{yA\phi}{m_\phi^2 + a\alpha^2 \frac{T^4}{\phi^2}}, \tag{6.23}$$

can be large and even become of the order of unity. Thus, both ϕ and $\tilde{N}$ decay through gauge interactions with decay rate. The decay rate of $\tilde{N}$ is estimated as

$$\Gamma \simeq \frac{1}{4\pi} g_2^2 m_{\tilde{N}} \times (\text{mixing})^2. \tag{6.24}$$

6.3.3 Lepton and baryon asymmetry

In this section, we evaluate the lepton number asymmetry generated through the Affleck-Dine mechanism with soft A-term SUSY breaking terms. Now, we can estimate the evolution of $n_{\Delta\tilde{N}}$ from eq.(6.14). The lepton number would fix when the AD-field $\tilde{N}$ starts to oscillate at $H_{\rm osc,N} \sim m_{\tilde{N}}$. With eqs.(6.19) and (6.20), this equation is solved as

$$n_{\Delta\tilde{N}}\big|_{\rm osc} \sim q_{\tilde{N}} \frac{yAM_p^4}{T_R^2} \delta_{\rm eff}, \tag{6.25}$$

where $\delta_{\rm eff} \sim \sin\left(\theta_{\tilde{N}} + 2\theta_\phi\right)$ is the effective CP phese.

It is straightforward to estimate the lepton asymmetry, but in our scenario, so far $n_{\Delta\tilde{N}}$ might be quite large at this rate. In order to reproduce the precise baryon number to explain the successful BBN, we need that a late time entropy production could dilute over abundant baryon asymmetry. One of the promising candidates of such an entropy production is saxion field σ (130). The decay width Γ_σ is given by

$$\Gamma_\sigma \simeq \frac{3\alpha_s^2}{64\pi^3}\frac{m_\sigma^3}{F_a^2} \tag{6.26}$$

where m_σ is the saxion mass and F_a is the axion decay constant. Further, for simplicity, we assume $m_\phi \simeq m_{\tilde{N}} \simeq m_\sigma$. After the moduli decay at the time Γ_σ^{-1}, the baryon number density is diluted as

$$\begin{aligned}\frac{n_B}{s} &\sim c_{\rm sph}\left.\frac{n_{\Delta N}}{s}\right|_{\Gamma_\sigma^{-1}} \\ &\sim \delta_{\rm eff}\frac{yA_N M_p T_\sigma}{m_{\tilde{N}}^3} \\ &\sim 6\times 10^{-11}\left(\frac{\delta_{\rm eff}}{0.01}\right)\left(\frac{y}{10^{-13}}\right)\left(\frac{A_N}{100\ \mathrm{GeV}}\right)\left(\frac{m_{\tilde{N}}}{50\ \mathrm{TeV}}\right)^{-3}\left(\frac{T_\sigma}{1\ \mathrm{GeV}}\right),\end{aligned} \tag{6.27}$$

where we utilize $c_{\rm sph} \simeq 8/23$. Therefore, sufficient baryon number asymmetry could be reproduced in our model.

Generally, we can usually take $H_{\mathrm{osc},\phi} \leq H_{\mathrm{osc},\tilde{\mathrm{N}}}$. As a result, the left-right asymmetry could be generated by such the difference. In this section, we will calculate the total lepton number focusing on only the right-handed sneutrino which produces the lepton number density by its decaying through the sphaleron process.

6.4 Cosmological implication

Since we have introduced the saxion to suppress overabundant baryon asymmetry, the abundance of saxion σ decays could be the candidate of the dark matter. Hence, we have to care that it is likely to overclose our universe. Here, we discuss one of the possible scenarios.

After the saxion decayed, the dark matter produced by the decays of σ remains being satisfy $n_{\rm DM} \simeq n_\sigma Br_{\rm DM}$, where $Br_{\rm DM}$ is the branching ratio from saxion to dark matter. If the freeze-out temperature of dark matter would be smaller than the reheating temperature and consequently the dark matter yield is determined by the non-thermal process of the saxion decay,

$$\frac{\rho_{\rm DM}}{s} \simeq \frac{m_{\rm DM}}{m_\sigma}T_\sigma Br_{\rm DM} \simeq T_\sigma Br_{\rm DM}, \tag{6.28}$$

where s is the entropy density of the universe. With this relation, we can estimate the relic abundance of dark matter using the ratio of the critical density to the current entropy density of the universe $\rho/s_0 \simeq 3.6h^2 \times 10^{-9}$,

$$\Omega_{\rm DM}h^2 \simeq m_{\rm DM}\frac{n_{\rm DM}}{s}\frac{s_0}{\rho} \simeq 10^{-8} \times \left(\frac{T_\sigma}{1\ \text{GeV}}\right)\left(\frac{Br_{\rm DM}}{1}\right), \tag{6.29}$$

with h being the dimensionless Hubble parameter. It suggests the relic abundance of dark matter are negligible for our universe.

6.5 Conclusion

Let us summarize our study briefly here. We have proposed an Affleck-Dine mechanism for the leptogenesis which is realized in the supersymmetric standard model with right-handed Dirac neutrino model. In our scenario, right-handed sneutrino $\tilde{N}$ and LH_u flat direction ϕ play an important in the Affleck-Dine mechanism with soft A-term SUSY breaking terms, where we identified these fields as the AD fields. After the AD fields trapped at the effective potential minimums, then finally AD fields roll down to the origin by decreasing magnitude of Hubble masses, which means that oscillation time of AD fields is generally different. Hence, the left-right asymmetry is generated, and we have calculated the total lepton number asymmetry focusing on only the right-handed sneutrino. If the right-handed sneutino decays in the early universe before the spharelon process occurs, it is found that the lepton number density is generated quite large. In order to prevent such overabundant lepton asymmetry, we showed that in particular, the saxion could do work well to reproduce the precise baryon asymmetry. Unfortunately, we do not show the cosmological implication detail so far. We think this treatment is not enough to investigate, and our future work on this model discussed here will involve understanding the comprehensive new framework on which the cosmological implications are also studied.

7

Summary and discussion

It is our dearest wish to understand the precise connection of the Planck scale to the electroweak scale that we have verified by experiments so far. Toward such our ultimate goal which is to build a model (theory) which explains everything, through this thesis, we stick to pragmatic models on about the cosmology, and we attempt to propose some of the inflation models and solution to the cosmological problems in the viewpoints of supersymmetry phenomenology, selectively. We hope that our study opens the window to new physics beyond the standard model, even deeper level of more fundamental physics.

In this thesis, we have proposed some extended models roughly including key ingredients for the construction of new comprehensive physics. This thesis is separated into two non-over-lapping parts: "inflation part" and "supersymmetry and cosmology part".

In chapter 3, we have studied the axion inflation model proposed recently within the framework of type IIB superstring theory with a particular emphasis on the sub-Planckian axion decay constant, $0.01 \lesssim f \lesssim 1.0$. Such an axion potential consists of the mixture of polynomial functions and sinusoidal functions with the periodicity $\phi \sim \phi + 2\pi/f$, represented as $V(\phi^m, \cos(\phi/f), \sin(\phi/f))$. For a small decay constant $f \ll 1$, such a potential can have many bumps, and the small field inflation can be realized on one of the plateaus. As a result, we have found that in such a model, the inflation energy scale and Hubble parameter could have the power law dependence on f and hence become rapidly small as f becomes small. We expect our concrete examples discussed in our paper can capture the generic features for a wider class of axion inflation consisting of the sinusoidal and polynomial terms with a sub-Planckian axion decay constant. Confirming such a generalization of our study is quite fascinating, and we have tried to present the analysis extending our studies here for a wider class of axion inflation models which can be explicitly derived from superstring theory.

Then, we also have discussed the general class of small-field axion inflation which is the mixture of polynomial and sinusoidal functions with an emphasis on the small axion decay constant, and finally found that the cosmological observables are written in terms of the axion decay constants in a systematic way. More detailed studies would be of great interest where we combine concrete mechanism for the moduli stabilization/uplifting, fix the mass scale of light moduli, choose a candidate for dark matter, and embed the QCD axion in superstring theory.

Further, we have studied a new type of moduli potential which is related to its stabilization. The result is that it is possible if some parameters are tuned even in the case for adding the p-lifting terms. Also, in this model, one of the light axions could derive the cosmological inflation if a proper potential is generated, as it is understood so far. Such axion phenomenology would be studied elsewhere.

Now, the idea that supersymmetry has something to do with not only inflation theory, but also possibly make a connection to the cosmological aspects, especially including the domain wall problems in the NMSSM and baryogenesis (leptogenesis) discussed in this thesis. After we remark on some aspects of cosmology in the context of Supersymmetry field theory, we have proposed our fascinating models in chapter 5 and chapter 6.

First, we have studied the cosmological implication of unstable domain walls in the NMSSM. We consider that the Z_3 symmetry is slight, but explicitly broken and the domain walls decay with the decay temperature. Such entropy production has significant implications in thermal history, they can dilute unwanted relics such as moduli, gravitino, LSP, and axion. We have pointed out that the decay temperature of several MeV dilutes various relics in several scenarios. If the energy density of the domain wall network decreases as $\rho_{DW} \propto a^{-1}$ during the domain wall domination, cosmological moduli problem in gravity mediation also might be relaxed.

Moreover, we have proposed an Affleck-Dine mechanism for the leptogenesis which is realized in the supersymmetric standard model with right-handed Dirac neutrino model. In our scenario, right-handed sneutrino $\tilde{N}$ and LH_u flat direction ϕ play an important role in the Affleck-Dine mechanism with soft A-term SUSY breaking terms, where we identified these fields as the AD fields. Then, the left-right asymmetry is generated, and we have calculated the total lepton number asymmetry focusing on only the right-handed sneutrino. We have pointed out that a sufficient amount of baryon asymmetry can be generated in our model. In order to prevent such the overabundant lepton asymmetry, we showed that in particular, the saxion could do work well to reproduce the precise baryon asymmetry.

The supersymmetry has something to do with the ideas of extension of the standard model, and possibly make a connection to other aspects of cosmology, including inflation model and baryogenesis (leptogenesis). We hope that supersymmetry would be experimentally verified in the future, and the discovery would become the beginning of the current understanding theories in high energy physics.

Appendix A

Conventions and notations

A.1 Conventions

First, let us define the general notation. Throughout this thesis, we employ natural units with $\hbar = c = 1$. Further, the reduced Plank mass,

$$M_p^{-2} \equiv 8\pi G = \left(2.4 \times 10^{18}\mathrm{GeV}\right)^{-2}, \tag{A.1}$$

is often set equal to one.

Our metric signature is $(+,\ -,\ -,\ -)$. We use t for physical time and overdots stand for derivatives with respect to physical time t. We also denote four-dimensinal space-time coordinates by x^μ, where μ runs $0,\ \cdots, 3$, while for three-dimensinal components we use index $i = 1, 2, 3$.

A.2 Notations of supersymmetry

The Pauli matrices are

$$\sigma^0 = \begin{pmatrix} 1 & 0 \\ 0 & 1 \end{pmatrix}, \quad \sigma^1 = \begin{pmatrix} 0 & 1 \\ 1 & 0 \end{pmatrix}, \quad \sigma^2 = \begin{pmatrix} 0 & -i \\ i & 0 \end{pmatrix}, \quad \sigma^3 = \begin{pmatrix} 1 & 0 \\ 0 & -1 \end{pmatrix}, \tag{A.2}$$

and by using above Pauli matrices, gamma matrices are defined as

$$\gamma^\mu = \begin{pmatrix} 0 & \sigma^\mu \\ \bar{\sigma}^\mu & 0 \end{pmatrix}, \qquad \gamma^5 \equiv i\gamma^0\gamma^1\gamma^2\gamma^3 = \begin{pmatrix} 1 & 0 \\ 0 & -1 \end{pmatrix}. \tag{A.3}$$

Note that we can find $\sigma^0 = \bar{\sigma}^0$ and $\sigma^{1,2,3} = -\bar{\sigma}^{1,2,3}$.

Depending on the van der Waerden notation, we define two-component spinors as ξ_α expressed with undotted indices, while with dotted indices like $\bar{\eta}^{\dot{\alpha}}$ to distinguish the transformation properties or left-right chirality. We contract spinor indices put in the form as

$$ {}^{\alpha}{}_{\alpha}\ , \quad \text{or} \qquad {}_{\dot{\alpha}}{}^{\dot{\alpha}} \tag{A.4}$$

Namely,

$$\xi \cdot \eta \equiv \xi^\alpha \eta_\alpha = -\xi_\alpha \eta^\alpha = \eta^\alpha \xi_\alpha = \eta \cdot \xi \tag{A.5}$$

and also

$$\bar{\xi} \cdot \bar{\eta} \equiv \bar{\eta} \cdot \bar{\xi} \tag{A.6}$$

in the same way. Here, the spinor indices are raised and lowered by using the asymmetric tensor, defined as

$$(i\sigma^2)^{\alpha\beta} \equiv \epsilon^{\alpha\beta}, \qquad (i\sigma^2)_{\alpha\beta} \equiv \epsilon_{\alpha\beta}, \qquad (i\sigma^2)^{\dot{\alpha}\dot{\beta}} \equiv \epsilon^{\dot{\alpha}\dot{\beta}}, \qquad (i\sigma^2)_{\dot{\alpha}\dot{\beta}} \equiv \epsilon_{\dot{\alpha}\dot{\beta}}, \tag{A.7}$$

and leading following forms,

$$\epsilon^{12} = \epsilon^{\dot{1}\dot{2}} = 1, \qquad \epsilon_{12} = \epsilon_{\dot{1}\dot{2}} = -1, \qquad \epsilon^{21} = \epsilon^{\dot{2}\dot{1}} = -1, \qquad \epsilon_{21} = \epsilon_{\dot{2}\dot{1}} = 1. \tag{A.8}$$

We close this section with defining the four-component Dirac spinors ψ_D and Majonara fermions ψ_M, which are written as following, respectively

$$\psi_D = \begin{pmatrix} \eta_\alpha \\ \bar{\xi}^{\dot{\alpha}} \end{pmatrix}, \qquad \psi_M = \begin{pmatrix} \eta_\alpha \\ \bar{\eta}^{\dot{\alpha}} \end{pmatrix}. \tag{A.9}$$

Appendix B

Moduli stabilization and radiative corrections

Here we mention about a new type of moduli stabilization scenario where the supersymmetric and supersymmetry-breaking minima are degenerate at the leading level. The inclusion of the loop-corrections originating from the matter fields resolves this degeneracy of vacua. One of the moduli could derive the cosmological inflation if a proper potential is generated. Such moduli phenomenology would be studied in chapter 3.

This content depends on our works Refs. (f) and (g).

B.1 Outlook

The superstring theory predicts six-dimensional compact space in addition to four-dimensional space-time. The size and shape of the 6D compact space are determined by moduli. Thus, moduli are a characteristic feature in the superstring theory on compact space. Indeed, moduli fields play important roles in the superstring theory and its four-dimensional low-energy effective field theory, in particular in particle phenomenology and cosmology. (See for a review, e.g. Refs. (52, 66).) Studies on physics relevant to moduli would provide a remnant of the superstring theory on compact space.

Gauge couplings, Yukawa couplings and other couplings in the 4D low-energy effective field theory are given by vacuum expectation values (VEVs) of moduli fields. In the phenomenological point of view, the spectrum of supersymmetric particles is sensitive to the supersymmetry (SUSY) breaking of moduli fields through the gravitational interactions between the moduli fields and matter fields (103, 131, 132, 133). This aspect would be relevant to dark matter physics, since the lightest superpartner is a candidate of dark matter. Moreover, the thermal history of the Universe highly depends on the dynamics of moduli fields as well as axion fields, which are the imaginary parts of moduli fields. From the theoretical point of view, these moduli fields are originating from the vector and tensor fields in low-energy effective action of the superstring theory as well as the higher-dimensional supergravity. The stabilization of the moduli field is one of the most important issues to realize a consistent low-energy effective action of the superstring theory.

The moduli potential is prohibited by the higher-dimensional gauge and Lorentz symmetries at the perturbative level. On the other hand, the nontrivial background fields and nonperturbative effects generate the moduli potential. Then, one can stabilize the moduli fields and also study the dynamics relevant to moduli fields. The vacuum structure of the moduli potential is of particular importance. For example, the flat direction of the moduli potential can drive cosmological inflation [1] and the lifetime of our Universe depends on the (meta)stability of the vacuum.

So far, there are several mechanisms to stabilize the moduli, in particular, closed string moduli fields, e.g., the Kachru-Kallosh-Linde-Trivedi (KKLT) scenario (44) and the LARGE volume scenario (50). (See, e.g., Ref. (66) and references therein.) In this paper, we propose a new type of moduli stabilization scenario by using the string-derived $\mathcal{N} = 1$ four-dimensional supergravity action. We find that the supersymmetric and SUSY-breaking vacua are degenerate at the tree level and they are independent of the F term of certain moduli fields. The loop effects originating from the matter fields generate the moduli potential and resolve this degeneracy of vacua.

B.2 Complex structure moduli

In sections B.2 and B.3, we consider two illustrative supergravity models where the moduli fields correspond to the complex structure modulus and Kähler modulus within the framework of the type IIB superstring theory. In both scenarios, we show that the

[1] See for the detail of moduli inflations as well as axion inflations, e.g. Ref. (12).

supersymmetric and SUSY-breaking vacua are degenerate at the leading level. The inclusion of the one-loop corrections from the matter fields resolves this degeneracy.

In the type IIB superstring theory on the Calabi-Yau (CY) orientifold, the Kähler potential of moduli fields is described by

$$K = -\ln\left(i\int_{\rm CY}\Omega\wedge\bar{\Omega}\right) - \ln(S+\bar{S}) - 2\ln\mathcal{V}, \tag{B.1}$$

where $\Omega(U_m)$ is the holomorphic three-form of the CY manifold and $\mathcal{V}(T_i)$ is the volume of the CY manifold. Here, S, U_m and T_i denote the dilaton, complex structure moduli and Kähler moduli, respectively.

The three-form flux can induce the superpotential (42)

$$W_{\rm flux} = \int_{\rm CY} G_3\wedge\Omega, \tag{B.2}$$

where $G_3 = F_3 - iSH_3$ is an imaginary self-dual three-form. Also nonperturbative effects such as D-brane instantons and gaugino condensations can generate the superpotential of S and T_i, e.g.,

$$W_{\rm np} = \sum_p A^{(p)}(U_m)e^{-a^{(p)}S - a_i^{(p)}T_i}, \tag{B.3}$$

where $A^{(p)}(U_m)$ represent the U_m-dependent one-loop corrections and $a^{(p)}$ and $a_i^{(p)}$ are the numerical constants.

B.2.1 The degenerate scalar potential

First, let us consider the following Kähler potential and superpotential based on the four-dimensional $\mathcal{N}=1$ supergravity:

$$K = -3\ln(U+\bar{U}), \qquad W = C_0 + C_1 U, \tag{B.4}$$

where $C_{0,1}$ are the complex constants. In the type IIB superstring theory on the CY orientifold, the modulus field U could be identified with one of the complex structure moduli of the CY manifold. We now assume that the other complex structure moduli and dilaton are stabilized at the minimum by the three-form fluxes (43). When the parameters $C_{0,1}$ are determined only by the three-form fluxes as well as VEVs of the other complex structure moduli, these would be of $\mathcal{O}(1)$. On the other hand, when the above superpotential appears from the instanton effects, $C_{0,1}$ are characterized as e^{-aT}, with T being a certain Kähler modulus of the CY manifold, and could be suppressed. In the following analysis, we treat $C_{0,1}$ as complex constants by further assuming that all the Kähler moduli are stabilized at the minimum by the other nonperturbative effects. When $C_{0,1}$ are of the order of unity, it is a challenging issue to stabilize the Kähler modulus at the scale above the mass of U. Conversely, when both $C_{0,1}$ are exponentially suppressed, one can achieve the above assumption as shown later. In the following, we use the parametrization as $C_1 = w_0$ and $C_0/C_1 = C$.

To see the degenerate supersymmetric and SUSY-breaking vacua, we calculate the scalar potential in the notation of $U = U_R + iU_I$ and $C = C_R + iC_I$,

$$V = e^K \left(K^{U\bar{U}}|D_U W|^2 - 3|W|^2\right) = -\frac{|w_0|^2}{6U_R^2}(3C_R + 2U_R), \tag{B.5}$$

where $K^{U\bar{U}}$ is the inverse of Kähler metric $K_{U\bar{U}} = \partial_U \partial_{\bar{U}} K$ and

$$D_U W = w_0 \left(-3\frac{C+U}{U+\bar{U}} + 1\right). \tag{B.6}$$

As a result, the scalar potential eq. (B.5) remains flat in the direction of U_I. On the other hand, from the extremal condition of U_R,

$$\frac{\partial V}{\partial U_R} = \frac{|w_0|^2}{6U_R^3}(6C_R + 2U_R) = 0, \tag{B.7}$$

U_R is stabilized at the minimum

$$U_{R,\mathrm{min}} = -3C_R, \tag{B.8}$$

where C_R should be negative to justify our low-energy effective action. Note that $|C_R|$ is typically of the order of unity in both scenarios: $C_{0,1} \simeq \mathcal{O}(1)$ and $C_{0,1} \simeq \mathcal{O}(e^{-aT})$. If $|C_R|$ is smaller than unity, the moduli space of U deviates from the large complex structure regime and our discussing logarithmic the Kähler potential is not reliable. It turns out that the mass squared of canonically normalized U_R,

$$\frac{K^{U\bar{U}}}{2}\frac{\partial^2 V}{\partial U_R^2} = \frac{2U_{R,\mathrm{min}}^2}{3}\frac{|w_0|^2}{3U_{R,\mathrm{min}}^3} = \frac{2|w_0|^2}{9U_{R,\mathrm{min}}}, \tag{B.9}$$

is positive and the vacuum energy,

$$V = -\frac{|w_0|^2}{6U_{R,\mathrm{min}}}, \tag{B.10}$$

is negative at this minimum. Note that the mass squared of canonically normalized U_R at this vacuum is taken smaller than the other moduli fields, in particular, the Kähler moduli. For example, when we consider the nonperturbative superpotential for the Kähler moduli irrelevant to our focus U, the Kähler moduli can be stabilized at certain minima by them and the mass squared of the overall Kähler modulus is given by $\mathcal{O}((2\pi\mathrm{Re}(T))^2|w_0|^2)$ for the KKLT scenario.

Although the vacuum energy is independent of U_I, the F-term of the modulus U depends on U_I,

$$F = -e^{K/2}K^{U\bar{U}}D_{\bar{U}}\bar{W}, \tag{B.11}$$

where

$$\mathrm{Re}(D_U W) = 0, \qquad \mathrm{Im}(D_U W) = w_0\left(-\frac{3(C_I+U_I)}{2U_{R,\mathrm{min}}}\right). \tag{B.12}$$

Thus, we find that the SUSY is preserved at $C_I+U_I=0$ and broken at $C_I+U_I\neq 0$, respectively. From the fact that the scalar potential is independent of U_I, supersymmetric and SUSY-breaking vacua are degenerate.

B.2.2 Loop corrections

The analysis in section B.2.1 shows that the vacuum energy is negative, $V<0$, and at the same time, the scalar potential remains flat in the direction of U_I. First, we introduce the uplifting sector to obtain the tiny cosmological constant. In particular, we assume that the U-independent potential induced by the anti-D-branes uplifts the anti-de Sitter vacuum to the Minkowski one such as the KKLT scenario [1]. Next, the nonvanishing F term of U gives rise to the soft terms of matter fields. These massive supersymmetric particles induce the U_I-dependent scalar potential through one-loop corrections (135):

$$\Delta V = \mathrm{Str}\frac{\mathcal{M}^4}{64\pi^2}\ln\left[\mathcal{M}^2/\Lambda^2\right]. \tag{B.13}$$

In the following analysis, we illustrate how we can stabilize U_I by one-loop effects. For such a purpose, we focus on the situation that the gauginos and supersymmetric scalar fields contribute to the one-loop corrections. The gaugino masses are provided by

$$M_a = \frac{1}{2}\frac{\partial \ln f_a}{\partial \ln \Phi^I}F^I, \tag{B.14}$$

[1] Uplifting by spontaneous F-term SUSY breaking is also possible (45, 134). Even in that case, the U_I direction would remain flat.

where $f_a(\Phi^I)$ with $a = U(1)_Y, SU(2)_L, SU(3)_C$ representing the gauge kinetic functions for the standard model gauge groups, respectively. On the other hand, the soft scalar masses are given by

$$m_i^2 = \frac{2}{3}V_0 - \partial_I \partial_{\bar{I}} Y_{i\bar{i}} |F^I|^2 + (\text{D–term}), \tag{B.15}$$

where

$$Y_{i\bar{i}} = e^{-K/3} Z_{i\bar{i}}, \tag{B.16}$$

with $Z_{i\bar{i}}$ being the Kähler metric of the matter fields.

To simplify our illustrating analysis, we assume that the typical soft scalar mass and gaugino mass mainly contribute to the one-loop potential. Then, those are characterized as

$$M = k_f F, \qquad m^2 = m_0^2 - k_m |F|^2, \tag{B.17}$$

where k_f and k_m are real constants and m_0^2 denotes the soft scalar mass induced by the U-independent F-term contributions. The gaugino mass may also have another contribution such as $M = k_f F + M_0$. Even in such a case, the following discussion is similar. For a simple illustration, we restrict ourselves to the above spectrum of superpartners.

By rescaling the F term of U, one can set $k_m = 1$, and the corresponding one-loop potential can be written by

$$64\pi^2 \Delta V = a_1 (c^2 - |F|^2)^2 \ln(c^2 - |F|^2) - a_2 F^4 \ln(a_3 |F|^2) + V_0, \tag{B.18}$$

where $c^2 = m_0^2/k_m$, $a_3 = k_f/k_m$ and $a_{1,2}$ correspond to the multiplicities of the scalars and gauginos, respectively. Now, we include the constant V_0 coming from the F terms of Kähler moduli and anti-D-brane effects to achieve the tiny cosmological constant at the vacuum. By using $\Delta\tilde{V} = 64\pi^2 \Delta V/a_2$, $a_0 = a_1/a_2$, and $\tilde{V}_0 = V_0/a_2$, the above scalar potential is simplified as

$$\Delta\tilde{V} = a_0 (c^2 - |F|^2)^2 \ln(c^2 - |F|^2) - F^4 \ln(a_3 |F|^2) + \tilde{V}_0. \tag{B.19}$$

The first derivative of the one-loop potential with respect to $|F|$ is given by

$$\Delta\tilde{V}' = -2|F| \left[2|F|^2 \ln(a_3 |F|^2) + |F|^2 + a_0 (c^2 - |F|^2) + 2a_0 (c^2 - |F|^2) \ln(c^2 - |F|^2) \right], \tag{B.20}$$

from which there are two possible minima leading to $|F| = 0$ and $|F| \neq 0$. To see the nonvanishing F, we draw the one-loop scalar potential as a function of $|F|$ by setting the following illustrative parameters:

$$a_0 = 1(-1), \qquad a_3 = 0.1, \qquad c = 1.2(0.2), \qquad \tilde{V}_0 \simeq -0.474(-0.00375), \tag{B.21}$$

on the left (right) panel in Figs. B.1 and B.2

$$a_0 = -1, \qquad a_3 = 0.1, \qquad c = 10^{-5}, \qquad \tilde{V}_0 \simeq -1.24 \times 10^{-19}, \tag{B.22}$$

in Fig. B.3. It turns out that the nonvanishing of $|F|$ depends on the sign of a_0 and the value of c.

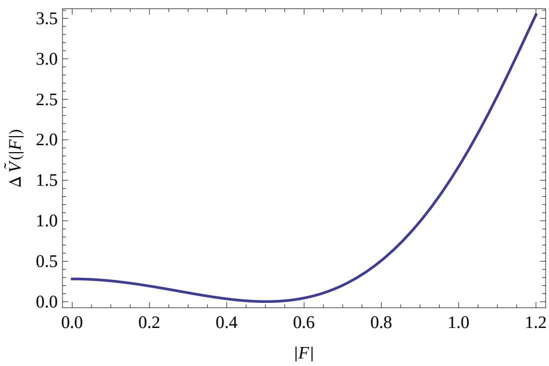

Figure B.1: - The one-loop scalar potential as a function of $|F|$. The parameters are set as $a_0 = 1, a_3 = 0.1, c = 1.2$

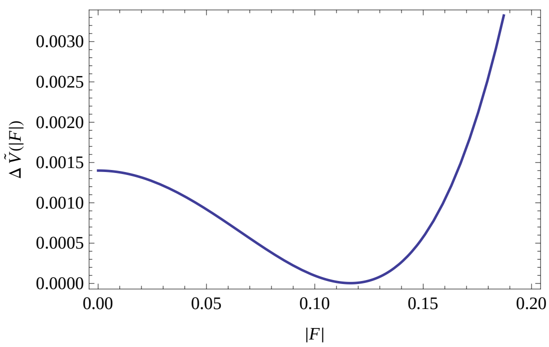

Figure B.2: - The one-loop scalar potential as a function of $|F|$. The parameters are set as $a_0 = -1, a_3 = 0.1, c = 0.2$

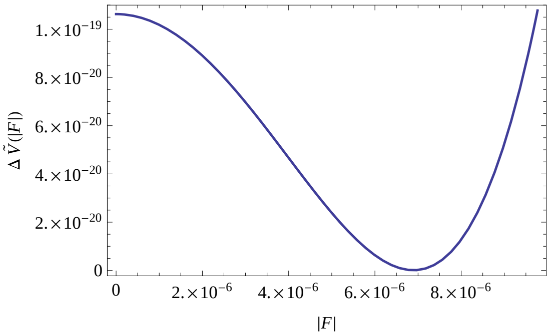

Figure B.3: - The one-loop scalar potential as a function of $|F|$ in the case of small c. The parameters are taken as $a_0 = -1, a_3 = 0.1, c = 10^{-5}$.

To discuss the vacuum structure of the one-loop scalar potential, we analytically derive the condition of vanishing $|F|$. From the second derivative of the one-loop potential with respect to $|F|$

$$\Delta\tilde{V}'' = -2\left(a_0c^2 - 7(a_0-1)|F|^2 + 6F^2\ln(a_3|F|^2) + 2a_0(c^2-3|F|^2)\ln(c^2-|F|^2)\right), \tag{B.23}$$

$\Delta\tilde{V}''$ becomes negative at the origin $|F| = 0$ for

$$-2\left(a_0c^2 + 2a_0c^2\ln c^2\right) \;<\; 0. \tag{B.24}$$

It implies that when $a_0 > 0$ and

$$c \;>\; \frac{1}{e^{1/4}} \simeq 0.78, \tag{B.25}$$

the minimum of $|F|$ is taken as $\mathcal{O}(1)$ because of the instability at $|F| = 0$. However, we assume that the other moduli fields are decoupled from our system and such a high-scale SUSY breaking is not reliable. Thus, when $a_0 > 0$, supersymmetric minimum $|F| = 0$ is favorable. In this case, the soft terms are determined by F terms of the Kähler moduli. Such a vanishing F term of U is also interesting from the aspects of the flavor structure of the matter fields. Indeed, Yukawa couplings among the standard model particles depend on the complex structure moduli through the compactification of an extra dimension as derived in the type IIB superstring theory with magnetized D-branes (53). Thus, a sizable F term of a complex structure modulus is dangerous for the flavor-changing processes among the supersymmetric particles, which are severely constrained in the low-scale SUSY-breaking scenario.

Finally, we discuss the possibility of nonvanishing F by adding the nonperturbative effects of U into the one-loop scalar potential. The nonperturbative effects of U are expected to appear through e.g. the gaugino condensation on hidden D-branes where the gauge kinetic function involves the U-dependent one-loop corrections (51). Since the real part of U is already stabilized by the superpotential in eq. (B.4), the potential of U_I can be extracted as

$$\Lambda^4 \cos(U_I/f + \theta_0), \tag{B.26}$$

where f is the typical decay constant and θ_0 is a real constant. In the following, we set $C_I = 0$ for simplicity. Then, the F term of U,

$$|F^U| = e^{K/2} K^{U\bar{U}} |D_U W| = 9W_0 U_I, \tag{B.27}$$

leads to the following total scalar potential:

$$V = \frac{1}{64\pi^2}\left[a_1(c^2 - |F|^2)^2 \ln(c^2 - |F|^2) - a_2|F|^4 \ln(a_3|F|^2)\right] + \Lambda^4 \cos\left(\frac{|F|}{9W_0 f}\right) + V_1. \tag{B.28}$$

Here, the constant V_1 is inserted to realize the tiny cosmological constant at the vacuum in a way similar to the previous scenario. By rescaling the parameters as

$$\tilde{V} \equiv 64\pi^2 V/a_2, \qquad a_0 \equiv a_1/a_2, \qquad \tilde{\Lambda} \equiv \Lambda(64\pi^2/a_2)^{1/4}, \qquad a_4 \equiv 9W_0 f, \qquad \tilde{V}_1 \equiv V_1(64\pi^2/a_2), \tag{B.29}$$

we analyze the following potential

$$\tilde{V} = a_0(c^2 - |F|^2)^2 \ln(c^2 - |F|^2) - F^4 \ln(a_3|F|^2) + \tilde{\Lambda}^4 \cos\left(\frac{|F|}{a_4}\right) + \tilde{V}_1. \tag{B.30}$$

Figure B.4 and figure B.5 shows that the nonvanishing $|F|$ is achieved even when a_0 is positive. Since the origin of c and $\tilde{\Lambda}$ are the nonperturbative effects, one can realize the low-scale SUSY-breaking scenario in this model.

We have assumed that loop corrections are dominant in the potential of U_I. When other nonperturbative effects are dominant, obviously U_I is stabilized by such nonperturbative effects and loop effects provide subdominant corrections.

B.3 Kähler moduli

In this section, we consider another example where the supersymmetric and SUSY-breaking minima are degenerate at the leading level.

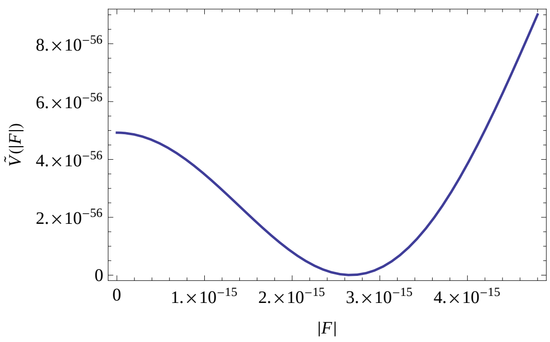

Figure B.4: - The one-loop scalar potential involving the nonperturbative correction in eq. (B.30) is drawn as a function of $|F|$. The parameters are set as $a_0 = a_3 = 1, a_4 = 10^{-15}, c = 5 \times 10^{-15}, \tilde{\Lambda} = 1.4 \times 10^{-14}, \tilde{V}_1 = 5.2 \times 10^{-56}$.

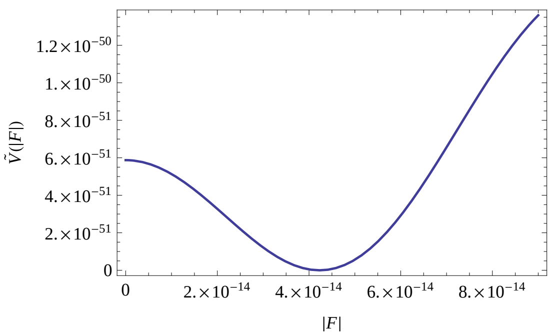

Figure B.5: - The parameters are set as $a_0 = a_3 = 1, a_4 = 10^{-15}, c = 9 \times 10^{-14}, \tilde{\Lambda} = 2.5 \times 10^{-13}, \tilde{V}_1 = 5.9 \times 10^{-51}$.

By use of the flux-induced superpotential eq.(B.2), the F-term scalar potential is calculated as

$$V_F = e^K\left[\sum_{I,J=S,U_m} K^{I\bar{J}} D_I W D_{\bar{J}} \bar{W} + \left(K^{T_i \bar{T}_j} K_{T_i} K_{\bar{T}_j} - 3\right)|W|^2\right]$$
$$= e^K\left[\sum_{I,J=S,U_m} K^{I\bar{J}} D_I W D_{\bar{J}} \bar{W}\right], \tag{B.31}$$

where $-3|W|^2$ is canceled by the no-scale structure of the Kähler moduli,

$$\sum_{i,j} K^{T_i \bar{T}_j} K_{T_i} K_{\bar{T}_j} - 3 = 0. \tag{B.32}$$

Note that the above no-scale structure is valid only at the tree level.

Then, the dilaton and complex structure moduli are stabilized at the minimum,

$$D_S W = 0, \qquad D_{U_m} W = 0, \tag{B.33}$$

which lead to the Minkowski minimum $V_F = 0$. When $W \neq 0$, the supersymmetry is broken by the F term of the Kähler moduli. In contrast to the previous section, we now assume that all the complex structure moduli and dilaton are stabilized by the flux-induced superpotential. Although the F terms of S and U vanish at this Minkowski minimum, the F terms of the Kähler moduli are nonvanishing, in general:

$$F^{T_i} = -e^{K/2} \sum_j K^{T_i \bar{T}_j} D_{\bar{T}_j} \bar{W} = -e^{K/2} \sum_j K^{T_i \bar{T}_j} K_{\bar{T}_j} \bar{W}, \tag{B.34}$$

when $W \neq 0$.

For simplicity, we study the model with the overall Kähler modulus with the CY volume $\mathcal{V} = (T + \bar{T})^{3/2}$. Then, the F term of the Kähler modulus is simplified as

$$F^T \simeq e^{K(S,U)/2} \frac{T + \bar{T}}{(T + \bar{T})^{3/2}} \bar{W} = e^{K(S,U)/2} \frac{\bar{W}}{(T + \bar{T})^{1/2}}. \tag{B.35}$$

Thus, supersymmetric and SUSY-breaking minima are also degenerate in a way similar to the previous section, since the scalar potential is independent of T and F^T. However, the supersymmetric vacuum corresponds to $\mathrm{Re}(T) \to \infty$, that is, the decompactification limit.

When the leading α' corrections are involved, the Kähler potential of the Kähler modulus is corrected as (67)

$$K = -2 \ln\left(\mathcal{V} + \frac{\xi}{2}\right), \tag{B.36}$$

where $\xi = -\frac{\chi(CY)\zeta(3)}{2(2\pi)^3 g_s^{3/2}}$ with χ and g_s being the Euler characteristic of CY and string coupling. These α'-corrections break the no-scale structure, and the scalar potential is generated as

$$V_F \simeq e^{K(S,U)} \frac{3\xi}{4\mathcal{V}^3} |W|^2. \tag{B.37}$$

The sign of ξ depends on the number of complex structure moduli and Kähler moduli. When the number of Kähler moduli is smaller than that of complex structure moduli, ξ is positive. In the case of single Kähler modulus, the F-term potential reduces to

$$V_F \simeq e^{K(S,U)} \frac{3\xi}{4(T+\bar{T})^{9/2}} |W|^2 = \frac{3\xi}{4(T+\bar{T})^{7/2}} |F^T|^2. \tag{B.38}$$

Along the same step outlined in section B.2, we take into account the loop corrections originating from the supersymmetric particles whose soft terms are dominated by the F term of the Kähler modulus. It is remarkable that the loop corrections give rise to the stabilization of $\mathrm{Re}(T)$ unlike the case in section B.2. Then, by assuming that the typical gaugino and supersymmetric scalar fields mainly contribute to the loop effects, the total scalar potential becomes

$$\begin{aligned}
V &\simeq \frac{3\xi}{4(T+\bar{T})^{7/2}} |F^T|^2 + \frac{1}{64\pi^2} \Bigg[a_1 \left(c^2 - \left(\frac{|F^T|}{T+\bar{T}} \right)^2 \right)^2 \ln \left(c^2 - \left(\frac{|F^T|}{T+\bar{T}} \right)^2 \right) \\
&\quad - a_2 \left(\frac{|F^T|}{T+\bar{T}} \right)^4 \ln \left(a_3 \left(\frac{|F^T|}{T+\bar{T}} \right)^2 \right) \Bigg] \\
&= \frac{3\xi}{4(T+\bar{T})^{3/2}} (\hat{F}^T)^2 + \frac{1}{64\pi^2} \left[a_1 \left(c^2 - \left(\hat{F}^T \right)^2 \right)^2 \ln \left(c^2 - \left(\hat{F}^T \right)^2 \right) \right. \\
&\quad \left. - a_2 \left(\hat{F}^T \right)^4 \ln \left(a_3 \left(\hat{F}^T \right)^2 \right) \right] \\
&= \frac{3\xi}{4e^{K(S,U)/2} W} (\hat{F}^T)^3 + \frac{1}{64\pi^2} \left[a_1 \left(c^2 - \left(\hat{F}^T \right)^2 \right)^2 \ln \left(c^2 - \left(\hat{F}^T \right)^2 \right) \right. \\
&\quad \left. - a_2 \left(\hat{F}^T \right)^4 \ln \left(a_3 \left(\hat{F}^T \right)^2 \right) \right],
\end{aligned} \tag{B.39}$$

where $\hat{F}^T \equiv |F^T|/(T+\bar{T})$. Here, we employ the same notation of section B.2 and W is chosen as a real constant, for simplicity.

By setting the illustrative parameters

$$a_1 = 10, \qquad a_2 = 3, \qquad a_3 = 8, \qquad c = 1.1, \qquad \xi = 1, \qquad e^{K(S,U)/2} W \simeq 60.42, \tag{B.40}$$

the scalar potential is drawn as in Fig. B.6. As a result, the degeneracy of vacua is resolved by the loop corrections. In contrast to the discussion in section B.2, the vanishing $|F^T| \propto (T+\bar{T})^{-1/2}$ corresponds to the unphysical domain $\mathrm{Re}(T) \to \infty$. Thus, the SUSY-breaking vacuum is selected. Indeed, the above illustrative parameters give rise to the high-scale SUSY-breaking minimum, where the vacuum expectation value of $\mathrm{Re}(T)$,

$$\mathrm{Re}(T) \simeq 9.9, \tag{B.41}$$

resides in a reliable range of the supergravity approximation. After canonically normalizing the modulus,

$$\hat{\sigma} = \sqrt{\frac{3}{2}} \ln \sigma, \tag{B.42}$$

with $\sigma = \mathrm{Re}(T)/\sqrt{2}$, its mass squared is evaluated as

$$m_{\hat{\sigma}}^2 \simeq 3.3 \times 10^{-2}, \tag{B.43}$$

in the reduced Planck unit, i.e. $m_{\hat{\sigma}} \simeq 0.18 \times M_{\mathrm{Pl}}$, which should be smaller than the other complex structure moduli and dilaton to justify our low-energy effective action. Since those complex structure moduli and dilaton fields have been stabilized at the SUSY-breaking minimum, their masses are typically greater than or equal to the gravitino mass $e^{K(S,U)/2} W/\mathcal{V} \simeq 6.9 \times 10^{-1}$ in our numerical example. Our situation is thus justified.

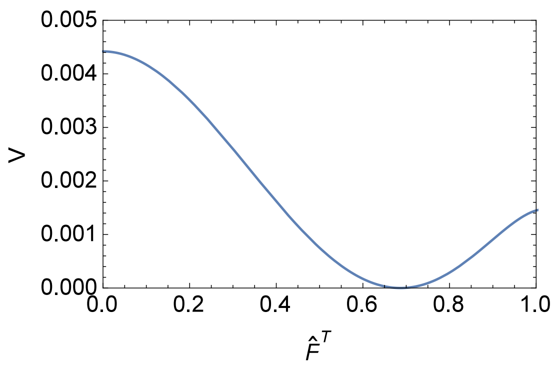

Figure B.6: - he scalar potential as a function of $\hat{F}^T$ by setting the parameters as in eq. (B.40).

Interestingly, the tuning of $e^{K(S,U)/2}W$ allows us to consider the tiny cosmological constant. In the above scenario, $\mathrm{Re}(T)$ can be stabilized at a fine value, but its imaginary part, i.e. the axion, remains massless.

B.4 Shhort summary

We have studied a new type of moduli potential and stabilization. In the model with the complex structure modulus U, the supersymmetric and SUSY-breaking minima are degenerate at the leading order. That is, the tree-level potential is independent of the F term of U, but depends on $\mathrm{Re}(U)$. The F term itself depends on $\mathrm{Im}(U)$. Loop effects due to $\mathrm{Im}(U)$-dependent gaugino and sfermion masses resolve the degeneracy of vacua and stabilize the axion $\mathrm{Im}(U)$. The SUSY vacuum or SUSY-breaking vacuum is selected depending on parameters in the potential. Low-scale SUSY breaking is also possible when additional proper nonperturbative effects are involved.

We have also studied the model with the Kähler modulus T. This model has the flat direction along both $\mathrm{Re}(T)$ and $\mathrm{Im}(T)$ at the leading level. The SUSY vacuum and SUSY-breaking vacuum are degenerate, but the SUSY vacuum corresponds to the decompactification limit $\mathrm{Re}(T) \to \infty$. In this model, the modulus F term depends only on $\mathrm{Re}(T)$. The real part $\mathrm{Re}(T)$ can be stabilized by inclusion of α'-corrections, and loop effects due to $\mathrm{Re}(T)$-dependent gaugino and sfermion masses. However, the axion $\mathrm{Im}(T)$ remains massless at this stage.

We can extend the model with the single Kähler modulus to the models with many Kähler moduli. Their real parts can be stabilized in a similar mechanism, but many axionic parts would remain light. Such axions would be interesting, e.g., for candidates of dark matter and the QCD axion. Also, one of the light axions could derive the cosmological inflation if a proper potential is generated. Moreover, these axions would be interesting from the viewpoint of a string axiverse. Such axion phenomenology would be studied elsewhere.

Appendix C

Preparation for the Affleck-Dine mechanism

Here, let us mention about the Noether current and Scalar potential in the supergravity (SUGRA). We will also summarize the Hubble induced mass-term and A-term briefly. We review what the Affleck-Dine mechanism is in chapter 6.

C.1 Nether current and asymmetric number density

We define the current of a scalar field ϕ as

$$J^{\mu} = i\alpha(\phi\partial^{\mu}\phi^{*} - \phi^{*}\partial^{\mu}\phi), \tag{C.1}$$

and the conserved charge as

$$Q = \int d^3x J^0(x) = i\alpha \int d^3x(\phi\dot{\phi}^{*} - \phi^{*}\dot{\phi}), \tag{C.2}$$

where α is a small arbitrary parameter (describing a displacement in space-time).

Using above definitions, with the equation of motion (or continuity equation) of a scalar field $\ddot{\phi} + 3H\dot{\phi} + V_{\phi} = 0$, we can obtain by integrating the equation for the evolution of the asymmetry,

$$\begin{aligned} \left[a^3 J^0\right](t) &= \int^t dt(-i\alpha)a^3\left(\phi V_{\phi} - \phi^{*}V_{\phi^{*}}\right) \\ J^0(t_0) &\sim (-i\alpha)\frac{1}{H_0}\left(\phi V_{\phi} - \phi^{*}V_{\phi^{*}}\right). \end{aligned} \tag{C.3}$$

In the second line, we use the approximation such that $\int^t dt \sim 1/H(t_0)(= 1/H_0)$. The difference of complex parts of the potential makes some currents, which plays an important role in our study (in chapter 6).

C.2 Scalar potential in the supergravity

In local supersymmetry (supergravity, SUGRA), the scalar potential becomes, in terms of Kähler potential K and superpotential W,

$$V = e^K \left(W_i (K^{-1})^i_j W^j - 3|W|^2 \right) + \text{D-terms} \ , \tag{C.4}$$

where $W_i = \partial_{\phi_i} W + W K_i$, $K_i = \partial_{\phi_i} K$, and $(K^{-1})^i_j$ is the inverse of the matrix $= \partial^2_{\phi_i \phi^{*j}} K$. Note that through this paper, we use the units where the reduced Planck mass $M_p = 2.4 \times 10^{18}$ GeV $= 1$ unless otherwise noted explicitly.

C.3 Hubble induced mass-term and A-term

During and inflation, the AD field obtains effective potentials from the energy density of inflaton I, When we introduce an inaflaton I. We consider the following the Kahler potential

$$K = |I|^2 + |\phi|^2 + \frac{c}{M_p^2} |I|^2 |\phi|^2, \tag{C.5}$$

where c is an $\mathcal{O}(1)$ constant. In the model, the scalar potential have

$$V \supset |F_I|^2 \left(1 + (1-c) \frac{|\phi|^2}{M_p^2} \right) . \tag{C.6}$$

Then, due to the above the terms, the AD field ϕ obtains an effective mass term of order the Hubble parameter during inflation:

$$V_H = c_H H^2 |\phi|^2, \quad \text{where} \qquad c_H = -3(c-1) \tag{C.7}$$

where H is the Hubble parameter at the giving time, and we use $|F_I|^2 = 3H^2 M_p^2$. This is called a Hubble induced mass-term.

The same procedure is applied for the Hubble induced A-term. We assume that there is a Kahler potential of $I|\phi|^2/M_p + c.c.$. It reads to

$$V_A \supset \left(- \frac{\lambda a_H}{n M_p^{n-3} H |\phi|^n} + c.c. \right) \tag{C.8}$$

where a_H is an $\mathcal{O}(1)$ constant.

These Hubble induced terms are playing important roles in our Affleck-Dine leptogenesis model.

Bibliography

[1] Tatsuo Kobayashi, Akane Oikawa, and Hajime Otsuka. New potentials for string axion inflation. *Phys. Rev.*, D93(8):083508, 2016. 3, 21, 22, 23, 25, 35, 36, 38, 40

[2] Shinji Tsujikawa. Introductory review of cosmic inflation. In *2nd Tah Poe School on Cosmology: Modern Cosmology Phitsanulok, Thailand, April 17-25, 2003*, 2003. 7, 8

[3] Alan H. Guth. The Inflationary Universe: A Possible Solution to the Horizon and Flatness Problems. *Phys. Rev.*, D23:347–356, 1981. [Adv. Ser. Astrophys. Cosmol.3,139(1987)]. 8

[4] K. Sato. Cosmological Baryon Number Domain Structure and the First Order Phase Transition of a Vacuum. *Phys. Lett.*, 99B:66–70, 1981. [Adv. Ser. Astrophys. Cosmol.3,134(1987)]. 8

[5] Andrei D. Linde. A New Inflationary Universe Scenario: A Possible Solution of the Horizon, Flatness, Homogeneity, Isotropy and Primordial Monopole Problems. *Phys. Lett.*, 108B:389–393, 1982. [Adv. Ser. Astrophys. Cosmol.3,149(1987)]. 8, 9, 10

[6] Andreas Albrecht and Paul J. Steinhardt. Cosmology for Grand Unified Theories with Radiatively Induced Symmetry Breaking. *Phys. Rev. Lett.*, 48:1220–1223, 1982. [Adv. Ser. Astrophys. Cosmol.3,158(1987)]. 8, 9, 10

[7] P. A. R. Ade et al. Planck 2013 results. XXII. Constraints on inflation. *Astron. Astrophys.*, 571:A22, 2014. 8, 15, 22, 25, 38, 40

[8] P. A. R. Ade et al. Planck 2015 results. XX. Constraints on inflation. *Astron. Astrophys.*, 594:A20, 2016. 8, 9, 15, 16, 17, 22, 25, 53

[9] Y. Akrami et al. Planck 2018 results. X. Constraints on inflation. 2018. 8, 9, 15, 19, 22

[10] Edward R. Harrison. Fluctuations at the threshold of classical cosmology. *Phys. Rev.*, D1:2726–2730, 1970. 12

[11] Ya. B. Zeldovich. A Hypothesis, unifying the structure and the entropy of the universe. *Mon. Not. Roy. Astron. Soc.*, 160:1P–3P, 1972. 12

[12] Daniel Baumann and Liam McAllister. *Inflation and String Theory*. Cambridge Monographs on Mathematical Physics. Cambridge University Press, 2015. 13, 14, 18, 20, 55, 118

[13] Masahiro Takada, Eiichiro Komatsu, and Toshifumi Futamase. Cosmology with high-redshift galaxy survey: neutrino mass and inflation. *Phys. Rev.*, D73:083520, 2006. 15

[14] Peter Adshead, Richard Easther, Jonathan Pritchard, and Abraham Loeb. Inflation and the Scale Dependent Spectral Index: Prospects and Strategies. *JCAP*, 1102:021, 2011. 15

[15] R. D. Peccei and Helen R. Quinn. CP Conservation in the Presence of Instantons. *Phys. Rev. Lett.*, 38:1440–1443, 1977. [,328(1977)]. 16

[16] Durmus A. Demir, Maxim Pospelov, and Adam Ritz. Hadronic EDMs, the Weinberg operator, and light gluinos. *Phys. Rev.*, D67:015007, 2003. 18

[17] Kaori Fuyuto, Junji Hisano, Natsumi Nagata, and Koji Tsumura. QCD Corrections to Quark (Chromo)Electric Dipole Moments in High-scale Supersymmetry. *JHEP*, 12:010, 2013. 18

[18] Katherine Freese, Joshua A. Frieman, and Angela V. Olinto. Natural inflation with pseudo - Nambu-Goldstone bosons. *Phys. Rev. Lett.*, 65:3233–3236, 1990. 18, 19, 21, 23, 41, 63

[19] Enrico Pajer and Marco Peloso. A review of Axion Inflation in the era of Planck. *Class. Quant. Grav.*, 30:214002, 2013. 18, 20

[20] Jihn E. Kim, Hans Peter Nilles, and Marco Peloso. Completing natural inflation. *JCAP*, 0501:005, 2005. 20

[21] Liam McAllister, Eva Silverstein, and Alexander Westphal. Gravity Waves and Linear Inflation from Axion Monodromy. *Phys. Rev.*, D82:046003, 2010. 20, 46

[22] Raphael Flauger, Liam McAllister, Enrico Pajer, Alexander Westphal, and Gang Xu. Oscillations in the CMB from Axion Monodromy Inflation. *JCAP*, 1006:009, 2010. 20

[23] Marcus Berg, Enrico Pajer, and Stefan Sjors. Dante's Inferno. *Phys. Rev.*, D81:103535, 2010. 20

[24] Joseph P. Conlon. Brane-Antibrane Backreaction in Axion Monodromy Inflation. *JCAP*, 1201:033, 2012. 20

[25] Kiwoon Choi and Jihn E. Kim. Harmful Axions in Superstring Models. *Phys. Lett.*, 154B:393, 1985. [Erratum: Phys. Lett.156B,452(1985)]. 21, 41, 51

[26] Tom Banks, Michael Dine, Patrick J. Fox, and Elie Gorbatov. On the possibility of large axion decay constants. *JCAP*, 0306:001, 2003. 21, 41, 51

[27] Peter Svrcek and Edward Witten. Axions In String Theory. *JHEP*, 06:051, 2006. 21, 41, 51, 97

[28] David H. Lyth. What would we learn by detecting a gravitational wave signal in the cosmic microwave background anisotropy? *Phys. Rev. Lett.*, 78:1861–1863, 1997. 21

[29] Nima Arkani-Hamed, Lubos Motl, Alberto Nicolis, and Cumrun Vafa. The String landscape, black holes and gravity as the weakest force. *JHEP*, 06:060, 2007. 22

[30] Michael Czerny and Fuminobu Takahashi. Multi-Natural Inflation. *Phys. Lett.*, B733:241–246, 2014. 22, 23, 41

[31] Marco Peloso and Caner Unal. Trajectories with suppressed tensor-to-scalar ratio in Aligned Natural Inflation. *JCAP*, 1506(06):040, 2015. 22

[32] Tatsuo Kobayashi, Daisuke Nitta, and Yuko Urakawa. Modular invariant inflation. *JCAP*, 1608(08):014, 2016. 22

[33] Arthur Hebecker, Patrick Mangat, Fabrizio Rompineve, and Lukas T. Witkowski. Winding out of the Swamp: Evading the Weak Gravity Conjecture with F-term Winding Inflation? *Phys. Lett.*, B748:455–462, 2015. 22, 25

[34] Susha Parameswaran, Gianmassimo Tasinato, and Ivonne Zavala. Subleading Effects and the Field Range in Axion Inflation. *JCAP*, 1604(04):008, 2016. 22, 43, 44

[35] Nana Cabo Bizet, Oscar Loaiza-Brito, and Ivonne Zavala. Mirror quintic vacua: hierarchies and inflation. *JHEP*, 10:082, 2016. 22

[36] Eva Silverstein and Alexander Westphal. Monodromy in the CMB: Gravity Waves and String Inflation. *Phys. Rev.*, D78:106003, 2008. 23, 41, 46, 63

[37] Tatsuo Kobayashi, Osamu Seto, and Yuya Yamaguchi. Axion monodromy inflation with sinusoidal corrections. *PTEP*, 2014(10):103E01, 2014. 23, 41

[38] Tetsutaro Higaki, Tatsuo Kobayashi, Osamu Seto, and Yuya Yamaguchi. Axion monodromy inflation with multi-natural modulations. *JCAP*, 1410(10):025, 2014. 23, 41

[39] Kiwoon Choi, Hyungjin Kim, and Seokhoon Yun. Natural inflation with multiple sub-Planckian axions. *Phys. Rev.*, D90:023545, 2014. 23, 41

[40] Michael Czerny, Tetsutaro Higaki, and Fuminobu Takahashi. Multi-Natural Inflation in Supergravity. *JHEP*, 05:144, 2014. 23, 41

[41] Hiroyuki Abe, Tatsuo Kobayashi, and Hajime Otsuka. Natural inflation with and without modulations in type IIB string theory. *JHEP*, 04:160, 2015. 23, 41

[42] Sergei Gukov, Cumrun Vafa, and Edward Witten. CFT's from Calabi-Yau four folds. *Nucl. Phys.*, B584:69–108, 2000. [Erratum: Nucl. Phys.B608,477(2001)]. 23, 119

[43] Steven B. Giddings, Shamit Kachru, and Joseph Polchinski. Hierarchies from fluxes in string compactifications. *Phys. Rev.*, D66:106006, 2002. 23, 119

[44] Shamit Kachru, Renata Kallosh, Andrei D. Linde, and Sandip P. Trivedi. De Sitter vacua in string theory. *Phys. Rev.*, D68:046005, 2003. 24, 55, 118

[45] Emilian Dudas, Chloe Papineau, and Stefan Pokorski. Moduli stabilization and uplifting with dynamically generated F-terms. *JHEP*, 02:028, 2007. 24, 121

[46] Hiroyuki Abe, Tetsutaro Higaki, Tatsuo Kobayashi, and Yuji Omura. Moduli stabilization, F-term uplifting and soft supersymmetry breaking terms. *Phys. Rev.*, D75:025019, 2007. 24

[47] Renata Kallosh and Andrei D. Linde. O'KKLT. *JHEP*, 02:002, 2007. 24

[48] Hiroyuki Abe, Tetsutaro Higaki, and Tatsuo Kobayashi. More about F-term uplifting. *Phys. Rev.*, D76:105003, 2007. 24

[49] Ralph Blumenhagen, Daniela Herschmann, and Florian Wolf. String Moduli Stabilization at the Conifold. *JHEP*, 08:110, 2016. 24

[50] Vijay Balasubramanian, Per Berglund, Joseph P. Conlon, and Fernando Quevedo. Systematics of moduli stabilisation in Calabi-Yau flux compactifications. *JHEP*, 03:007, 2005. 24, 55, 118

[51] D. Lust and S. Stieberger. Gauge threshold corrections in intersecting brane world models. *Fortsch. Phys.*, 55:427–465, 2007. 35, 48, 125

[52] Ralph Blumenhagen, Boris Kors, Dieter Lust, and Stephan Stieberger. Four-dimensional String Compactifications with D-Branes, Orientifolds and Fluxes. *Phys. Rept.*, 445:1–193, 2007. 35, 48, 55, 117

[53] D. Cremades, L. E. Ibanez, and F. Marchesano. Computing Yukawa couplings from magnetized extra dimensions. *JHEP*, 05:079, 2004. 36, 124

[54] Hiroyuki Abe, Kang-Sin Choi, Tatsuo Kobayashi, and Hiroshi Ohki. Higher Order Couplings in Magnetized Brane Models. *JHEP*, 06:080, 2009. 36

[55] Masahiro Kawasaki, Kazunori Kohri, and Takeo Moroi. Hadronic decay of late - decaying particles and Big-Bang Nucleosynthesis. *Phys. Lett.*, B625:7–12, 2005. 37

[56] Masahiro Kawasaki, Kazunori Kohri, and Takeo Moroi. Big-Bang nucleosynthesis and hadronic decay of long-lived massive particles. *Phys. Rev.*, D71:083502, 2005. 37

[57] Kensuke Akita, Tatsuo Kobayashi, Akane Oikawa, and Hajime Otsuka. Moduli mediation without moduli-induced gravitino problem. *JHEP*, 05:178, 2016. 37, 38, 40, 49

[58] E. D. Stewart, M. Kawasaki, and T. Yanagida. Affleck-Dine baryogenesis after thermal inflation. *Phys. Rev.*, D54:6032–6039, 1996. 37

[59] Dong-hui Jeong, Kenji Kadota, Wan-Il Park, and Ewan D. Stewart. Modular cosmology, thermal inflation, baryogenesis and predictions for particle accelerators. *JHEP*, 11:046, 2004. 37

[60] Masahiro Kawasaki and Fuminobu Takahashi. Late-time entropy production due to the decay of domain walls. *Phys. Lett.*, B618:1–6, 2005. 38, 40, 49, 85, 90, 97

[61] Eran Palti and Timo Weigand. Towards large r from [p, q]-inflation. *JHEP*, 04:155, 2014. 46

[62] Nemanja Kaloper and Lorenzo Sorbo. A Natural Framework for Chaotic Inflation. *Phys. Rev. Lett.*, 102:121301, 2009. 46

[63] Liam McAllister, Eva Silverstein, Alexander Westphal, and Timm Wrase. The Powers of Monodromy. *JHEP*, 09:123, 2014. 46

[64] Ian Affleck and Michael Dine. A New Mechanism for Baryogenesis. *Nucl. Phys.*, B249:361–380, 1985. 53, 79, 101

[65] Michael Dine, Lisa Randall, and Scott D. Thomas. Baryogenesis from flat directions of the supersymmetric standard model. *Nucl. Phys.*, B458:291–326, 1996. 53, 79

[66] Luis E. Ibanez and Angel M. Uranga. *String theory and particle physics: An introduction to string phenomenology.* Cambridge University Press, 2012. 55, 117, 118

[67] Katrin Becker, Melanie Becker, Michael Haack, and Jan Louis. Supersymmetry breaking and alpha-prime corrections to flux induced potentials. *JHEP*, 06:060, 2002. 57, 127

[68] Rudolf Haag, Jan T. Lopuszanski, and Martin Sohnius. All Possible Generators of Supersymmetries of the s Matrix. *Nucl. Phys.*, B88:257, 1975. [,257(1974)]. 68

[69] Sidney R. Coleman and J. Mandula. All Possible Symmetries of the S Matrix. *Phys. Rev.*, 159:1251–1256, 1967. 68

[70] Stephen P. Martin. A Supersymmetry primer. pages 1–98, 1997. [Adv. Ser. Direct. High Energy Phys.18,1(1998)]. 69, 73

[71] F. Gabbiani, E. Gabrielli, A. Masiero, and L. Silvestrini. A Complete analysis of FCNC and CP constraints in general SUSY extensions of the standard model. *Nucl. Phys.*, B477:321–352, 1996. 70

[72] Yasuhiro Okada, Masahiro Yamaguchi, and Tsutomu Yanagida. Upper bound of the lightest Higgs boson mass in the minimal supersymmetric standard model. *Prog. Theor. Phys.*, 85:1–6, 1991. 73

[73] Y. Okada, Masahiro Yamaguchi, and T. Yanagida. Renormalization group analysis on the Higgs mass in the softly broken supersymmetric standard model. *Phys. Lett.*, B262:54–58, 1991. 73

[74] Howard E. Haber and Ralf Hempfling. Can the mass of the lightest Higgs boson of the minimal supersymmetric model be larger than m(Z)? *Phys. Rev. Lett.*, 66:1815–1818, 1991. 73

[75] John R. Ellis, Giovanni Ridolfi, and Fabio Zwirner. Radiative corrections to the masses of supersymmetric Higgs bosons. *Phys. Lett.*, B257:83–91, 1991. 73

[76] John R. Ellis, Giovanni Ridolfi, and Fabio Zwirner. On radiative corrections to supersymmetric Higgs boson masses and their implications for LEP searches. *Phys. Lett.*, B262:477–484, 1991. 73

[77] Ulrich Ellwanger, Cyril Hugonie, and Ana M. Teixeira. The Next-to-Minimal Supersymmetric Standard Model. *Phys. Rept.*, 496:1–77, 2010. 74, 84, 94

[78] Pierre Fayet. Supergauge Invariant Extension of the Higgs Mechanism and a Model for the electron and Its Neutrino. *Nucl. Phys.*, B90:104–124, 1975. 74, 84

[79] Pierre Fayet. Supersymmetry and Weak, Electromagnetic and Strong Interactions. *Phys. Lett.*, 64B:159, 1976. 74

[80] Pierre Fayet. Spontaneously Broken Supersymmetric Theories of Weak, Electromagnetic and Strong Interactions. *Phys. Lett.*, 69B:489, 1977. 74

[81] Pierre Fayet. Relations Between the Masses of the Superpartners of Leptons and Quarks, the Goldstino Couplings and the Neutral Currents. *Phys. Lett.*, 84B:416, 1979. 74

[82] Hans Peter Nilles, M. Srednicki, and D. Wyler. Weak Interaction Breakdown Induced by Supergravity. *Phys. Lett.*, 120B:346, 1983. 74

[83] J. M. Frere, D. R. T. Jones, and S. Raby. Fermion Masses and Induction of the Weak Scale by Supergravity. *Nucl. Phys.*, B222:11–19, 1983. 74

[84] J. P. Derendinger and Carlos A. Savoy. Quantum Effects and SU(2) x U(1) Breaking in Supergravity Gauge Theories. *Nucl. Phys.*, B237:307–328, 1984. 74

[85] John R. Ellis, J. F. Gunion, Howard E. Haber, L. Roszkowski, and F. Zwirner. Higgs Bosons in a Nonminimal Supersymmetric Model. *Phys. Rev.*, D39:844, 1989. 74

[86] Manuel Drees. Supersymmetric Models with Extended Higgs Sector. *Int. J. Mod. Phys.*, A4:3635, 1989. 74

[87] Alexander Vilenkin. Cosmic Strings and Domain Walls. *Phys. Rept.*, 121:263–315, 1985. 74

[88] S. A. Abel. Destabilizing divergences in the NMSSM. *Nucl. Phys.*, B480:55–72, 1996. 75

[89] Christopher F. Kolda, Stefan Pokorski, and Nir Polonsky. Stabilized singlets in supergravity as a source of the mu - parameter. *Phys. Rev. Lett.*, 80:5263–5266, 1998. 75

[90] C. Panagiotakopoulos and K. Tamvakis. Stabilized NMSSM without domain walls. *Phys. Lett.*, B446:224–227, 1999. 75, 90

[91] A. Vilenkin and E. P. S. Shellard. *Cosmic Strings and Other Topological Defects*. Cambridge University Press, 2000. 75, 86

[92] E. Komatsu et al. Seven-Year Wilkinson Microwave Anisotropy Probe (WMAP) Observations: Cosmological Interpretation. *Astrophys. J. Suppl.*, 192:18, 2011. 78

[93] A. D. Sakharov. Violation of CP Invariance, C asymmetry, and baryon asymmetry of the universe. *Pisma Zh. Eksp. Teor. Fiz.*, 5:32–35, 1967. [Usp. Fiz. Nauk161,no.5,61(1991)]. 78, 101

[94] M. Fukugita and T. Yanagida. Baryogenesis Without Grand Unification. *Phys. Lett.*, B174:45–47, 1986. 78

[95] V. A. Kuzmin, V. A. Rubakov, and M. E. Shaposhnikov. On the Anomalous Electroweak Baryon Number Nonconservation in the Early Universe. *Phys. Lett.*, 155B:36, 1985. 78

[96] S. Yu. Khlebnikov and M. E. Shaposhnikov. The Statistical Theory of Anomalous Fermion Number Nonconservation. *Nucl. Phys.*, B308:885–912, 1988. 78, 81, 102

[97] Jeffrey A. Harvey and Michael S. Turner. Cosmological baryon and lepton number in the presence of electroweak fermion number violation. *Phys. Rev.*, D42:3344–3349, 1990. 78, 81, 102

[98] P. A. R. Ade et al. Planck 2013 results. XV. CMB power spectra and likelihood. *Astron. Astrophys.*, 571:A15, 2014. 78, 101

[99] Takeo Moroi and Hitoshi Murayama. The Minimal supersymmetric leptogenesis. *JHEP*, 07:009, 2000. 79

[100] Tony Gherghetta, Christopher F. Kolda, and Stephen P. Martin. Flat directions in the scalar potential of the supersymmetric standard model. *Nucl. Phys.*, B468:37–58, 1996. 79

[101] Jihn E. Kim and Hans Peter Nilles. The mu Problem and the Strong CP Problem. *Phys. Lett.*, 138B:150–154, 1984. 83

[102] Tatsuo Kobayashi, Hiroki Makino, Ken-ichi Okumura, Takashi Shimomura, and Tsubasa Takahashi. TeV scale mirage mediation in NMSSM. *JHEP*, 01:081, 2013. 84, 87, 99

[103] Kiwoon Choi, Kwang Sik Jeong, Tatsuo Kobayashi, and Ken-ichi Okumura. Little SUSY hierarchy in mixed modulus-anomaly mediation. *Phys. Lett.*, B633:355–361, 2006. 84, 118

[104] K. Choi, A. Falkowski, Hans Peter Nilles, M. Olechowski, and S. Pokorski. Stability of flux compactifications and the pattern of supersymmetry breaking. *JHEP*, 11:076, 2004. 84, 85

[105] Kiwoon Choi, Kwang Sik Jeong, and Ken-ichi Okumura. Phenomenology of mixed modulus-anomaly mediation in fluxed string compactifications and brane models. *JHEP*, 09:039, 2005. 84

[106] Motoi Endo, Masahiro Yamaguchi, and Koichi Yoshioka. A Bottom-up approach to moduli dynamics in heavy gravitino scenario: Superpotential, soft terms and sparticle mass spectrum. *Phys. Rev.*, D72:015004, 2005. 84

[107] Ya. B. Zeldovich, I. Yu. Kobzarev, and L. B. Okun. Cosmological Consequences of the Spontaneous Breakdown of Discrete Symmetry. *Zh. Eksp. Teor. Fiz.*, 67:3–11, 1974. [Sov. Phys. JETP40,1(1974)]. 84, 89

[108] S. A. Abel, Subir Sarkar, and P. L. White. On the cosmological domain wall problem for the minimally extended supersymmetric standard model. *Nucl. Phys.*, B454:663–684, 1995. 84, 89

[109] Koichi Hamaguchi, Kazunori Nakayama, and Norimi Yokozaki. NMSSM in gauge-mediated SUSY breaking without domain wall problem. *Phys. Lett.*, B708:100–106, 2012. 84, 90

[110] Kenji Kadota, Masahiro Kawasaki, and Ken'ichi Saikawa. Gravitational waves from domain walls in the next-to-minimal supersymmetric standard model. *JCAP*, 1510(10):041, 2015. 84

[111] Motoi Endo, Koichi Hamaguchi, and Fuminobu Takahashi. Moduli-induced gravitino problem. *Phys. Rev. Lett.*, 96:211301, 2006. 85, 95

[112] Yoshimi Kanehata, Tatsuo Kobayashi, Yasufumi Konishi, Osamu Seto, and Takashi Shimomura. Constraints from Unrealistic Vacua in the Next-to-Minimal Supersymmetric Standard Model. *Prog. Theor. Phys.*, 126:1051–1076, 2011. 85

[113] E. W. Kolb and M. S. Turner. *The Early Universe*. Addison-Wesley, 1990. 89

[114] William H. Press, Barbara S. Ryden, and David N. Spergel. Dynamical Evolution of Domain Walls in an Expanding Universe. *Astrophys. J.*, 347:590–604, 1989. 89

[115] Mark Hindmarsh. Level set method for the evolution of defect and brane networks. *Phys. Rev.*, D68:043510, 2003. 89

[116] Theodore Garagounis and Mark Hindmarsh. Scaling in numerical simulations of domain walls. *Phys. Rev.*, D68:103506, 2003. 89

[117] A. M. M. Leite and C. J. A. P. Martins. Scaling Properties of Domain Wall Networks. *Phys. Rev.*, D84:103523, 2011. 89, 90

[118] A. M. M. Leite, C. J. A. P. Martins, and E. P. S. Shellard. Accurate Calibration of the Velocity-dependent One-scale Model for Domain Walls. *Phys. Lett.*, B718:740–744, 2013. 89

[119] Takashi Hiramatsu, Masahiro Kawasaki, and Ken'ichi Saikawa. On the estimation of gravitational wave spectrum from cosmic domain walls. *JCAP*, 1402:031, 2014. 89

[120] M. Kawasaki, Kazunori Kohri, and Naoshi Sugiyama. MeV scale reheating temperature and thermalization of neutrino background. *Phys. Rev.*, D62:023506, 2000. 90

[121] Steen Hannestad. What is the lowest possible reheating temperature? *Phys. Rev.*, D70:043506, 2004. 90

[122] Kazuhide Ichikawa, Masahiro Kawasaki, and Fuminobu Takahashi. The Oscillation effects on thermalization of the neutrinos in the Universe with low reheating temperature. *Phys. Rev.*, D72:043522, 2005. 90

[123] David G. Cerdeno, C. Munoz, and Osamu Seto. Right-handed sneutrino as thermal dark matter. *Phys. Rev.*, D79:023510, 2009. 94

[124] Pierre Sikivie. Axion Cosmology. *Lect. Notes Phys.*, 741:19–50, 2008. [,19(2006)]. 97

[125] Hiroyuki Abe, Tatsuo Kobayashi, and Hajime Otsuka. Towards natural inflation from weakly coupled heterotic string theory. *PTEP*, 2015(6):063E02, 2015. 97

[126] T. Asaka and M. Kawasaki. Cosmological moduli problem and thermal inflation models. *Phys. Rev.*, D60:123509, 1999. 98

[127] Antonio Riotto and Mark Trodden. Recent progress in baryogenesis. *Ann. Rev. Nucl. Part. Sci.*, 49:35–75, 1999. 101

[128] D. N. Spergel et al. Wilkinson Microwave Anisotropy Probe (WMAP) three year results: implications for cosmology. *Astrophys. J. Suppl.*, 170:377, 2007. 101

[129] Hitoshi Murayama and T. Yanagida. Leptogenesis in supersymmetric standard model with right-handed neutrino. *Phys. Lett.*, B322:349–354, 1994. 102

[130] Motoi Endo and Fuminobu Takahashi. Non-thermal Production of Dark Matter from Late-Decaying Scalar Field at Intermediate Scale. *Phys. Rev.*, D74:063502, 2006. 108

[131] Vadim S. Kaplunovsky and Jan Louis. Model independent analysis of soft terms in effective supergravity and in string theory. *Phys. Lett.*, B306:269–275, 1993. 118

[132] A. Brignole, Luis E. Ibanez, and C. Munoz. Towards a theory of soft terms for the supersymmetric Standard Model. *Nucl. Phys.*, B422:125–171, 1994. [Erratum: Nucl. Phys.B436,747(1995)]. 118

[133] Kiwoon Choi, Adam Falkowski, Hans Peter Nilles, and Marek Olechowski. Soft supersymmetry breaking in KKLT flux compactification. *Nucl. Phys.*, B718:113–133, 2005. 118

[134] Oleg Lebedev, Hans Peter Nilles, and Michael Ratz. De Sitter vacua from matter superpotentials. *Phys. Lett.*, B636:126–131, 2006. 121

[135] Sidney R. Coleman and Erick J. Weinberg. Radiative Corrections as the Origin of Spontaneous Symmetry Breaking. *Phys. Rev.*, D7:1888–1910, 1973. 121